

# DISSERTATION | DOCTORAL THESIS

Titel | Title

The prevalence and diversity of labial cartilages in sharks and their facets of utilization during prey capture

verfasst von | submitted by

Claudia Klimpfinger BSc BEd MSc MEd

angestrebter akademischer Grad | in partial fulfilment of the requirements for the degree of  
Doktorin der Naturwissenschaften (Dr.rer.nat.)

Wien | Vienna, 2025

Studienkennzahl lt. Studienblatt |  
Degree programme code as it appears on the  
student record sheet:

UA 796 605 426

Dissertationsgebiet lt. Studienblatt | Field of  
study as it appears on the student record  
sheet:

Erdwissenschaften

Betreut von | Supervisor:

Univ.-Prof. Dipl.-Geol. Dr. Jürgen Kriwet



# Table of Content

<b>ACKNOWLEDGEMENTS</b> .....	<b>5</b>
<b>ABSTRACT</b> .....	<b>6</b>
<b>ZUSAMMENFASSUNG</b> .....	<b>7</b>
<b>CHAPTER 1: INTRODUCTION</b> .....	<b>9</b>
1.1 GENERAL INFORMATION .....	9
1.2 SHARKS AND THEIR FEEDING MECHANISMS .....	9
1.2.1 Ram-Feeding .....	11
1.2.2 Suction-Feeding.....	11
1.2.3 Biting .....	12
1.2.4 Filter-Feeding.....	13
1.3 LABIAL CARTILAGES IN SHARKS.....	14
1.4 MAIN OUTLINE AND OBJECTIVES OF THE CHAPTERS 2 TO 4 .....	16
1.4.1 Outline of Chapter 2 .....	16
1.4.2 Outline of Chapter 3 .....	17
1.4.3 Outline of Chapter 4 .....	18
REFERENCES .....	19
<b>CHAPTER 2: GROWTH TRAJECTORIES OF PRENATAL EMBRYOS OF THE DEEP-SEA SHARK <i>CHLAMYDOSELACHUS</i> <i>ANGUINEUS</i> (CHONDRICHTHYES)</b> .....	<b>23</b>
AUTHOR INFORMATION .....	23
BIBLIOGRAPHY .....	23
ABSTRACT .....	25
INTRODUCTION .....	25
MATERIALS AND METHODS .....	27
<i>Ethical statement</i> .....	27
<i>Staging</i> .....	27
<i>Measurements</i> .....	27
<i>Geometric morphometric analyses</i> .....	27
RESULTS .....	28
<i>Stages</i> .....	28
<i>Analysis of linear measurements</i> .....	29
<i>Shape variation of body and head</i> .....	30
<i>Head allometry variation</i> .....	31
DISCUSSION .....	32
CONCLUSIONS .....	34
REFERENCES.....	35
<b>CHAPTER 3: COMPARATIVE MORPHOLOGY OF LABIAL CARTILAGES IN SHARKS (CHONDRICHTHYES, ELASMOBRANCHII)</b> .....	<b>39</b>
AUTHOR INFORMATION .....	39
BIBLIOGRAPHY .....	39
ABSTRACT .....	41
INTRODUCTION .....	41
MATERIALS AND METHODS.....	42
RESULTS.....	43
DISCUSSION .....	49
CONCLUSIONS.....	51
REFERENCES .....	51
<b>CHAPTER 4: MORPHOLOGICAL VARIABILITY AND FUNCTION OF LABIAL CARTILAGES IN SHARKS (CHONDRICHTHYES, ELASMOBRANCHII)</b> .....	<b>55</b>
AUTHOR INFORMATION .....	55
BIBLIOGRAPHY .....	55
ABSTRACT.....	57

INTRODUCTION .....	57
MATERIALS AND METHODS .....	58
<i>Morphological Descriptions</i> .....	59
RESULTS .....	60
<i>Morphological Descriptions</i> .....	60
<i>Interpretations</i> .....	67
DISCUSSION .....	69
<i>Number of Labial Cartilages</i> .....	69
<i>Shapes of Labial Cartilages</i> .....	70
<i>Labial Cartilage Mobility and Adaptations for Special Feeding Strategies</i> .....	70
<i>Labial Cartilage Combinations</i> .....	72
CONCLUSIONS .....	73
REFERENCES .....	74
<b>CHAPTER 5: CONCLUDING REMARKS AND FUTURE PERSPECTIVES .....</b>	<b>79</b>
REFERENCES .....	82
<b>SUPPLEMENTARY MATERIALS .....</b>	<b>83</b>
MANUSCRIPT 1 .....	83
MANUSCRIPT 2 .....	84
MANUSCRIPT 3 .....	87
CONCLUSIONS .....	93

# ACKNOWLEDGEMENTS

I would like to thank all the people who encouraged and supported me throughout the years. First of all, I would like to thank my supervisor and co-author Jürgen Kriwet for his great help, advice and assistance which turned me into the right direction whenever I lost my way. Your encouragement, guidance and positivity were a great help to accomplish all the years of studying and research up to this final point.

Also, I want to thank all the other members of the Evolutionary Morphology Group who made this journey a social and fun experience and who provided great ideas, help and feedback for my work and presentations. I learned a lot of you guys and hopefully will continue to do so in the future.

A special thanks goes to my co-authors Faviel López-Romero and Sho Tanaka and the anonymous peer-reviewers, without whom the publications would not have been possible.

Thank you, Viktoria Zechmayer for your help in proof-reading this dissertation and the preceding manuscripts.

Very affectionate thanks to some of the most important people in my life: thank you, Florian Zechmayer, my love, for all your patience, support, and endless love. Thanks to my mother, Elisabeth Klimpfinger and my sister, Anita Klimpfinger, for their emotional support at all times and their deep believe in me.

Finally, I want to thank all my friends and family for supporting and encouraging me over the whole time.

It took me almost eight years, which of course were interrupted by different jobs, the academic studies to become a teacher, a pandemic and finally my teaching career, but eventually I mastered all the way with all your support, and I want to thank you all for your long breath. At last, I succeeded.

## ABSTRACT

Sharks are part of the Earth-fauna since more than 300 million years. Today they are globally distributed and have occupied many different ecological niches – ranging from tiny ectoparasites, like the cookie-cutter shark, over big apex predators, like the great white shark, up to gigantic planktivores, like the whale shark. Since old times sharks were used to investigate the evolution of vertebrates, especially concerning the evolution of moveable jaws. Though one part of the jaws, the labial cartilages, was mostly overlooked and undescribed. During the research on the growth-trajectories of an ancient-morphotyped deep sea shark (*Chlamydoselachus anguineus*), those labial cartilages caught my interest. Since I barely found information on those structures in a quick search I started to engage myself with the research of labial cartilages in sharks.

Labial cartilages are a primeval part of the shark jaws that is either preserved, reduced or extended in present shark species. Therefore, the scope of labial cartilages within different shark species ranges anywhere between zero and five pairs. It emerges that number, shape and position of labial cartilages is rather an evidence on the feeding strategy of sharks than displaying a phylogenetic connection. I used published computed tomographic scans (ct-scans) of sharks and extensive literature research on labial cartilages, shark jaws and feeding behaviors to comply the different constellations of labial cartilages with documented feeding behaviors. After sighting more than 100 ct-scans of different shark species and extensive literature research I was able to form a hypothesis on the connection of the different constellations of labial cartilages and the feeding methods in sharks.

My research lead up to the following three conclusions: 1) the more labial cartilages are present, the more dominant is the usage of suction during feeding; 2) the more anterior the onset of the labial cartilages and the more robust they are, the stronger is the produced suction; 3) a strong reduction of labial cartilages is a secondary adaptation to ram-feeding behavior.

# ZUSAMMENFASSUNG

Haie gehören schon seit über 300 Millionen Jahren zur Fauna der Erde. Heute sind sie weltweit verbreitet und haben die verschiedensten ökologischen Nischen besetzt – von winzigen Ektoparasiten, wie dem Zigarrenhai, über große Apex-Prädatoren, wie dem weißen Hai, bis hin zu gigantischen Planktonfressern, wie dem Walhai. Besonders interessant sind sie seit jeher um die Evolution der Wirbeltiere, insbesondere die der beweglichen Kiefer, zu erforschen und nachzuvollziehen. Ein Nebenteil der Kiefer, die sogenannten Labialknorpel, sind bei diesen Forschungsarbeiten allerdings häufig unerwähnt geblieben. Bei der Erforschung des Wachstumsverlaufes einer ursprünglich geformten Tiefsee-Hai-Art (*Chlamydoselachus anguineus*) fielen mir diese Labialknorpel ins Auge und nachdem ich bei einer schnellen Recherche kaum Informationen zu diesen Strukturen finden konnte, beschäftigte ich mich intensiver mit ihrer Erforschung. Die Labialknorpel sind ein ursprünglicher Teil der Hai-Kiefer, der bei den heutigen Haien erhalten, reduziert oder verstärkt entwickelt vorliegt. So kommt es, dass Hai-Arten alles zwischen null und fünf Paaren an Labialknorpeln besitzen können. Es zeichnet sich jedoch ab, dass die Anzahl, Ausformung und Position der Labialknorpel weniger phylogenetische Verbindungen anzeigen, als vielmehr einen Hinweis auf die Beutefang- und Nahrungsaufnahmemethode bergen. Ich nutzte publizierte computertomographische Scans (ct-Scans) von Haien und betrieb Literaturrecherche zu den Labialknorpeln und den Fressverhalten verschiedener Hai-Arten, um die verschiedenen Labialknorpelkonstellationen in Einklang mit den dokumentierten Fressverhalten zu bringen. Nach Sichtung von über 100 ct-Scans verschiedener Hai-Arten und ausgedehnter Literaturrecherche konnte ich eine Hypothese für die Verbindung von verschiedenen Labialknorpelkonstellationen mit der Methode der Nahrungsaufnahme bei Haien aufstellen. Es ergeben sich die folgenden drei Konklusionen: 1) je mehr Labialknorpel vorliegen, desto dominanter ist die Verwendung von Sog bei der Nahrungsaufnahme; 2) je weiter anterior die Labialknorpel ansetzen und je kräftiger sie ausgeprägt sind, desto stärker ist der erzeugte Sog; 3) eine starke Reduktion der Labialknorpel ist eine sekundäre Anpassung an ein rammendes Fressverhalten (sogenanntes „ram-feeding“).





# **CHAPTER 1: INTRODUCTION**

*„The sea, once it casts its spell, holds one in its net of wonder forever.“  
– Jacques Yves Cousteau*

## **1.1 General information**

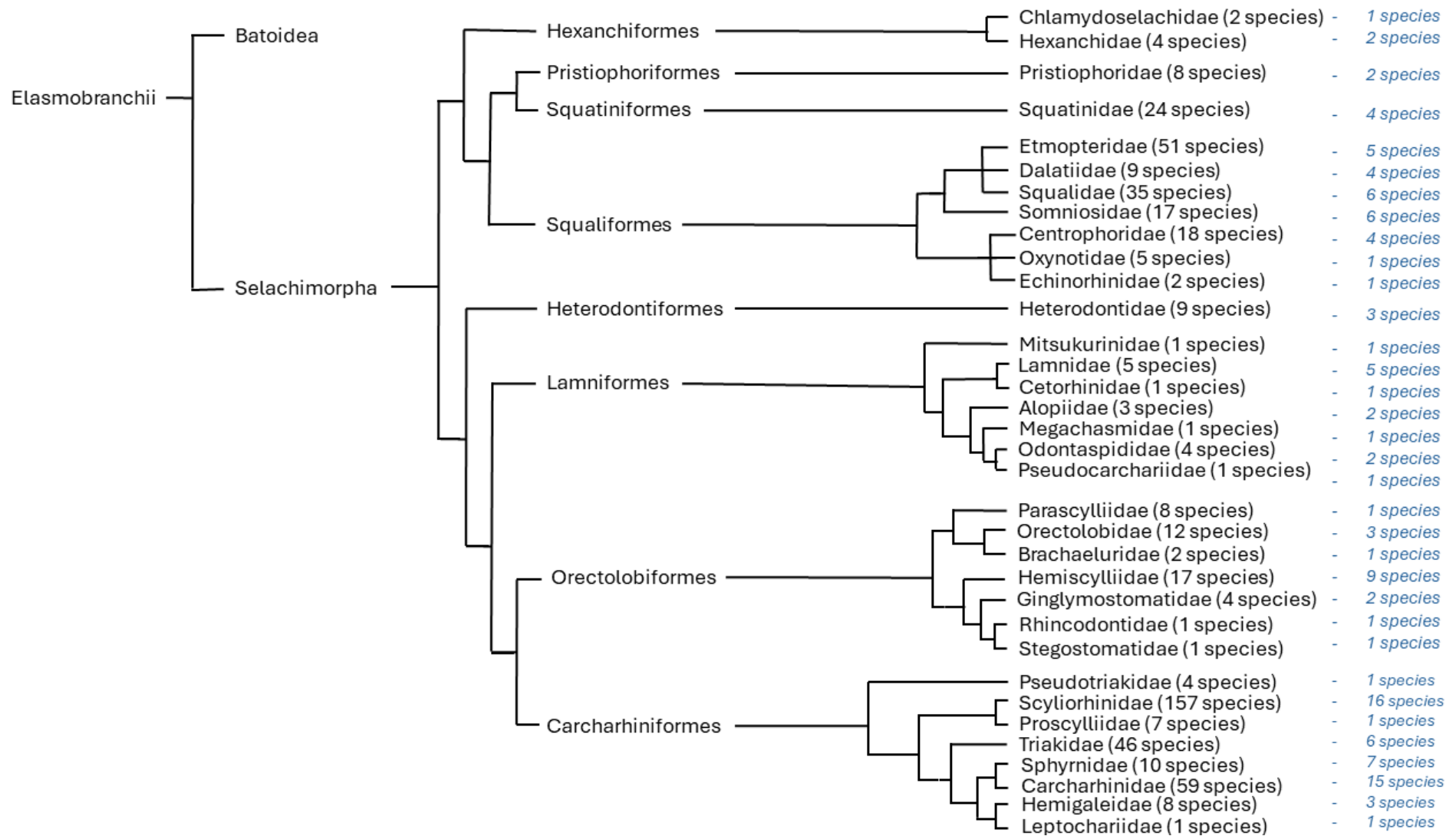
Chondrichthyan fishes are among the oldest creatures on planet Earth, considering that they have been around since about 400 million years (Grogan et al. 2012; Brazeau & Friedman 2015). This group comprises chimeras, sharks, skates and rays, which are clustered into elasmobranchs (sensu Maisey 2012), comprising sharks, skates and rays, and holocephalans, comprising only chimeras. Sharks alone are merged under the group of Selachimorpha (sensu Vélez-Zuazo & Agnarsson 2011) that currently includes 537 living shark species ([www.catalogueoflife.org](http://www.catalogueoflife.org) – Bánki et al. 2024), grouping into 8 Orders and 31 Families (Vélez-Zuazo & Agnarsson 2011). [

Figure 1]

Sharks are present in almost every part of the World's oceans, from polar to tropical regions and from shallow to deep waters, some species are even capable of living in fresh waters (Compagno 1990). They have conquered many different ecological niches and display a large variety of body shapes, ranging from large apex predators and giant planktivores over medium sized opportunistic feeders, active hunters, and ambush predators down to small opportunists and tiny ectoparasites (Huber et al. 2019). Since all sharks are predators of some kind, they play an important role in the worlds' ecosystems by controlling populations, not only of smaller animals – like most teleosts do – but also of animals larger than themselves. (Ferretti et al. 2010)

## **1.2 Sharks and their feeding mechanisms**

All sharks are predatory in some way with prey items ranging from zooplankton to cetaceans, and they display a large variety of prey-capture methods, even though their feeding apparatus consists only of a quite limited number of elements (Motta & Huber 2012). There are four basic feeding strategies distinguished: ram-feeding, suction-feeding, biting and filter-feeding. The large variety of prey capture methods seen in extant sharks is based on various combinations of two or more of those basic strategies with different proportions of the basic strategies incorporated. (Moss 1977; Huber 2006; Wilga et al. 2007; Motta & Huber 2012; Ramsay 2012; Ferry et al. 2015; Huber et al. 2019)



**Figure 1** Phylogenetic tree of Elasmobranchii (after Vélez-Zuazo & Agnarsson 2011 and sharksrays.org 2025, last accessed on 01.01.2025) including all presently known families with described species numbers in brackets (according to catalogueoflife.org 2024) and species numbers examined in the course of this PhD-Project in blue italics after the hyphen.

### 1.2.1 Ram-Feeding

Ram-feeding species tend to ‘over-swim’ their prey, moving at fast speed and opening the mouth in the last possible moment to grab the prey item, so to avoid the bow-wave and a possible escape of the prey [Figure 2]. Ram-feeding is discussed to be either a quite common or the least common prey capture method among sharks (Motta & Huber 2012; Huber et al. 2019). This discussion relies on the definition of ram-feeding. It is, as explained above, the engulfment of relatively stationary prey, but the definitions differ, whether it only includes smaller prey items that can be taken up completely (Huber et al. 2019) or if it also includes larger prey items, which are additionally decreased in size by biting (Motta & Huber 2012). In the latter case a combination of ram-feeding and biting is obvious, but the opinions differ regarding whether ram-feeding is the prey-capture mechanism and biting is just an additional processing (Motta & Huber 2012), or if this combination makes biting the prey capture mechanism all by itself (Huber et al. 2019). In correlation to the objectives of this work, I follow the definition by Motta & Huber (2012), making ram-feeding the prey capture process and biting a processing activity. Ram-feeding is found to some extent in many shark species and is especially well established in requiem (Carcharhinidae) and mackerel sharks (Lamnidae). A very prominent example is the great white shark (*Carcharodon carcharias*) that is largely known to hit its prey at high speed, occasionally even leaving the water in its prey capture attempts when the prey is localized close to the surface (Tricas 1985; Motta & Huber 2012).

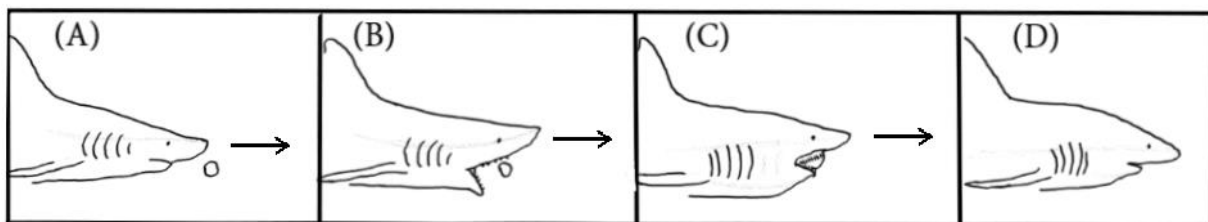


**Figure 2** Ram-feeding sequence sketch (adapted from Motta & Huber 2012). (A) Approaching the prey item, (B) jaw expansion at the latest possible moment, (C) engulfing of prey with upper jaw protrusion, (D) retraction of upper jaw and pharyngeal transport of prey item.

### 1.2.2 Suction-Feeding

In aquatic vertebrates a pervasive ability is the use of suction to draw prey into the mouth cavity or to compensate for the bow-wave caused by the forward movement of the predator. In a dense medium such as water, suction is a very efficient way to capture prey. A circular mouth opening, the capability of jaw protrusion and enlargement of the mouth

cavity enhance the suction capabilities of aquatic vertebrates (Nauwelaerts et al. 2006; Ferry et al. 2015; Wainwright et al. 2015). Sharks too use suction to different extent. The most effective suction feeders, for example the Japanese wobbegong (*Orectolobus japonicus*), rely exclusively on suction for prey capturing, even enhancing their strong suction by using it close to the ground (Motta & Huber 2012). Also, strong labial cartilages, a comparatively small mouth opening, and strong abductor muscles are typical for suction-dependent species (Moss 1977; Motta & Huber 2012). It is even suggested that suction-feeding developed in chondrichthyans earlier than it did in bony fishes, dating early suction-feeding back to the Carboniferous (359 Ma) (Coates et al. 2019).

Suction-feeding, or inertial suction, works by decreasing the pressure in the mouth cavity due to a rapid expansion causing a negative pressure gradient, which subsequently draws the prey item into the mouth of the predator [Figure 3]. Depending on the intensity of the suction used, it can compensate for the predators' forward movement when attacking or even drag the prey item into the mouth of a predator remaining stationary (Motta & Huber 2012; Huber et al. 2019). Especially in some carpet shark species (*Orectolobiformes*) suction is established as main or sole feeding mechanism. Besides those specialists, variations in suction intensity are very common in many shark species as part of their hunting and feeding strategies, as it is in other aquatic vertebrates (Ferry et al. 2015; Wainwright et al. 2015).

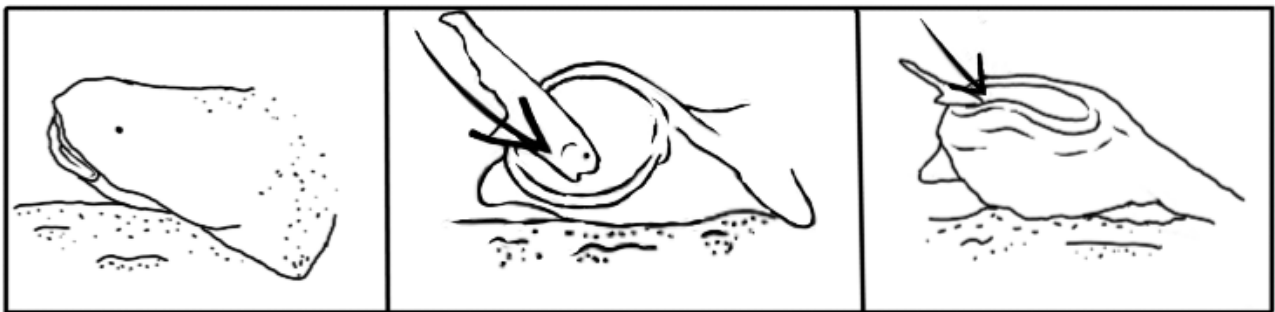


**Figure 3** Suction-feeding in the pacific angel shark (*Squatina californica*). As an ambush predator it buries itself in the sand and uses a strong suction flow to capture its prey. (Redrawn after freely available photos)

### 1.2.3 Biting

LCs and the suction they support are not the sole way of capturing elusive prey. The deep living goblin shark (*Mitsukurina owstoni*) and the megamouth shark (*Megachasma pelagios*) are known to have extremely protrusible jaws (Nakaya et al. 2008, Nakaya et al. 2016) that facilitate the capturing of prey when moving at a rather slow pace, hence

extreme jaw protrusion must be taken into account when it comes to prey capturing behaviors as a special case of biting behavior.

Biting is suggested to be the most ancient or basal prey capture method in sharks (Wilga et al. 2007; Huber et al. 2019). It is a process in which the shark has to be very close to the prey object. It includes actively overtaking and subsequently grasping the prey with the teeth and ripping or cutting a piece of flesh out of the prey. This is often only a method of prey manipulation but can clearly be taken as feeding mechanism on carcasses or stationary prey items close to the ground. Mostly biting occurs in combination with ram- and/ or suction-feeding. (Motta & Huber 2012; Huber et al. 2019)

Typical species using biting (almost always in combination with suction to some extent) are the ectoparasitic cookie cutter sharks (*Isistius spp.*), that attach to larger prey animals and bite a crater-shaped piece of flesh out of their prey's body engulfing large pieces of flesh that reach up to 4.6% of their body mass (Grace et al. 2023). Also, the durophagous horn shark (*Heterodontus francisci*) uses biting, preceded by a short burst of suction, to consume its hard shelled, often sessile prey (Huber et al. 2005). Another example is the sharpnose sevengill shark (*Heptranchias perlo*), which is suspected to bite into its prey items and then rip out pieces by short jerky backwards movements, a foraging strategy that was also observed in the broadnose sevengill shark (*Notorynchus cepedianus*) (Ebert 1991; Kryukova & Kuznetsov 2020).

#### **1.2.4 Filter-Feeding**

Filter-Feeding is only used by three shark species (whale shark *Rhincodon typus*, basking shark *Cetorhinus maximus*, megamouth shark *Megachasma pelagios*), which feed on tiny plankton organisms by intake of water into their mouth and filtering the plankton by gill rakers or special pads anterior to the gills, as seen in *Rhincodon typus* (Cade et al. 2020). At least four different kinds of filter feeding mechanisms are known in sharks. Surface ram filter feeding (= surface active feeding) and sub-surface ram filter feeding (= passive feeding) occur when the shark steadily swims through the water with an open mouth [Figure 4 B], the terms 'active' and 'passive' are related to the swimming effort. This behavior is seen in whale sharks and basking sharks and probably also is displayed by the megamouth shark. Vertical suction feeding (= bottling) [Figure 4 A] is only known from the whale shark, which positions its body vertically with the mouth close to the surface and sucks up water and plankton by a rapid mouth-expansion (Motta et al. 2010, Cade et al. 2020). The megamouth shark is also considered to perform engulfment feeding, a strategy

that is typical for humpback whales. It engulfs a large amount of water using its extraordinarily large buccal cavity and filters the plankton with its gill rakers after the mouth closed and the water is pushed out steadily (Nakaya et al. 2008).

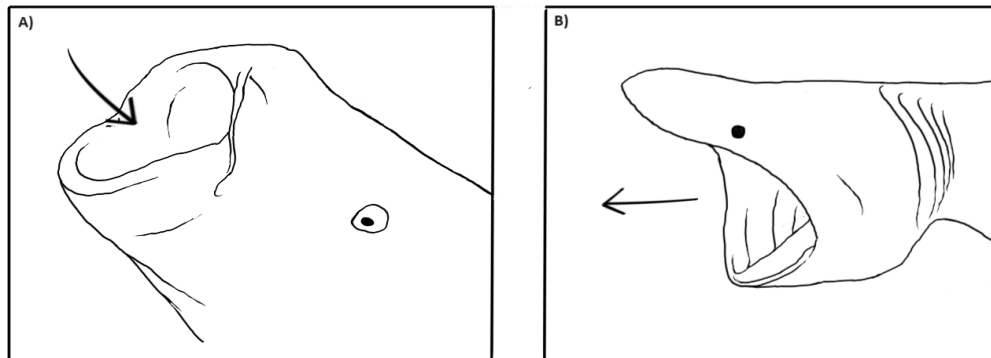


**Figure 4** Filter-feeding in sharks. A) whaleshark (*Rhincodon typus*) using “bottling”, thus sucking water and plankton into its mouth stationed close to the surface; B) basking shark (*Cetorhinus maximus*) using ram filter-feeding. (Redrawn after freely available photographs)

### 1.3 Labial Cartilages in Sharks

Labial Cartilages (LCs) are cartilaginous structures located labial to the jaws, with their onset, shape and number varying significantly between shark species [Figure 5]. LCs are almost always, but not exclusively, connected to some kind of suction. They are often, but not necessarily enclosed in labial folds that can be detected along the jaw line. Usually they move anterior and, depending on their onset location, lateral when the mouth is opened. With the forward movement the mouth corners are enclosed, and the mouth opening is given a more stable frame by these cartilages, whereas lateral movement enlarges the mouth cavity and therefore intensifies the flow of water into the mouth cavity [Figure 6].

The evolutionary origins of these skeletal structures are not yet completely understood, and their functions originally were considered to strengthen and mobilize mouth corners (Smith 1937), subsequently to be “without functional utility” (Veran 1995) and finally to be of use in prey capturing and feeding (Motta & Wilga 2001). LCs occur in members of all groups of chondrichthyan fishes (e.g., Dean et al 2007; Dearden et al. 2021; Lopez-Romero et al. 2022) but, concerning sharks, they generally have been mentioned only in a couple of studies concerning the prey capturing and feeding mechanisms of some species (e.g., Fouts & Nelson 1999; Edmonds et al. 2001; Huber et al. 2005; Motta et al. 2008; McNeil et al. 2016; Grant et al. 2018) without being the main objective of a study focusing on their variety and corresponding functionality up to now. Consequently, no comparative

morphological analyses of LCs in sharks are available to better understand whether they comprise phylogenetic or functional signals, or both. With this thesis, I intend to fill this gap. Over the course of my doctoral studies, I examined the LCs of different shark species carefully so to propose an overview on their variety as well as a connection between LC-type and its range of function during prey capture and feeding. Rays and skates, the Batomorphii, which represent the sister groups to sharks were not considered here, but the results of this study provide a solid foundation for analyzing LCs in rays and skates.

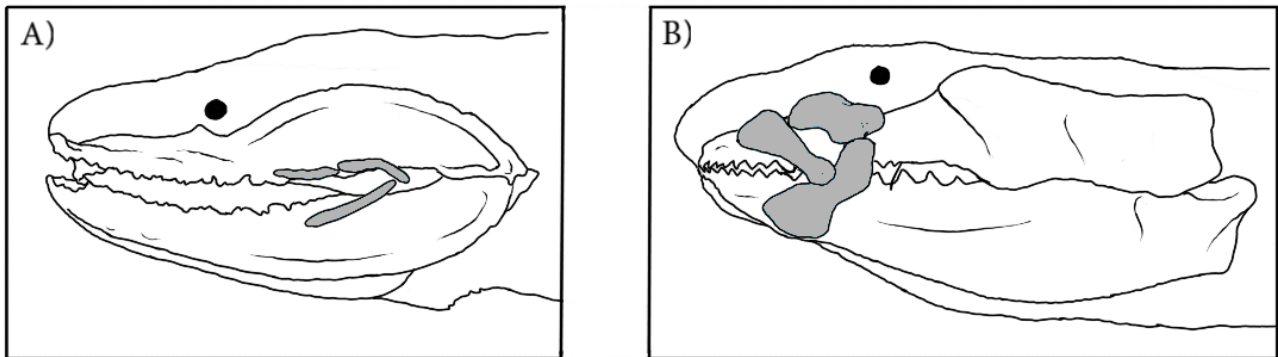


**Figure 5** Examples of labial cartilages in sharks to display the large variety drawn after evaluated CT-scans. A) frilled shark (*Chlamydoselachus anguineus*), B) angel shark (*Squatina squatina*)

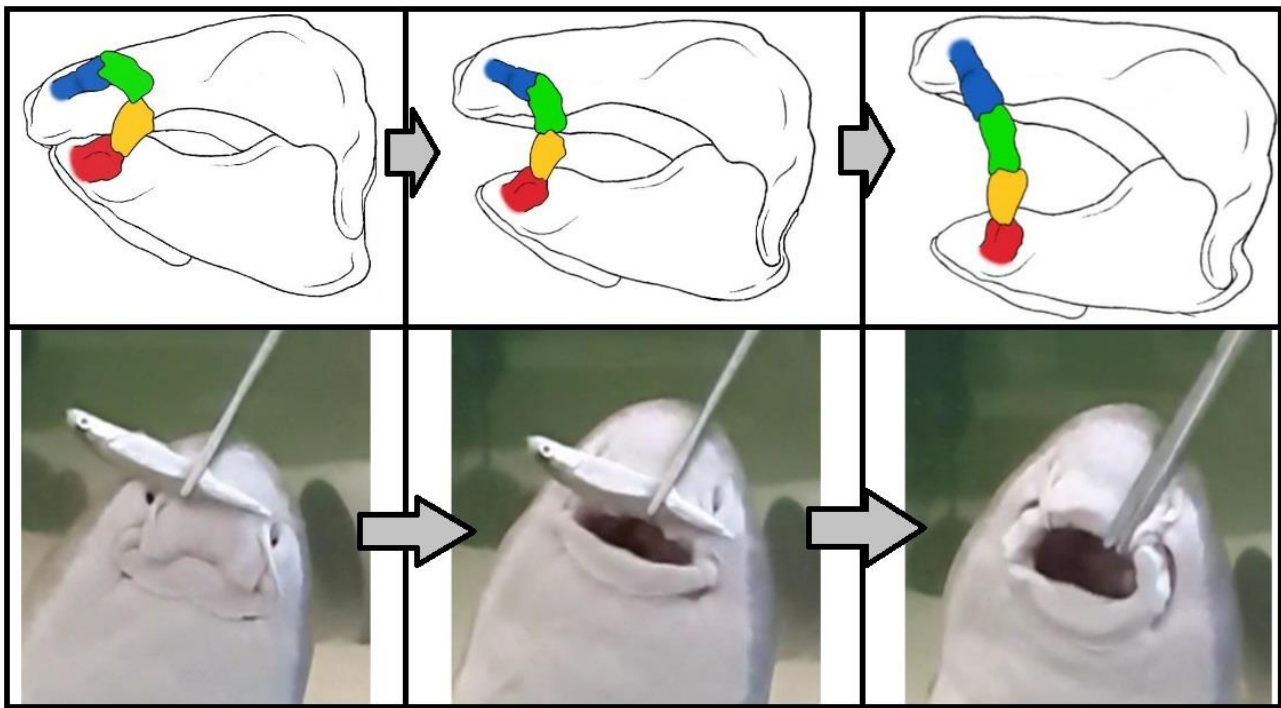


**Figure 6** Labial cartilage movement while feeding in the brown banded bamboo shark (*Chiloscyllium punctatum*) drawn after evaluated CT-scans. Color-code in the sketch: blue = LC1, green = LC2, orange = LC3.1, red = LC3

Photos from the wet lab of the University of Vienna by Manuel Staggl

## 1.4 Main outline and objectives of the chapters 2 to 4

As I detected labial cartilages very early in the ontogenetic development of an ancient-looking deep-sea shark (*Chlamydoselachus anguineus*) the main outline of this PhD-Project changed from the initial aim to study the traits of deep-sea sharks to studying the occurrence of labial cartilages in sharks and their influence on their hunting and feeding strategies.

### **1.4.1 Outline of Chapter 2**

This first publication represents an analysis of the growth trajectories in the frilled shark (*Chlamydoselachus anguineus*), a so-called “living fossil” (Smith 1937) that is considered to display a rather ancient body shape (eel-like body, multi-cuspid teeth, terminal mouth position) comparable to the shapes known from extinct taxa far back in deep time. Due to this considerably ancient body morphotype the changes during ontogenetic development were particularly interesting because the shifts in growth may provide information on the evolution of body shapes. The resulting shape shifts and trends in pigmentation during the embryonic development are intended to be used as a comparison for the embryonic development in other shark species.

I conducted linear length measurements, and my colleague F. Lopez-Romero performed additional morphometric analyses and CT-scans of some embryos were generated to better visualize skeletal structures. Together we installed a staging scheme for the embryonic development of the frilled shark.

Our analyses showed an allometric growth pattern in frilled shark embryos and a size dimorphism between sexes that is contrary to the one observed in adults. Furthermore, the rather late shift in mouth position from ventral to terminal leads to the suggestion that a terminal mouth position is more likely to be a derived rather than a plesiomorphic character, rejecting the hypothesis of the frilled shark being a plesiomorphic shark.

One striking morphological feature in the prepared CT-scans, as well as in the cleared and stained embryos, were the labial cartilages (LCs) [Figure 7] appearing very early in the shark's development, but their origin could not be established and remained obscured. It soon became clear that almost no information about these skeletal elements exists in the literature apart from few general considerations and descriptions in single species (see above). This ultimately led to a reorientation of my dissertation project, as my collaborator decided to focus on ontogenetic aspects of cartilaginous fish in the further course of his doctoral thesis.



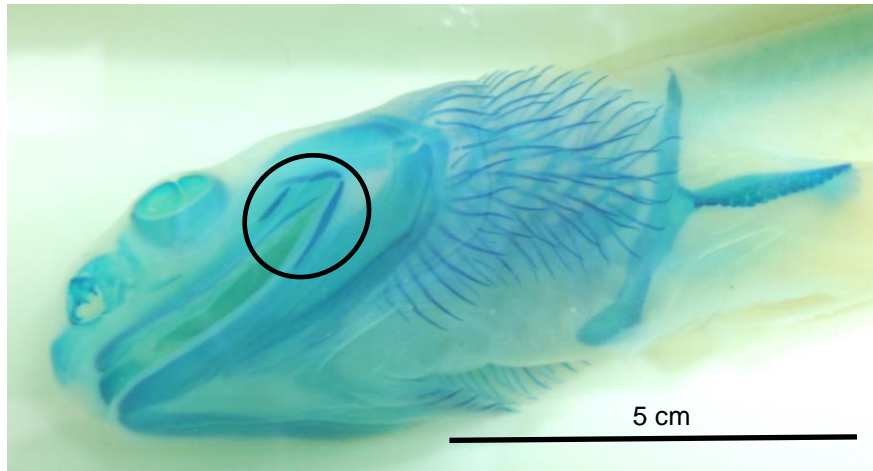


**Figure 7** Cleared and stained embryo of the frilled shark (*Chlamydoselachus anguineus*) with skeletal elements, including labial cartilages (encircled), clearly visible. (Specimen number: 1986.5.27A4 School of Marine Science and Technology, Tokai University, Japan)

#### 1.4.2 Outline of Chapter 3

In chapter three I established the occurrence of labial cartilages (LCs) in different shark species and tried to provide an overview of the variety of LCs in combination with the jaw structure in a first step. The high diversity and the often-missing characterization of LCs in species descriptions made this work more complex than assumed in the beginning. I reconstructed the jaws and LCs of different shark species from published CT-scans.

Using scans provided on figshare.com (Brázeau et al. 2017) reconstructing and marking the jaws and LCs, employing the Amira software, I was able to compare the LCs of 86 out of 537 currently present shark species, covering 27 out of 31 recent shark families.

I introduced a generally usable numeration system, differentiating between LC1, LC2, LC2.1, LC3 and LC3.1, following a description by Wu (1994) who hypothesized the partition of smaller LCs (LC2.1 and LC3.1) from the original three LCs. Also, I grouped those 86 species into eight morphogroups considering their jaw shape as well as the number, position and arrangement of the present LCs. From fossil arrangements and a hypothetical neoselachian ancestor (Compagno 1977) as well as the frequent presence of the same number of LC pairs, I deduced that three pairs is probably the primordial number of LCs, resulting in the assumption that more or less than three pairs of LCs display a derived condition.

The established morphogroups synergize (1) species that primarily use ram-feeding and display between zero and two pairs of LCs; (2) species of the dalatiid family, which act as

ectoparasites and suck onto larger prey cutting out chunks of flesh and therefore display a unique jaw shape and LC arrangement; (3) members of the orectolobid family, which are the only ones possessing five pairs of LCs and using strong suction being highly adapted ambush predators; (4) the family of angel sharks, with their three to four pairs of very strong, very far anterior located LCs; (5) all species who use suction mostly in combination with biting or ram-feeding and possessing three or four pairs of LCs; (6) species with three pairs of rather slender LCs probably using a minor suction; (7) special shaped LCs of the deepwater lantern sharks (Etmopteridae), possessing two pairs of labially-curved LCs and (8) the horn sharks (Heterodontidae), possessing two pairs of short LCs that are protruding labially also during the resting position. A connection of the feeding behavior and the number, shape and position of the LCs became obvious.

#### **1.4.3 Outline of Chapter 4**

In the further course of this PhD-Project I enlarged the sample number and investigated at least one species of every extant shark family using 3D reconstructions of computer tomographic (CT) and micro-computer tomographic (micro-CT) scans mainly provided online by Brázeau et al. ([www.figshare.com](http://www.figshare.com)) and Corrigan et al. (<https://sharkrays.org>). Also, an extensive literature research and personal observations were conducted to find out more about the LCs in sharks and how they influence the feeding behaviors of sharks.

With a general overview of features like position, number, size and shape of the LCs present I produced a dichotomous identification key for the different LC types excluding all species without any LCs. Since a reduction usually starts with LC2, then LC3 and last LC1 the number of types is highest in LC1, followed by LC3, and least in the additional LCs 2.1 and 3.1. In addition, based on current knowledge of feeding strategies in well-researched species, I concluded what combination of LC types leads to which kind of feeding behavior. This overview can be used on rare, endangered or extinct shark species where only dead individuals or skeletons are found, to get an insight on their feeding strategies and probably also their hunting strategies.

## References

- Bánki, O., Roskov, Y., Döring, M., Ower, G., Hernández Robles, D. R., Plata Corredor, C. A., Stjernegaard Jeppesen, T., Örn, A., Vandepitte, L., Hobern, D., Schalk, P., DeWalt, R. E., Ma, K., Miller, J., Orrell, T., Aalbu, R., Abbott, J., Adlard, R., Aedo, C., et al., 2024, *Catalogue of Life Checklist* (Version 2024-02-22), Catalogue of Life  
<https://doi.org/10.48580/dfvll>
- Brazeau M. & Friedman M., 2015, *The origin and early phylogenetic history of jawed vertebrates*, Nature, Volume 520, pp. 490-497, doi: 10.1038/nature14438
- Brazeau M., Kamminga P., De Bruin P.W. & Geleijns J., 2017, *X-ray computed tomography library of shark anatomy and lower jaw surface models*, figshare Collection,  
<https://doi.org/10.6084/m9.figshare.c.3662366.v1>
- Cade D.E., Levenson J.J., Cooper R., de la Parra R., Webb D.H. & Dove A.D.M., 2020, *Whale sharks increase swimming effort while filter feeding, but appear to maintain high foraging efficiencies*, Journal of Experimental Biology, Volume 223, pp. 1-13,  
doi: 10.1242/jeb.224402
- Catalogue of Life*, available online: <https://www.catalogueoflife.org/> (last accessed on 01.01.2025)  
– by Bánki O. et al.
- Chondrichthyan Tree of Life*, available online: <https://sharksrays.org/> (last accessed on 20.03.2024). – by Corrigan S., Naylor G. & Yang L.
- Coates M.I., Tietjen K., Olsen A.M. & Finarelli J.A., 2019, *High-performance suction feeding in an early elasmobranch*, Science Advances, Volume 5, eaax2742
- Compagno L.J.V., 1977, *Phyletic Relationships of Living Sharks and Rays*, American Zoology, Volume 17, pp. 303-322
- Compagno L.J.V., 1990, *Alternative life-history styles of cartilaginous fishes in time and space*, Environmental Biology of Fishes, Volume 28, pp. 33-75,  
<https://doi.org/10.1007/BF00751027>
- Corrigan, S.; Naylor, G.; Yang, L. The Chondrichthyan Tree of Life Project: Taking Stock of the World's Sharks and Rays, Copyright Experiment 2023. Available online:  
<https://experiment.com/projects/the-chondrichthyan-tree-of-life-project-taking-stock-of-the-world-s-sharks-and-rays> (accessed on 20.03.2024).
- Dean M.N., Bizzarro J.J. & Summers A.P., 2007, *The evolution of cranial design, diet and feeding mechanisms in batoid fishes*, Integrative and Comparative Biology, Volume 47, pp. 7-81
- Dearden R.P., Mansuit R., Cuckovic A., Herrel A., Didier D. Tafforeau P. & Pradel A., 2021, *The morphology and evolution of chondrichthyan cranial muscles: A digital dissection of the elephantfish *Callorhynchus milii* and the catshark *Scyliorhinus canicular**, Journal of Anatomy, Volume 238, pp. 1082-1105, doi: 10.1111/joa.13362

- Ebert D.A., 1991, *Observations on the predatory behaviour of the sevengill shark Notorynchus cepedianus*, South African Journal of marine Sciences, Volume 11, pp. 455-465
- Edmonds M.A., Motta P.J. & Hueter R.E., 2001, *Food capture kinematics of the suction feeding horn shark, Heterodontus francisci*, Environmental Biology of Fishes, Volume 62, pp. 415-427
- Ferretti F., Worm B., Britten G.L., Heithaus M.R. & Lotze H.K., 2010, *Patterns and ecosystem consequences of shark declines in the ocean*, Ecology Letters, Volume 13, pp. 1055-1071, doi: 10.1111/j.1461-0248.2010.01489.x
- Ferry L.A., Paig-Tran E.M. & Gibb A.C., 2015, *Suction, Ram, and Biting: Deviations and Limitations to the Capture of Aquatic Prey*, Integrative and Comparative Biology, Volume 55, Number 1, pp. 97-109, doi:10.1093/icb/icv028
- figshare.com, available online: <https://doi.org/10.6084/m9.figshare.c.3662366.v1> (last accessed on 20.03.2024) – by Brázeau et al.
- Grace M.A., Huber D., Travis K., Doozey M.H., Ford J., Decker S. & Mann J., 2023, *Simulating cookiecutter shark bites with a 3D-printed jaw-dental model*, Zoomorphology, Volume 142, pp. 253-264, doi: 10.1007/s00435-022-00586-0
- Grant S.M., Sullivan R. & Hedges K.J., 2018, *Greenland shark (Somniosus microcephalus) feeding behavior on static fishing gear, effect of SMART (Selective Magnetic and Repellent-Treated) hook deterrent technology, and factors influencing entanglement in bottom longlines*, PeerJ, Volume 6:e4751, doi:10.7717/peerj.4751
- Grogan E.D., Lund R. & Greenfest-Allen E., 2012, *The Origin and Relationships of Early Chondrichthyans* IN: Biology of Sharks and their Relatives – Second Edition. Editors: J.C. Carrier, J.A. Musick & M.R. Heithaus, CRC Press, Taylor & Francis Group, Florida; U.S.A., ISBN 978-1—4398-3926-3; pp. 3-30
- Huber D.R., Eason T.G., Hueter R. E. & Motta P.J., 2005, *Analysis of the bite force and mechanical design of the feeding mechanism of the durophagous horn shark Heterodontus francisci*, Journal of Experimental Biology, Volume 208, pp. 3553-3571, doi: 10.1242/jeb.01816
- Huber D.R., 2006, *Cranial biomechanics and feeding performance of sharks*, Dissertation University of South Florida, Paper 2566, <http://scholarcommons.usf.edu/etd/2566>
- Huber D.R., Claes J.M., Mallefet J. & Herrel A., 2009, *Is Extreme Bite Performance Associated with Extreme Morphologies in Sharks?*, Physiological and Biochemical Zoology, Volume 82, Number 1, pp. 20-28, doi: 10.1086/588177
- Huber D.R., Wilga C.D., Dean M., Ferry L., Gardiner J., Habegger L., Papastamatiou Y., Ramsay J. & Whitenack L., 2019, *Feeding in Cartilaginous Fishes: An Interdisciplinary Synthesis* IN: Feeding in Vertebrates – Evolution, Morphology, Behavior, Biomechanics. Editors: V. Bels

- & I.Q. Whishaw, Springer Nature Switzerland AG, ISBN 978-3-030-13738-0; pp. 231-295, doi: 10.1007/978-3-030-13739-7
- Kryukova N.V. & Kuznetsov A.N., 2020, *Suboccipital muscle of sharpnose sevengill shark *Heptanchias perlo* and its possible role in prey dissection*, Journal of Morphology, Volume 281, pp. 842-861, doi: 10.1002/jmor.21142
- López-Romero F.A., Beria F., Abed-Navandi D. & J. Kriwet, 2022, *Early shape divergence of developmental trajectories in the jaw of galeomorph sharks*, Frontiers in Zoology, Volume 19:7, pp. 1-11, doi: 10.1186/s12983-022-00452-1
- McNeil B., Lowry D., Larson S. & Griffing D., 2016, *Feeding Behavior of Subadult Sixgill Sharks (*Hexancus griseus*) at a Bait station*, PlosOne, doi: 10.1371/journal.pone.0156730
- Moss S.A., 1977, *Feeding Mechanisms in Sharks*, American Zoology, Volume 17, pp. 355-364
- Motta P.J., Hueter R.E., Tricas T.C., Summers A.P., Huber D.R., Lowry D., Mara K.R., Matott M.P., Whitenack L.B. & Wintzer A.P., 2008, *Functional Morphology of the Feeding Apparatus, Feeding Constraints, and Suction Performance in the Nurse Shark *Ginglymostoma cirratum**, Journal of Morphology, Volume 269; pp. 1041-1055, doi: 10.1002/jmor.10626
- Motta P.J., Maslanka M., Hueter R.E., Davis R.L., de la Parra R., Mulvany S.L., Habegger M.L., Strother J.A., Mara K.R., Gardiner J.M., Tyminski J.P. & Zeigler L.D., 2010, *Feeding anatomy, filter-feeding rate, and diet of whale sharks *Rhincodon typus* during surface ram filter feeding off the Yucatan Peninsula, Mexico*, Zoology, Volume 113, pp. 199-212, doi: 10.1016/j.zool.2009.12.001
- Motta P.J. & Huber D.R., 2012, *Prey Capture Behavior and Feeding Mechanics of Elasmobranchs* IN: *Biology of Sharks and Their Relatives – Second Edition*. Editors: J.C. Carrier, J.A. Musick and M.R. Heithaus, CRC Press, Taylor & Francis Group, Florida, ISBN 978-1-4398-3926-3
- Nakaya K., Matsumoto R. & Suda K., 2008, *Feeding strategy of the megamouth shark *Megachasma pelagios* (Lamniformes: Megachasmidae)*, Journal of Fish Biology, Volume 73, pp. 17-34, doi: 10.1111/j.1095-8649.2008.01880.x
- Nakaya K., Tomita T., Suda K. Sato K., Ogimoto K., Chappell A. Sato T., Takano K. & Yuki Y., 2016, *Slingshot feeding of the goblin shark *Mitsukurina owstoni* (Pisces: Lamniformes: Mitsukurinidae)*, Scientific Report, Volume 6, pp. 1-10, doi: 10.1038/srep27786
- Nauwelaerts S., Wilga C., Sanford C. & Lauder G., 2006, *Hydrodynamics of prey capture in sharks: effects of substrate*, Journal of the Royal Society Interface, Volume 4, pp. 341-345, doi: 10.1098/rsif.2006.0180
- Ramsay J.B., 2012, *A comparative investigation of cranial morphology, mechanics, and muscle function in suction and bite feeding sharks*, Dissertation University of Rhode Island, UMI Number 3526224, ProQuest LLC.

- Smith B.G., 1937, *The Anatomy of the frilled shark Chlamydoselachus anguineus* Garman IN: The Bashford Dean Memorial Volume Archaic Fishes, Part 2. Editor: E.W. Gudger, Published by the Trustees of the American Museum of Natural History, New York
- Tricas T.C., 1985, *Feeding Ethology of the White Shark, Carcharodon carcharias*, Memoirs of the Southern California Academy of Sciences, Volume 9, pp. 81-91
- Veran M., 1995, *Are the labial cartilages of Chondrichthyens homologous to the labial bone of the primitive fossil Actinopterygians?*, Geobios, M.S. Volume 19, pp. 161-166
- Vélez-Zuazo X. & Agnarsson I., 2011, *Shark tales: A molecular species-level phylogeny of sharks (Selachimorpha, Chondrichthyes)*, Molecular Phylogenetics and Evolution, Volume 58, pp. 207-217, doi: 10.1016/j.jmpev.2010.11.018
- Wainwright P.C., McGee M.D, Longo S.J. & Hernandez L.P., 2015, *Origins, Innovations, and Diversification of Suction Feeding in Vertebrates*, Integrative and Comparative Biology, Volume 55, Number 1, pp. 134-145, doi: 10.1093/icb/icv026
- Wilga C.D., Wainwright P.C. & Motta P.J., 2000, *Evolution of jaw depression mechanics in aquatic vertebrates: insights from Chondrichthyes*, Biological Journal of the Linnean Society, Volume 71, pp. 165-185, doi: 10.1006/bijl.2000.0436
- Wilga C.D., 2002, *A functional analysis of jaw suspension in elasmobranchs*, Biological Journal of the Linnean Society, Volume 75, pp. 483-502,
- Wilga C.D., Motta P.J. & Sanford C.P., 2007, *Evolution and ecology of feeding in elasmobranchs*, Integrative and Comparative Biology, Volume 47, Number 1, pp. 55-69, doi: 10.1093/icb/icm029
- Wu E.H., 1994, *Kinematic Analysis of Jaw Protrusion in Orectolobiform Sharks: A New Mechanism for Jaw Protrusion in Elasmobranchs*, Journal of Morphology, Volume 222, pp. 175-190

# **CHAPTER 2: GROWTH TRAJECTORIES OF PRENATAL**

## **EMBRYOS OF THE DEEP-SEA SHARK**

### ***CHLAMYDOSELACHUS ANGUINEUS***

### **(CHONDRICHTHYES)**

#### **Author Information**

López-Romero F.<sup>1\*</sup>, Klimpfinger C.<sup>2</sup>, Tanaka S.<sup>3</sup> & Kriwet J.<sup>4</sup>

<sup>1</sup> Dr. Faviel Alejandro López-Romero, Department of Paleontology, University of Vienna, Vienna, Austria

\* Corresponding Author: Faviel A. López-Romero faviel.alejandro.lopez.romero@univie.ac.at

<sup>2</sup> Dr. Sho Tanaka, Faculty of Marine Science and Technology, Tokai University, Shizuoka Shimizu-ku, Japan

<sup>3</sup> Claudia Klimpfinger MSc.MEd., Department of Paleontology, University of Vienna, Vienna, Austria

<sup>4</sup> Prof. Dr. Jürgen Kriwet, Department of Paleontology, University of Vienna, Vienna, Austria

Own contributions: I developed this project together with my colleague (F.A. L.-R.) and our supervisor (J. K.). I conducted linear measurements, for which I chose characteristic landmarks and took the measurements from digital photographs which included a scale. I carried out statistical analysis using Microsoft Excel (which were later adapted to R by my colleague for unity reasons). I contributed to the staging by describing the pigmentation and the dimensions of eyes, jaws and body in coherence with the linear measurements taken before. I wrote parts of the introduction, the material and results part concerning the linear measurements, as well as parts of the staging and the discussion.

#### **Bibliography**

López-Romero F.A., Klimpfinger C., Tanaka S. & Kriwet J., 2020, Growth trajectories of prenatal embryos of the deep-sea shark *Chlamydoselachus anguineus* (Chondrichthyes), Journal of Fish Biology, Volume 97, pp. 212-224, doi: 10.1111/jfb.14352



Processing status: Published





# Growth trajectories of prenatal embryos of the deep-sea shark

## *Chlamydoselachus anguineus* (Chondrichthyes)

Faviel A. López-Romero<sup>1</sup>  | Claudia Klimpfinger<sup>1</sup> | Sho Tanaka<sup>2</sup> | Jürgen Kriewel<sup>1</sup> 

<sup>1</sup>Department of Paleontology, University of Vienna, Vienna, Austria

<sup>2</sup>School of Marine Science and Technology, Faculty of Marine Science and Technology, Tokai University, Shizuoka Shimizu-ku, Japan

### Correspondence

Faviel A. López-Romero, Department of Paleontology, University of Vienna, Geozentrum, Althanstrasse 14, 1090 Vienna, Austria.

Email:

faviel.alejandro.lopez.romero@univie.ac.at

### Funding information

Universität Wien

### Abstract

*Chlamydoselachus anguineus*, Garman 1884, commonly called the frilled shark, is a deep-sea shark species occurring up to depths of 1300 m. It is assumed to represent an ancient morphotype of sharks (e.g., terminal mouth opening, more than five gill slits) and thus is often considered to represent plesiomorphic traits for sharks. Therefore, its early ontogenetic developmental traits are important for understanding the evolution of its particular phenotype. Here, we established six stages for prenatal embryos and used linear measurements and geometric morphometrics to analyse changes in shape and size as well as their timing during different embryonic stages. Our results show a change in head shape and a relocation of the mouth opening at a late stage of development. We also detected a negative allometric growth of the head and especially the eye compared to the rest of the body and a sexual dimorphism in total body length, which differs from the known data for adults. A multivariate analysis of covariance shows a significant interaction of shape related to the logarithm of centroid size and developmental stage. Geometric morphometrics results indicate that the head shape changes as a covariate of body size while not accounting for differences between sexes. The growth pattern of stages 32 and 33 indicates a shift in head shape, thus highlighting the moment in development when the jaws start to elongate anteriorly to finally achieve the adult condition of terminal mouth opening rather than retaining the early embryonic subterminal position as is typical for sharks. Thus, the antero-terminal mouth opening of the frilled shark has to be considered a derived feature.

### KEYWORDS

development, frilled shark, geometric morphometrics, jaw development, ontogeny

## 1 | INTRODUCTION

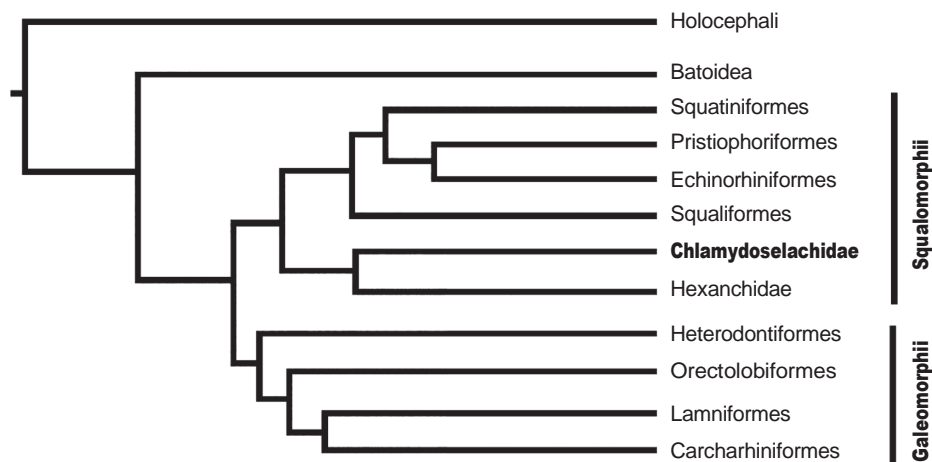
Samuel W. Garman described in 1884 an extraordinary shark, which he named the frilled shark, *Chlamydoselachus anguineus* Garman, 1884. Subsequently, Gudger and Smith (1933) described its anatomy in detail based on four adult females. The first description of its embryonic

development was presented some years later by Gudger (1940). The frilled shark is assigned to its own family, the Chlamydoselachidae (Figure 1), which is believed to be the oldest living family of elasmobranchs (Garman, 1884; Gudger & Smith, 1933; Goto & Hashimoto, 1976; Goto, 1991; Tanaka *et al.*, 1990, 2013), although its affinities with Palaeozoic sharks was cautioned by Maisey and

This is an open access article under the terms of the Creative Commons Attribution License, which permits use, distribution and reproduction in any medium, provided the original work is properly cited.

© 2020 The Authors. Journal of Fish Biology published by John Wiley & Sons Ltd on behalf of The Fisheries Society of the British Isles.

FIGURE 1 Phylogenetic position of *C. anguineus*, simplified after Amaral *et al.* (2017)



Wolfram (1984). The status of various morphological traits (plesiomorphic *versus* apomorphic) in this shark thus remains ambiguous. The embryonic development of elasmobranchs has become a major topic of focus for developmental biologists and also evolutionary palaeobiologists in recent years because it enables researchers to gain deeper insights into plesiomorphic and apomorphic morphologies and often mirrors the species' evolutionary path.

The habitat of the frilled shark is cold waters with a wide but discontinuous distribution where it occurs in water depths between 100 and 1300 m (Compagno, 1984; Shiobara *et al.*, 1987). It is considered a benthopelagic shark feeding on cephalopods, bony fish and even smaller sharks (Kiralı *et al.*, 2000; Kubota *et al.*, 1991). It has an elongated, eel-like body and it grows up to an average total length (TL) of 150 cm with a maximum reported TL of 196 cm (Gudger & Smith, 1933). Maturity is reached at a TL of 100 cm in males and 140 cm in females. Ebert and Compagno (2009) identified the populations around South Africa as separate species, *Chlamydoselachus africana*, that differs from the frilled shark in a smaller number of vertebrae, spiral valve and pectoral fin radial counts.

A prominent characteristic of the frilled shark is its elongated eel-like body, which is very distinctive from other elasmobranch species. The head is dorso-ventrally flattened, and its mouth is the most terminal positioned one in all shark species, except the whale shark *Rhincodon typus*, which is a filter-feeder (Compagno, 1984). The frilled shark bears six gill slits including the first left and right gill slits, which are ventrally connected and form the eponymous frill (Smith, 1937). The number of gill slits is assumed to be a secondary increase in number since in most other shark species only five gill-slits are present, and in the frilled shark the additional arch might have evolved independently from other hexanchoid sharks (Shirai, 1992).

Frilled sharks are aplacental viviparous with a year-round mating and breeding season. Usually there are two to 10 embryos in each litter. They hatch within the mother's uterus when they reach a TL of 5.5 cm and remain there, feeding on their yolk sack until they are born at a TL of 40–60 cm (Tanaka *et al.*, 1990). The gestation period of *C. anguineus* is the longest period known for all vertebrates, lasting 3.5 years, and the growth rate of the embryos is around 10–17 mm

per month (Tanaka *et al.*, 1990), although the gestation period estimation can be as low as 1–2 years (Compagno, 1984; Gudger & Smith, 1933).

The apparent ancient habitus, development and morphology of its teeth were considered in previous studies to better understand early evolutionary patterns in gnathostomes (Goto & Hashimoto, 1976; Goto, 1987; Smith *et al.*, 2018). However, developmental aspects of the external morphology that might provide information on character evolution in this and probably related taxa have not been considered up to now. The relationships between growth and changes in shape are relevant because they have an impact on the phenotypic diversity within species. Identifying the developmental moment when morphological change occurs is of utmost importance to comprehend how specific traits are established and how they vary among individuals. Studies of the ontogeny of morphology illustrate that developmental processes can help to identify constraints in morphological diversities as well as give examples for broader possible morphologies (Bolzan *et al.*, 2015; Cardini & Polly, 2013; Cheverud, 1982; Loy *et al.*, 1998; Openshaw & Keogh, 2014; Zelditch *et al.*, 2000). Despite these effects being more noticeable by comparing different but related species, there are other effects within the same species that could show how a defined shape is acquired. Some of the underlying processes in ontogenetic shape shift involve a decoupling caused by changes throughout the life cycle (Cvijanovic *et al.*, 2014; Loy *et al.*, 1998; McGowan, 1988; Rose *et al.*, 2015; Strauss & Fuiman, 1985) or adaptations to particular feeding mechanisms or behaviours, both of which can influence the morphology of the individual (Bergmann & Motta, 2005; Bolzan *et al.*, 2015; Frédérich *et al.*, 2008; Genbrugge *et al.*, 2011; Meyer, 1990; Russo *et al.*, 2007). Particularly in elasmobranchs these patterns have been unambiguously observed and they contribute to the exploitation of possible resources throughout their life history (Dean *et al.*, 2007; Wilga *et al.*, 2016).

Earlier studies on the development of elasmobranchs have mainly focused on general descriptions of particular body parts and their anatomy (Balfour, 1881; El-Toubi, 1952; Harrison, 1931; Holmgren, 1940; Jollie, 1971). However, only a few have attempted to present a staging system, which is useful for comparisons with other species (Ballard

*et al.*, 1993; Castro & Wourms, 1993; Didier *et al.*, 1998; Rodda & Seymour, 2007; Maxwell *et al.*, 2008; Onimaru *et al.*, 2018). Most recently, studies have focused on post-embryonic developmental traits (Fu *et al.*, 2016; Litherland *et al.*, 2009; Tomita *et al.*, 2018) and underlying developmental mechanisms (Adachi & Kuratani, 2012; Barry & Crow, 2017; Compagnucci *et al.*, 2013; Cooper *et al.*, 2017; Debais-Thibaud *et al.*, 2011; Eames *et al.*, 2007; Freitas *et al.*, 2007; Gillis *et al.*, 2012; O'Shaughnessy *et al.*, 2015). Because of their long generation time and reproduction mode, developmental studies of elasmobranchs are often difficult (Coolen *et al.*, 2008), and the diversity of descriptions on embryonic development consists of sporadic bycatches (Francis & Duffy, 2005; Gilmore *et al.*, 1983; Joung & Hsu, 2005; Tanaka *et al.*, 1990). Staging the development into sequences is fundamental to understand possible mechanisms operating at defined stages, which may have an impact on the phenotypic result. The goal of this study is to present new insights into the developmental changes of several morphological traits, especially the development of the anterior mouth opening in the frilled shark, which differs from the subterminal condition in most other sharks, to better understand the origins of its peculiar appearance.

## 2 | MATERIALS AND METHODS

### 2.1 | Ethical statement

The embryos used for the study were obtained from a survey conducted from 1981 to 1988 in the Suruga Bay, Japan, the samples from which are stored in the University of Shimizu, as described in Tanaka *et al.* (1990). Only individuals preserved in 70% ethanol were used for the analysis, and no tissue sampling or killing was involved in the present study.

### 2.2 | Staging

Since there is no existing staging scheme for embryos of the frilled shark, we used different published information (see below) for comparison and to establish a staging sequence for the embryos. We also assumed that the embryos with the smallest body length are those from early developmental stages whereas the largest individuals are from later developmental stages.

We used 51 embryos (32 females, 19 males) from Suruga Bay, Japan. Forty-three embryos were photographed using a Sony DSC-H9 (Sony Corp., Tokyo, Japan) with a macro lens, whereas the remaining nine individuals were photographed using an Olympus E-3 (Olympus Corp., Tokyo, Japan) camera with a 14–54 mm lens. All the photographs contain a scale next to the objects. Staging of the embryos was conducted by comparison of our individuals with descriptions and drawings from E.W. Gudger (1940) as well as the staging protocol of the lesser spotted dogfish *Scyliorhinus canicula* by Ballard *et al.* (1993) and the staging protocol of the brown-banded bamboo shark *Chiloscyllium punctatum* by Onimaru *et al.* (2018). The lesser spotted dogfish is a galeomorph shark and spends parts of its lifetime in deeper waters too, which is why we chose it, and there is

complete staging of the brown-banded bamboo shark, which made it a useful comparison. The description of the staging of the chimaeroid fish *Callorhynchus milii* by Didier *et al.* (1998) was used for a comparison of the embryonic development of elasmobranchs with their sister group, the Holocephali, providing possibly another ancient morphotype. Accordingly, we identified categories from stage 31 up to stage 36. For each stage the following number of individuals was used: stage 31 ( $n = 1$ ; female), stage 32 ( $n = 3$ ; 2 females, 1 male), stage 33 ( $n = 8$ ; 5 females, 3 males), stage 34 ( $n = 10$ ; 9 females, 1 male), stage 35 ( $n = 14$ ; 9 females, 5 males), stage 36 ( $n = 15$ ; 6 females, 9 males).

### 2.3 | Measurements

Linear measurements were defined by 11 landmarks set on each individual giving eight measuring distances (Figure 2a). The landmarks were chosen to be characteristic points, which can be identified easily in every picture. For the statistics and growth comparisons the TL was used as independent variable and values for body length (BL), head length (HL), caudal fin length (CF), upper jaw (UJ), lower jaw (LJ), and the diameter of the eye in vertical (EV) and horizontal (EH) plane were plotted and regressed to the predicted value using the package basicTrendline (Mei *et al.*, 2018) for R Cran 3.6.1 (2019).

### 2.4 | Geometric morphometric analyses

A subset of 22 embryos out of the original sample of 51 specimens was chosen for subsequent analysis of shape with geometric morphometrics, since this subset presented no bending deformation that could lead to biased results in the shape. The number of individuals of each stage for this analysis were: stage 32 ( $n = 2$ ), stage 33 ( $n = 4$ ), stage 34 ( $n = 3$ ), stage 35 ( $n = 4$ ), stage 36 ( $n = 9$ ). The shapes were defined according to two-dimensional landmarks and semi-landmarks, and the landmark coordinates were digitized using tpsDIG2 v.2.18 (Rohlf, 2002) (Figure 2b,c). The landmark coordinates were digitized twice on each individual and subject to a principal component analysis (PCA) to assess the accuracy of landmark capture.

Each subset of landmark coordinates was aligned by a generalized Procrustes superimposition as implemented in geomorph (v. 3.0.5) R package (Adams & Otárola-Castillo, 2013). This method eliminates differences in size, position and orientation, and leaves only shape variation remaining for the analysis (Rohlf & Slice, 1990). Because each subset of landmark coordinates contains several semi-landmarks the variation regarding its position along the curve was assessed considering the minimum bending energy between the target shape and the mean shape (Gunz and Mitteroecker, 2013). After superimposition, the Procrustes coordinates were used for a PCA to visualize the sources of variation in the specimens. Thin-plate spline deformation grids were included to assist in illustrating the changes in shape from the mean along each PC axis as well as the minimum and maximum

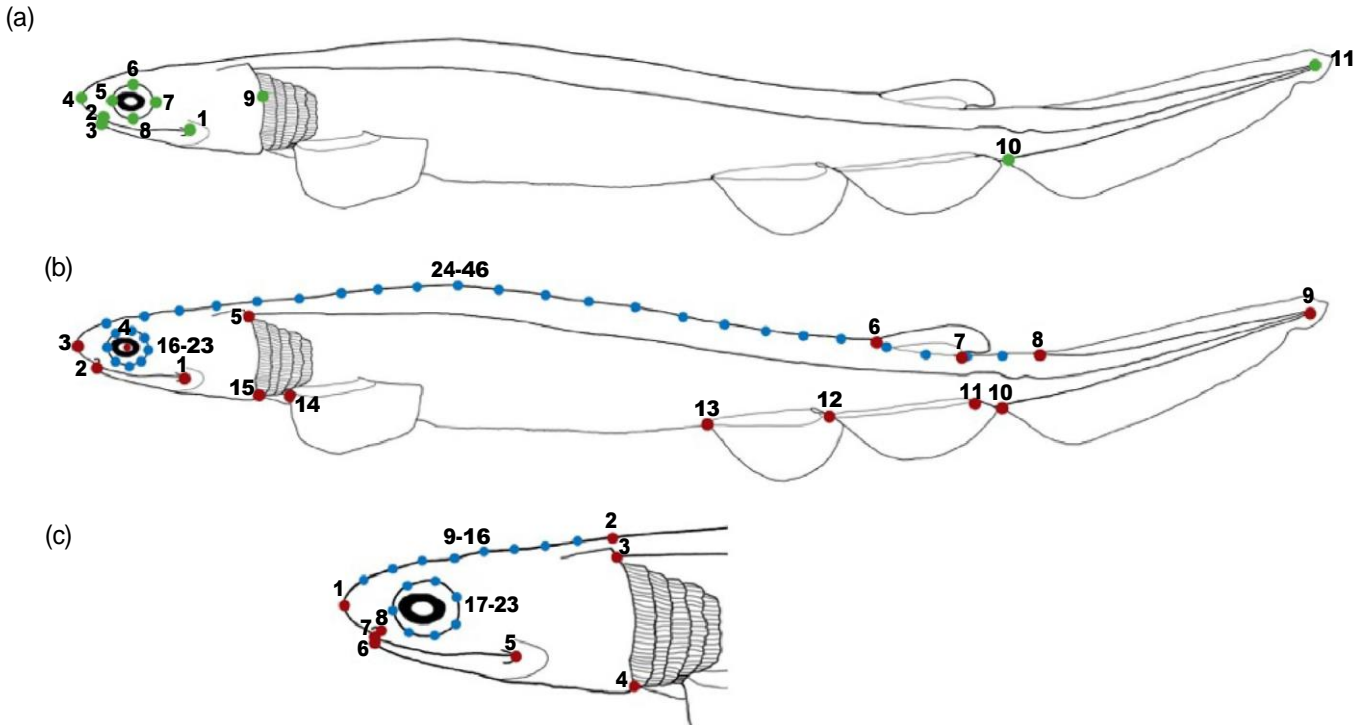


**FIGURE 2** Position of the landmarks defined to estimate the variation in linear measurements and shape in *C. anguineus*. (a) Linear measurements landmarks (green dots): 1–2, upper jaw length; 1–3, lower jaw length; 4–9, head length; 5–7, eye diameter horizontal; 6–8, eye diameter vertical; 9–10, body length; 10–11, caudal fin length; 4–11, total length. (b) Body landmarks (red dots = landmarks; blue dots = semi-landmarks): 1, labial cartilage articulation; 2, rostral edge of lower jaw; 3, rostrum; 4, eye center; 5, lateral line-frill origin conjunction; 6, anterior insertion of dorsal fin; 7, posterior insertion of dorsal fin; 8, anterior insertion of caudal fin; 9, caudal fin posterior end; 10, anterior-ventral insertion of caudal fin; 11, posterior insertion of anal fin; 12, anterior insertion of anal fin; 13, anterior insertion of pelvic fin; 14, anterior insertion of pectoral fin; 15, ventral origin of frill; 16–23, eye perimeter; 24–46, dorsal profile. (c) Head of *C. anguineus* embryo at stage 36 of development. The eight landmarks (red dots) and 15 semilandmarks (blue dots) are indicated in the corresponding anatomical positions: 1, rostrum; 2, posterior dorsal edge of head; 3, posterior dorsal side of frill; 4, posterior ventral side of frill; 5, labial cartilage articulation; 6, rostral edge of lower jaw; 7, rostral edge of upper jaw; 8, nostril; 9–16, dorsal craniofacial profile; 17–23, eye circumference

along those axes. The variation of head and body shape related to the size of the embryo was estimated by a multivariate analysis of covariance (MANCOVA) using the information of size as the logarithm of the centroid size (the square root of the sum of the squared distances of all the landmark coordinates), developmental stages, sex and the interactions between these variables. For statistical significance Goodall's F-ratio and randomized residual permutation procedure (10,000 iterations) were used (Collyer *et al.*, 2015). Significance in the interaction terms with (Shape ~ log(Csize)\*Stage) and (Shape ~ log(Csize)\*Sex) were interpreted as a difference in allometric trajectories between the stages or sexes of the individuals. A pairwise test for slope homogeneity was conducted with the advanced.procD.lm function in geomorph when the interactions were significant to assess the slope changes between developmental stages. Statistical significance rejecting the null hypothesis for a common slope was assessed by permutation using 10,000 iterations. The pairwise comparison of stage angle slopes was estimated in degrees. The shape change associated with the developmental stage was observed as a function of the regression of shape on the log-transformed centroid size. The slopes of each developmental stage were plotted as the predicted shape scored against the log-transformed centroid size.

### 3 | RESULTS

#### 3.1 | Stages

##### 3.1.1 | Stage 31

The LJ barely reaches the posterior end of the eye while the UJ extends to about the middle of the eye. The head shape is rounded, and pigmentation starts to surround the eye. The pectoral and pelvic fins are formed, with the pelvic fins being broader than the pectoral fins. No trace of the median fin fold is found in between the unpaired fins (Figure 3a). Embryos described by Gudger (1940) do not correspond to this size in morphology since the mouth of the described embryos are still in the diamond shape stage. The closer ones resembling the indicated stage are 32–34 mm

##### 3.1.2 | Stage 32

The LJ starts protruding and the rostrum starts to change its position from its former ventral position to a more dorsal, anterior-pointing



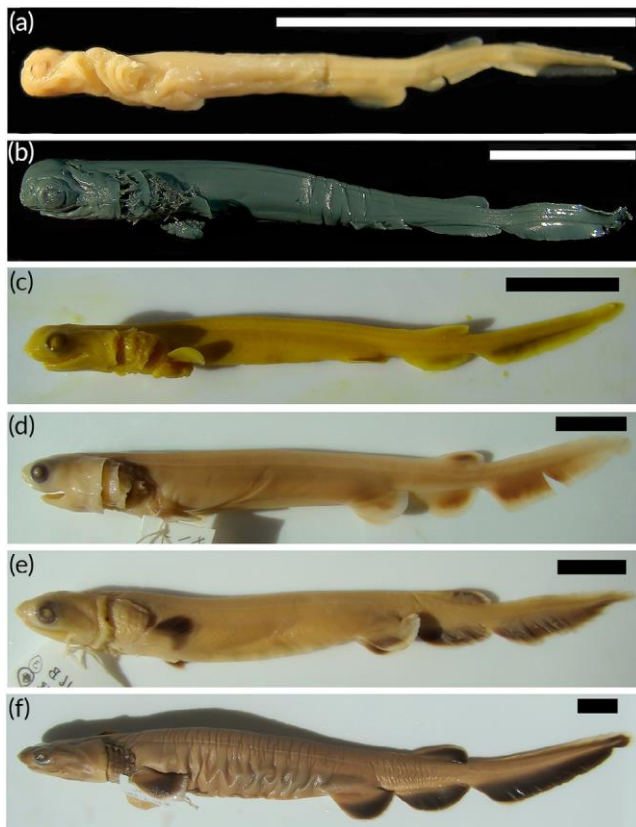


FIGURE 3 Fixed embryos of *C. anguineus* representing the developmental stages: (a) stage 31, (b) stage 32, (c) stage 33, (d) stage 34, (e) stage 35, and (f) stage 36. Scale bars: 20 mm

position. Eye pigmentation becomes darker and surrounds the lens completely; still there is no pigmentation on the body. The pectoral and pelvic fins are longer than in the previous stage and the dorsal and anal fins are already well developed and separated from the caudal fin. All the unpaired fins start to show slight pigmentation along the margins. Small gill filaments are visible and there is a slight frilling on gills two to six (Figure 3b). Approximately corresponding to Gudger (1940) these embryos have a TL of 54–55 mm.

### 3.1.3 | Stage 33

The jaws are recognizably longer compared to the previous stage. The LJ extends anteriorly to the margin of the eye. The head is smaller and more compact, and the snout depicts a slightly pointed shape in a lateral view with the rostrum pointing anteriorly. The eyes are completely pigmented now, and the unpaired fins show an incipient dark pigmentation. Both paired fins (pectoral and pelvic) become longer and take in adult shapes, including an upcoming dark pigmentation on the margins. The caudal fin appears to turn upwards. There are no external gill filaments recognizable anymore. The lateral line starts to appear (Figure 3c). The embryos depicted by Gudger (1940) are heavily deformed; the closest one described appears to correspond to the 66 mm embryo.

### 3.1.4 | Stage 34

Both jaws are extending forward, surpassing eye level, and meanwhile have nearly the same length. The snout is now blunter and points straight forward. The body becomes pigmented with a brownish shade. Pectoral and pelvic fins elongate and become broader, the lower caudal lobe already shows the adult form. The body, between pectoral and pelvic fins, becomes more elongated (Figure 3d). The embryo described by Gudger (1940) at 103 mm could correspond in morphology to this stage.

### 3.1.5 | Stage 35

The LJ almost reaches its terminal position. The snout is pointed in lateral view and the nasal capsules are in their final positions. The bases of the paired fins are well developed and the dorsal and anal fins are already similar to the ones seen in adults. The lateral line system is more defined than in the stages before but not completely developed yet. Frills are occurring on the first gill (Figure 3e). The embryo at 124 mm by Gudger (1940) is the most similar.

### 3.1.6 | Stage 36

The mouth opening now reaches its final terminal position. The head is slightly dorso-ventrally compressed and the snout is more prominent. The body pigmentation is now complete and more intense than before with the fins (both paired and unpaired) being darker than the body. Paired fins now also reach their adult shape and the unpaired fins have grown a little broader to reach final shape, including the appearance of the terminal notch in the caudal fin. Frills are well visible and detected on all gills and the lateral line is clearly defined (Figure 3f). The embryos from 185 to 240 mm described by Gudger (1940) correspond to this stage.

## 3.2 | Analysis of linear measurements

The 51 measured embryos generally show an allometric growth pattern in most of the measured distances. Starting with the means of the TL we have to acknowledge that there are more females than males in this sample with the smallest and the biggest individual both being females. Still, males are significantly bigger than the females ( $t$ -test,  $P = 0.03$ ) (Figure 4a). The same applies to many measured distances, which undergo an elongation during development (e.g., BL and CF) (Figure 4a). Analysing the distribution of lengths between head (defined by LM 4 and 9), body (defined by LM 9 and 10) and tail (defined by LM 10 and 11) it is noticeable that the head is the shortest body part, which also elongates the least.

The body, understood as everything between head and tail, is the longest part with the highest tendency to further growth (Figure 4b), and grows proportionally at the same rate as the CF, while the HL also keeps growing but at a lower rate compared to the BL and

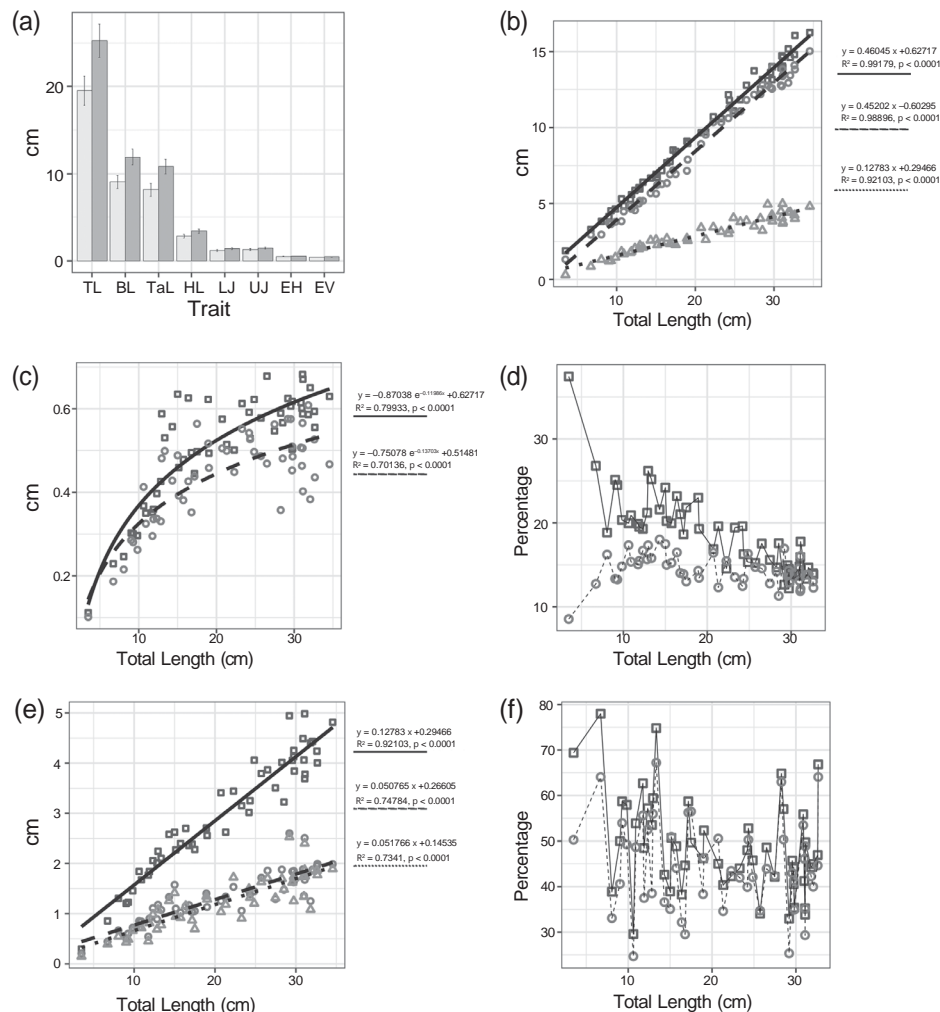


**FIGURE 4** Linear measurement analysis of the embryos of *C. anguineus*. (a) Averages with standard error bars for each of the linear measurements from the landmarks described in Figure 2a Sex (□) Female, (▣) Male. (b) Relation of the BL, CF and HL as a variable of the total length (□) BL, (◊) CF, (Δ) HL. (c) Eye length in both horizontal and vertical diameter. (□) EH, (○) EV. (d) Proportion changes of the eye diameter and head length through development. (□) EH-%HL, (◊) HL-%TL. (e) Length growth of the head, and upper and lower jaw (□) HL, (◊) UJ, (Δ) LJ. (f) Growth of the upper and lower jaw as percentage of the head length. (□) UJ-%HL, (○) LJ-%HL. BL, body length; CF, caudal fin length; HL, head length; EH, eye diameter horizontal; EV, eye diameter vertical; EH-%HL, eye diameter horizontal percentage of head length; HL-%TL, head length percentage of total length; UJ, upper jaw length; LJ, lower jaw length; UJ-%HL, upper jaw percentage of head length; LJ-%HL, lower jaw percentage of head length

CF. Comparing the EV to the EH, a slight elliptical shape on the horizontal axis can be noticed, which might increase in postnatal development (Figure 4c). When considering the EH as a percentage of HL, it is noticeable that the eye in relation to the head decreases in size while the head continues to grow in relation to the TL (Figure 4d).

Analysing the growth rate of the mouth opening in connection with the growth of the head it seems that the jaws grow at a relatively slower rate compared to the head. There is a visible difference between the UJ and the LJ at all times, with the UJ being always longer than the LJ, resulting in a constant gap. These differences, however, are not noticeable in the proportion of the UJ and LJ to the HL as a function of the TL (Figure 4e). On average the UJ is 0.1 cm longer than the LJ, but this is not significant ( $P > 0.5$ ). Both jaws appear to grow little through the measured developmental stages. Furthermore, a convergence of the jaw as a percentage of the head is discernible in

both parts of the jaw (Figure 4f). This would lead, according to the linear trend, to closure of the gap between UJ and LJs, with both of them reaching the same length.

### 3.3 | Shape variation of body and head

Estimating the ratio of the mean squares of the individuals and replicates from a nested ANOVA showed a repeatability of 0.97. A discriminant function analysis on the replicate measurements after a PCA revealed that each capture session could not be assigned as different groups ( $P = 0.5$ ) (Supporting Information Figure S1). The PCA shows that for both the body and the head configuration the PC1 and PC2 account for over 81.9% and 62.7%, respectively, of the total variation (Figure 5). For the body shape, the PC1 is related to the dorsal

curvature and the upwards position of the caudal fin tip. However, this shape change might be related to the bending effect of preservation. Nevertheless, the positive values of PC1 shows that the later stages (34, 35 and 36) are grouped in this area, while the earliest stages share the negative side of PC1 (Figure 5a). The Unbend function in tpsUtil was tried in an attempt to eliminate the deformation effect, but without success. PC2 also describes shape changes similar as in PC1. In this case the deformation effects also seem to be part of the preservation bending, with some differences between developmental stages. Earlier stages seem to have a more straightened dorsal side of the body, which might tend to curve as development proceeds. Since these effects could not be removed from the analysis, we focused mainly on the head shape configuration for further analysis.

The head shape along PC1 describes a more rounded craniofacial profile on the negative values (Figure 5b), a longer distance from the origin of the maxilla to the preorbital region, and the postorbital region of the head appears to be elongated as development progresses. The UJ and LJ also elongate. In the earlier stages, the anterior tips are positioned slightly at the middle of the eye, and as development continues the tips extend anteriorly to surpass the anterior margin of the orbit. The shift in the elongation of the jaws is first recognizable with the UJ. At earlier stages, the UJ starts to protrude along with the rostrum while the LJ only reaches the terminal position

at around stages 34 and 35. Both jaw tips are at the same terminal position at stage 36.

The orbit also appears to be larger in earlier developmental stages in relation to the BL, but appears to slow its growth in the later stages. Later shape changes during development become more apparent in a more straightened frontonasal profile with the tip of the rostrum turning upwards and also a longer postorbital region. PC2 describes the position of the eye from the middle to a more dorsal location and a more flattened head shape, although this is not reflected as a shape change related to a particular developmental stage. The head shape was not sufficient to determine sexual dimorphism among the individuals analysed (Supporting Information Figure S2). However, since the sampling size for each stage does not include both sexes for all the developmental stages, the morphospace might not be accurate. Perhaps the inclusion of more male specimens for the earlier stages might provide a better picture to investigate possible sexual dimorphism patterns in the future.

### 3.4 | Head allometry variation

Since there were differences in the head shape related to developmental stage, a MANCOVA was performed to examine interactions between shape, size, stage and sex (Table 1). The head shape

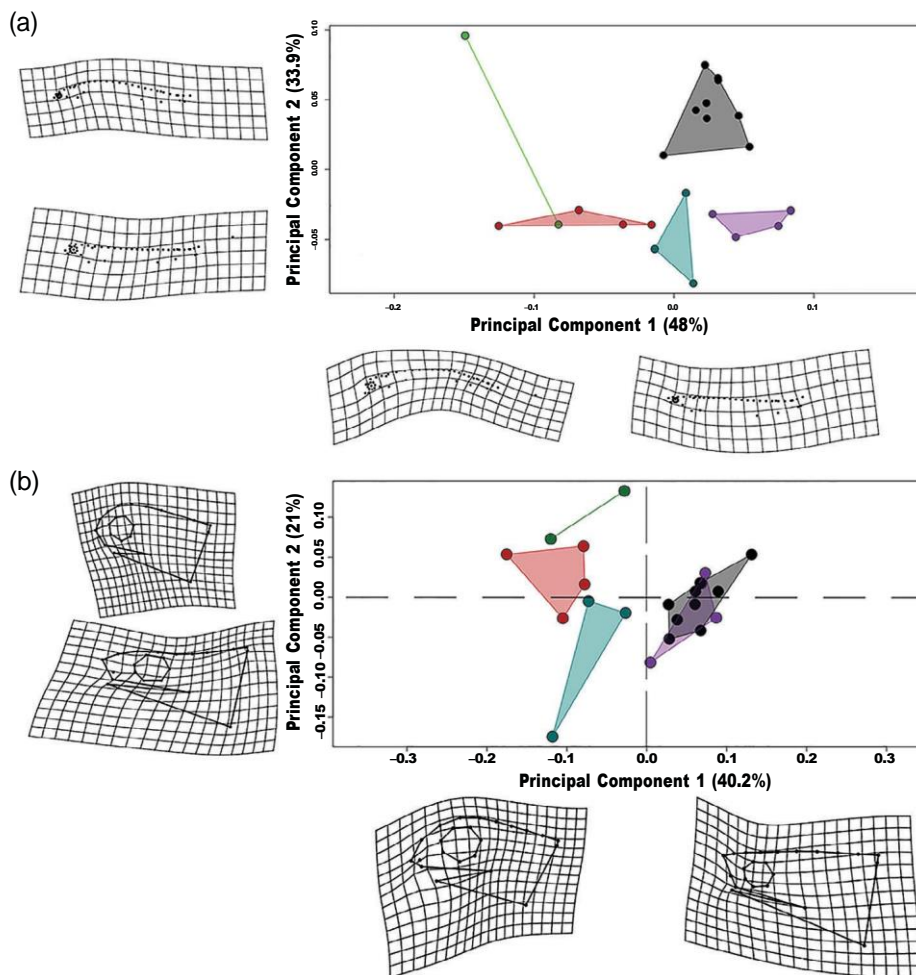


FIGURE 5 PCA of the body and head shape variation in *C. anguineus*. (a) Body shape variation due to deformation effects by the preservation of the individuals. (b) Head shape variation among frilled shark embryos through development. Colours indicate the developmental stage: (●) stage 32; (●) stage 33; (●) stage 34; (●) stage 35; (●) stage 36

differences are mainly explained by size ( $r^2 = 0.397$ ) and developmental stage ( $r^2 = 0.162$ ). The significant interactions of size and developmental stage in both configurations suggest that allometric slopes might differ between developmental stages. When we compared this covariation of head shape assuming the sex as an important factor and its interaction to the centroid size, we observed that the interaction is slightly significant (Table 1). The allometric slope plots show that some developmental stages differ in the intercept and that the intercept of later stages takes place in the upward  $y$  axis (Figure 6). After the confirmation of significant interactions between size and developmental stages and also sex (Table 1), a pairwise slope test was conducted to reveal divergence points during the development of the head shape or if there was an effect of sexual dimorphism related to size and shape. The results suggest that the earliest stages are the ones where the shape starts to shift (stages 32 and 33), and we noticed changes in most traits of the head, like the upward shift of the rostrum and the onset of jaw protrusion. However, there were no differences between the sexes and probably other characters could be more useful in the compared stages (Table 2). Taking the Procrustes distances from the mean configuration of the individuals plotted against the PC1 scores revealed that the earlier stages are the ones with the highest variation in shape, and as development progresses the later stages tend to converge towards the mean shape and their variation is reduced overall (Figure 7).

#### 4 | DISCUSSION

The characters selected for the definition of the developmental stages follow the definitions of morphological-based landmarks rather than a time- or length-based system. This is due to the variable gestation periods between several elasmobranch species (Ballard *et al.*, 1993; Didier *et al.*, 1998; Maxwell *et al.*, 2008; Rodda & Seymour, 2007), with the frilled shark having probably the longest gestation period of up to 3.5 years (Tanaka *et al.*, 1990). Overall the stages were well defined and subsequent analyses reflected the grouping of the individuals belonging to their respective stage. Since it is assumed that the frilled sharks represent a basal elasmobranch group, the introduction of a

staging scheme and the subsequent description of the development of specific traits is of particular interest to understand the origin of its peculiar morphology. Some of the most noticeable changes are related to the development of the jaws and the rostrum. While almost all other elasmobranch species display a ventrally, subterminally located mouth opening, which reaches its final position at a quite early stage [around stage 28 in catsharks and bamboo sharks (Ballard *et al.*, 1993; Onimaru *et al.*, 2018)], the rather terminal positioned mouth opening in the frilled shark starts to move to its future position at stages 31–32 and reaches the final position near the end of the embryonic development. In the winter skate *Leucoraja ocellata*, Maxwell *et al.* (2008) point out that the change in the position of the jaws starts at an even earlier stage (stage 27) and that this shift in timing can be related to the specialized dorso-ventrally flattened body shape.

Other characters such as the paired and unpaired fins seem to be more variable throughout development. We were not able to detect a median fin fold from which the unpaired fins develop (Mabee *et al.*, 2002). However, it is expected that by the time of the formation of the pectoral and pelvic fins this structure might already be absent (Witten & Huysseune, 2007). Several studies point at specific events during ontogeny where certain shape changes occur and are central for particular adaptations (Genbrugge *et al.*, 2011; McGowan, 1988; Meyer, 1990; Rose, 2009; Russo *et al.*, 2007). We observed in our sample a larger shape variation in the early stages and we were able to estimate the moment of morphologic convergence to one defined specific morphology. Finally, the staging of the frilled shark embryos will allow further comparisons with other elasmobranch species at similar stages to improve the understanding of character evolution.

Sexually related dimorphism in body size is known in several groups of vertebrates (Adkins-Regan & Reeve, 2014; Arak, 1988; da Silva *et al.*, 2017; Francis & Duffy, 2005; Malmgren and Tholleson, 1999; Monnet & Cherry, 2002; Rogers *et al.*, 2017; Woolbright, 1983). Elasmobranchs tend to display sexual dimorphism in size (Francis & Duffy, 2005; Rogers *et al.*, 2017; Rolim *et al.*, 2015; Semba *et al.*, 2011) and even in specific characters like the mouth shape of the small-spotted catshark, which is, for example, longer and narrower in males than females (Ellis and Shackley, 1995). In some species, like the Caribbean

TABLE 1 Covariance of shape and size related to ontogenetic changes (stages) and sex of the individuals

Head shape	Df	SS	MS	$R^2$	$F$	$P$
log (Csize)	1	0.20022	0.200216	0.39715	17.2306	0.0001
Stage	4	0.08204	0.020511	0.16274	1.7651	0.0002
log (Csize):Stage	4	0.08244	0.020611	0.16353	1.7737	0.0001
Residuals	12	0.13944	0.011620			
Total	21	0.50414				
log (Csize)	1	0.12443	0.124434	0.31974	9.7884	0.0001
Sex	1	0.01469	0.014686	0.03774	1.1553	0.1165
log(Csize):Sex	1	0.02123	0.021229	0.05455	1.6699	0.0201
Residuals	18	0.22882	0.012712			
Total	21	0.38917				

Note. Df, degrees of freedom; SS, sum of squares; MS, mean squares;  $R^2$ , coefficient of determination;  $F$ ,  $F$  ratio;  $P$ ,  $P$  value. Bold indicates significant  $P$  values.



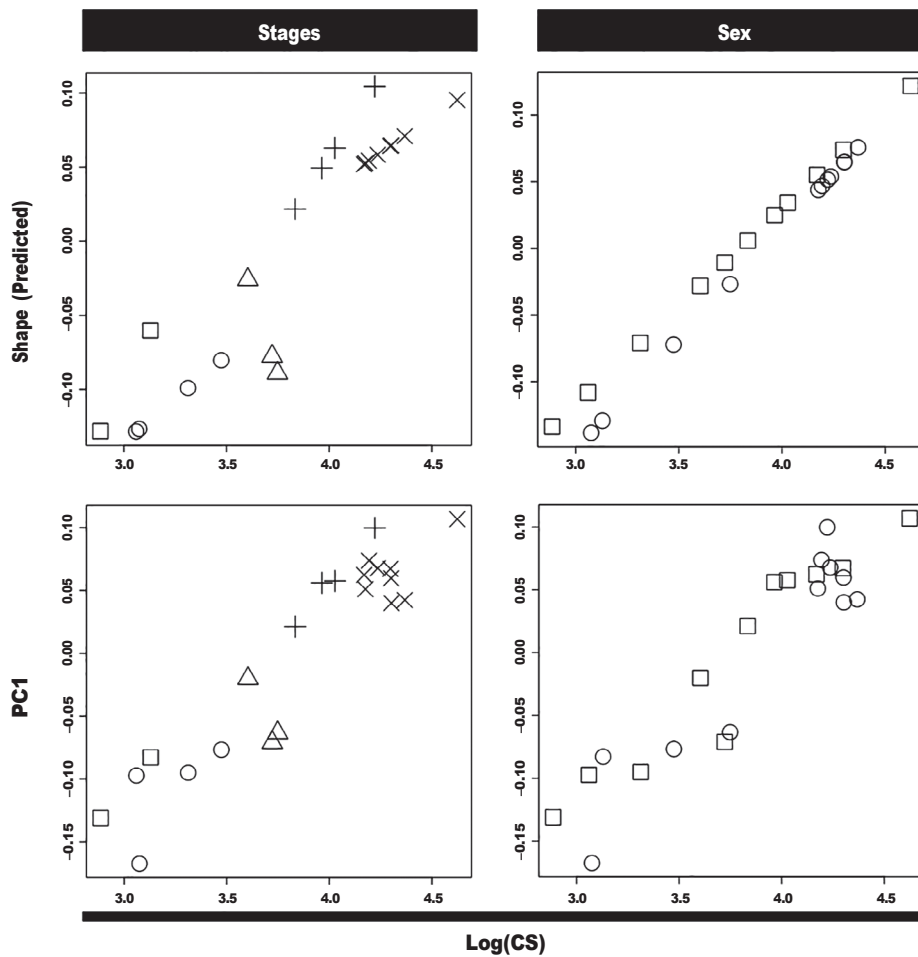


FIGURE 6 Allometric slopes and shape variation of the head of *C. anguineus* as a function of logarithm of centroid size. Both developmental stages and sex are compared. (□) stage 32; (○) stage 33; (△) stage 34; (+) stage 35; (×) stage 36; (□) female (○) male

	Stage 32	Stage 33	Stage 34	Stage 35	Stage 36
Stage 32	—	<i>0.0138</i>	0.6098	0.3613	<i>0.0082</i>
Stage 33	79.75450	—	0.1869	0.2159	0.9095
Stage 34	130.76903	101.16381	—	0.3618	0.1973
Stage 35	81.77449	108.39498	108.2021	—	0.1835
Stage 36	62.84690	83.97788	114.0396	81.93991	—

Note. Upper half (cut diagonally) indicates *P* values and lower half indicates angles. Significant *P* values reported in bold.

TABLE 2 Pair-wise *post hoc* test of allometric slope angles between stages and sexes of the individuals

sharpnose shark *Rhizoprionodon porosus* or the smalltail shark *Carcharhinus porosus*, several measurements of head, body and fins indicate that males are generally larger than females (Barbosa Martins *et al.*, 2015). In the case of the frilled shark linear measurements of adults (adulthood being defined by sexual maturity) indicate that females, conversely, are generally larger than the males without this difference in size being particularly noticeable at birth (Tanaka *et al.*, 1990). Both sexes still experience the same shape changes during development, which is displayed by the nonsignificant difference between their allometric slopes.

The linear measurements in our sample show that the males are significantly larger than the females even though there was a larger

number of females in the sample, including the largest and smallest individuals. This discrepancy in total BL between the embryonic or newly born female and the sexually mature one leads us to the suggestion that females either grow faster or that they grow over a longer period of time before reaching sexual maturity. As a trend, deep-sea elasmobranch species have lower growth rates, greater longevity and late age at maturity (Rigby & Simpfendorfer, 2013). In a paper by Girard and Du Buit (1999) a comparison of the growth rate differences between sexes of two viviparous deep sea shark species – the Portuguese dogfish *Centroscyrmus coelolepis* and the leafscale gulper shark *Centrophorus squamosus* – was drawn and showed that the females were larger in TL in both embryonic stages and as adults.

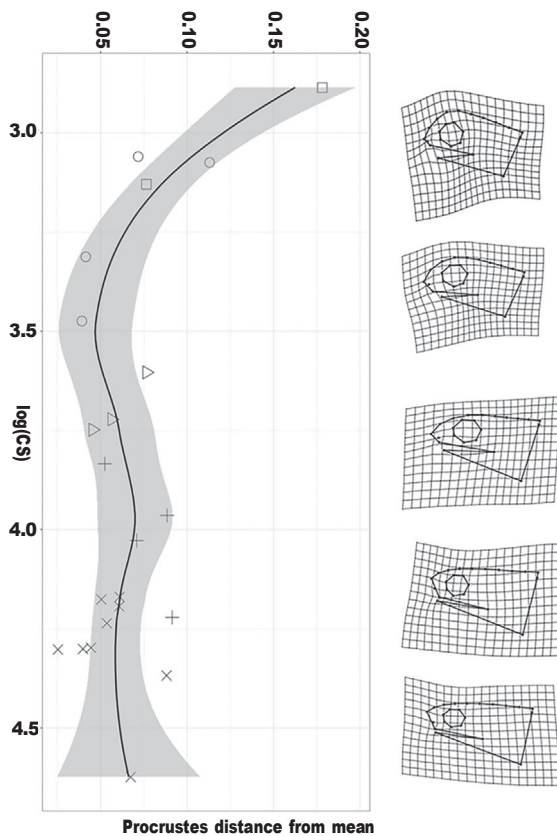


FIGURE 7 Shape divergence of the head of *C. anguineus* as a function of Procrustes distance from mean to the logarithm of centroid size (solid line; grey shading = 95% confidence interval) of the head shape through the development. (○) stage 32; (△) stage 33; (×) stage 34; (+) stage 35; (×) stage 36

From our samples we cannot observe this difference clearly since at later stages the sample size is not large enough to display such trends.

The eye diameter was measured vertically and horizontally and showed only a very small amount of growth in both distances from the smallest to the largest embryo, reaching a plateau, which might continue its growth at a slower pace throughout the life of the individuals. Litherland *et al.* (2009) showed that eye growth differs significantly between the sandbar shark *Carcharhinus plumbeus*, which inhabits coastal waters, and the shortspine spurdog *Squalus mitsukurii*, which inhabits deeper waters of the continental shelf. In their paper Litherland *et al.* (2009) suggest that the growth through lifetime takes place due to constant adaptations to the current surrounding of the individual. Perhaps the eyes of the frilled shark present this pattern since there is only little light in the water depths at which they live. The eye size of the frilled shark, in percentage of the head of recently hatched individuals of different size, could provide more support on its possible adaptations.

The jaws elongate quite constantly with the growth of the head, as shown by their length measurements. The constant difference of UJ and LJ (the LJ being the shorter one) leads to an observable gap, which can be detected in every stage and is also known from adult individuals (Smith, 1967). From our results, the loss of the gap can neither be observed in late embryonic stages nor in adults and is

probably a deviation due to skewed effect. Nonetheless a shrinking of the size of the gap between the two jaws is detectable during development, displayed in lateral view.

The craniofacial traits are of particular interest because many species have an observable trend that helps to explain the developmental basis of particular adaptations according to the development of the craniofacial traits (Ahi, 2016; Eames & Schneider, 2008; Hall *et al.*, 2014). Morphological changes within the same elasmobranch species previously were detected by functional analysis of the feeding apparatus. The displayed shifts in individuals were related to a change of diet during ontogeny, which also involved a change in size and bite performance of the feeding apparatus (Fahle and Thomason, 2008; Fu *et al.*, 2016; Huber *et al.*, 2008; Lowry & Motta, 2008; Wilga *et al.*, 2016). In some cases, similar morphologies of different species seemingly evolved multiple times independently (Dean *et al.*, 2007). However, most of these changes occur during postnatal development and reflect trends the juveniles experience while growing up. While analysing the jaw growth of the frilled shark we noticed that the shape changes and elongation of the jaws occur later in embryonic development, compared with other elasmobranch species, and continue up to the latest stage we analysed. Although the frilled shark has been positioned as a primitive form of elasmobranch (Goto & Hashimoto, 1976), several studies suggest that some of its characters (especially the jaw suspension and number of gill slits) could be derived (Amaral *et al.*, 2017; Bustamante *et al.*, 2016; Soares and de Carvalho, 2013; Tanaka *et al.*, 2013). The developmental

sequence of jaws in other species could shed light on the changes we observed, since – as pointed out by Maxwell *et al.* (2008) in *Leucoraja ocellata* – some of these derived features can occur at earlier stages, as in the case of the jaws. It is noteworthy, however, that the jaws start to develop in a subterminal position as is typical for most sharks, but reach a terminal position late in development through anterior elongation of the jaws.

The caudal fin is another interesting structure as it appears not to change its shape at all throughout the stages we analysed. It has been reported that the caudal fin shape changes in other species like the tiger shark, *Galeocerdo cuvier*, the great white shark, *Carcharodon carcharias*, and the spiny dogfish, *Squalus acanthias* (Fu *et al.*, 2016; Reiss & Bonnan, 2010; Tomita *et al.*, 2018), which might reflect a shift in function towards their apex predator niche or possibly a bio-mechanical response to swimming mode. We found that in the frilled shark the caudal fin seems to experience only very little change in shape. However, since our sample comprises prenatal individuals only, it is possible that the caudal fin experiences shape changes after birth. Therefore, we cannot assess if certain prenatal shape constraints are related to deep-sea adaptations for sure or if there are changes in postnatal development to give the frilled shark its specialized phenotype.

## 5 | CONCLUSIONS

We present for the first time a comparison of the embryos of the aplacental viviparous deep-sea frilled shark through several stages,

which serves as a reference point for further studies among other elasmobranch species. The characters we analysed highlight the changes that the frilled shark experience in prenatal ontogeny. Although the changes appear to be remarkable, it should be kept in mind that the gestation period in this species is one of the longest known. Nevertheless, by using the size as a proxy of developmental time, we can estimate that overall some traits change relatively fast while others change at a slower pace. The highly variable shape in earlier stages and the subsequent convergence towards the mean shape is prominent and suggests a tendency to reduce its variability when the organism approaches a terminal stage in development. Regarding the sexual dimorphism, a difference in the mean TL was detected that differs from the size dimorphism in mature individuals. This character might display growth variation within postnatal individuals and might continue throughout the lifespan of this shark. Finally, a set of traits that could be useful to determine a general adaptation to deep-sea environments is difficult to assess, but further studies on eye development might provide new insights. Furthermore, we provide additional evidence that suggests that the terminal position of the jaws in elasmobranchs could be a derived trait rather than a plesiomorphic condition as is generally assumed.

#### ACKNOWLEDGEMENTS

We are grateful to Dr Brian Metscher at the Theoretical Biology Department in the Universität Wien for additional material for earlier stages of the frilled shark. We also thank two anonymous reviewers whose comments helped to improve the manuscript.

#### AUTHORS' CONTRIBUTIONS

F.A.L.-R., C.K. and J.K. conceived/designed the study. C.K. and F.A.L.-R. collected the raw data and performed the analyses. F.A.L.-R., C.K., J.K. and S.T. wrote the manuscript. All authors gave final approval for publication.

#### ORCID

Favie A. López-Romero  <https://orcid.org/0000-0001-6500-0747>

Jürgen Kriwet  <https://orcid.org/0000-0002-6439-8455>

#### REFERENCES

- Adachi, N., & Kuratani, S. (2012). Development of head and trunk mesoderm in the dogfish, *Scyliorhinus torazame*: I. Embryology and morphology of the head cavities and related structures. *Evolution and Development*, 14, 234–256.
- Adams, D. C., & Otarola-Castillo, E. (2013). Geomorph: An R package for the collection and analysis of geometric morphometric shape data. *Methods in Ecology and Evolution*, 4, 393–399.
- Adkins-Regan, E., & Reeve, H. K. (2014). Sexual dimorphism in body size and the origin of sex determination systems. *American Naturalist*, 183, 519–536.
- Ahi, E. P. (2016). Signalling pathways in trophic skeletal development and morphogenesis: Insights from studies on teleost fish. *Developmental Biology*, 420(1), 11–31.
- Amaral, C. R. L., Pereira, F., Silva, D. A., Amorim, A., & de Carvalho, E. F. (2017). The mitogenomic phylogeny of the Elasmobranchii (Chondrichthyes). *Mitochondrial DNA Part A*, 20, 1–12.
- Arak, A. (1988). Sexual dimorphism in body size: A model and a test. *Evolution*, 42, 820–825.
- Balfour, F. (1881). On the development of the skeleton of the paired fins of Elasmobranchii, considered in relation to its bearing on the nature of the limbs of the vertebrata. *Proceedings of the Zoological Society of London*, 1881, 662–671.
- Ballard, W. W., Mellinger, J., & Lechenault, H. (1993). A series of normal stages for development of *Scyliorhinus canicula*, lesser spotted dogfish (Chondrichthyes: Scyliorhinidae). *Journal of Experimental Zoology*, 267, 318–336.
- Barbosa Martins, A. P., da Silva Filho, E., Manir Feitosa, L., Nunes e Silva, L. P., da Silva de Almeida, Z., & Silva Nunes, J. L. (2015). Sexual dimorphism of sharks from the Amazonian equatorial coast. *Universitas Scientiarum*, 20(3), 297–304.
- Barry, S. N., & Crow, K. D. (2017). The role of HoxA11 and HoxA13 in the evolution of novel fin morphologies in a representative batoid (*Leucoraja erinacea*). *EvoDevo*, 8, 24.
- Bergmann, G. T., & Motta, P. J. (2005). Diet and morphology through ontogeny of the nonindigenous Mayan cichlid '*Cichlasoma (Nandopsis)*' *urophthalmus* (Günther 1862) in southern Florida. *Environmental Biology of Fishes*, 72, 205–211.
- Bolzan, D. P., Pessôa, L. M., Peracchi, A. L., & Strauss, R. E. (2015). Allometric patterns and evolution in Neotropical nectar-feeding bats (Chiroptera, Phyllostomidae). *Acta Chiropterologica*, 17, 59–73.
- Bustamante, C., Bennett, M. B., & Ovenden, J. R. (2016). Genotype and phylogenomic position of the frilled shark *Chlamydoselachus anguineus* inferred from the mitochondrial genome. *Mitochondrial DNA Part B*, 1 (1), 18–20.
- Cardini, A., & Polly, P. D. (2013). Larger mammals have longer faces because of size-related constraints on skull form. *Nature Communications*, 4, 2458.
- Castro, J. I., & Wourms, J. P. (1993). Reproduction, placentation, and embryonic development of the Atlantic sharpnose shark, *Rhizoprionodon terraenovae*. *Journal of Morphology*, 218, 257–280.
- Cheverud, J. M. (1982). Relationships among ontogenetic, static, and evolutionary allometry. *American Journal of Physical Anthropology*, 59, 139–149.
- Collyer, M. L., Sekora, D. J., & Adams, D. C. (2015). A method for analysis of phenotypic change for phenotypes described by high-dimensional data. *Heredity*, 115, 357–365.
- Compagno, L. J. V. (1984). *Sharks of the world. An annotated and illustrated catalogue of shark species known to date* (Vol. 4). Rome: FAO of the United Nations.
- Compagnucci, C., Debais-Thibaud, M., Coolen, M., Fish, J., Griffin, J. N., Bertocchini, F., ... Depew, M. J. (2013). Pattern and polarity in the development and evolution of the gnathostome jaw: both conservation and heterotopy in the branchial arches of the shark, *Scyliorhinus canicula*. *Developmental Biology*, 377, 428–448.
- Coolen, M., Menuet, A., Chassoux, D., Compagnucci, C., Henry, S., Lévêque, L., Da Silva, C., Gavory, F., Samain, S., Wincker, P., Thermes, C., D'Aubenton-Carafa, Y., Rodriguez-Moldes, I., Naylor, G., Depew, M., Sourdain, P., & Mazan, S. (2008). The dogfish *Scyliorhinus canicula*: A reference in jawed vertebrates. *CSH Protocols*, pdb. emo111, 431–446.
- Cooper, R. L., Martin, K. J., Rasch, L. J., & Fraser, G. J. (2017). Developing an ancient epithelial appendage: FGF signaling regulates early tail denticle formation in sharks. *EvoDevo*, 8, 8.
- Cvijanovi, c, M., Ivanovi, c, A., Kalezi, c, M. L., & Zelditch, M. L. (2014). The ontogenetic origins of skull shape disparity in the *Triturus cristatus* group. *Evolution and Development*, 16, 306–317.
- da Silva, F. A. M., Silva de Oliveira, L., Souza Nascimento, L. R., Andrade Machado, F., & Costa Prudente, A. L. (2017). Sexual dimorphism and ontogenetic changes of Amazonian pit vipers (*Bothrops atrox*). *Zoologischer Anzeiger*, 271, 15–24.
- Dean, M. N., Bizzarro, J. J., & Summers, A. P. (2007). The evolution of cranial design, diet and feeding mechanisms in batoid fishes. *Integrative and Comparative Biology*, 47, 70–81.
- Debais-Thibaud, M., Oulion, S., Bourrat, F., Laurenti, P., Casane, D., & Borday-Birraux, V. (2011). The homology of odontodes in gnathostomes: insights from *Dlx* gene expression in the dogfish, *Scyliorhinus canicula*. *BMC Evolutionary Biology*, 11, 307.

- Didier, A. D., Leclair, E. E., & Vanbuskirk, D. R. (1998). Embryonic staging an external features of development of the Chimaeroid Fish, *Callorhynchus milii* (Holocephali, Callorhynchidae). *Journal of Morphology*, 236, 25–47.
- Eames, B. F., Allen, N., Young, J., Kaplan, A., Helms, J. A., & Schneider, R. A. (2007). Skeletogenesis in the swell shark *Cephaloscyllium ventriosum*. *Journal of Anatomy*, 210, 542–554.
- Eames, B. F., & Schneider, R. A. (2008). The genesis of cartilage size and shape during development and evolution. *Development*, 135, 3947–3958.
- Ebert, D. A., & Compagno, L. J. V. (2009). *Chlamydoselachus africana*, a new species of frilled shark from southern Africa (Chondrichthyes, Hexanchiformes, Chlamydoselachidae). *Zootaxa*, 2173, 1–18.
- Ellis, J. R., & Shackley, S. E. (1995). Ontogenetic changes and sexual dimorphism in the head, mouth and teeth of the lesser spotted dogfish. *Journal of Fish Biology*, 47, 155–164.
- El-Toubi, M. R. (1952). The development of the chondrocranium of the spiny dogfish, *Acanthias vulgaris* (*Squalus acanthias*). Part I. Neurocranium, mandibular and hyoid arches. *Journal of Morphology*, 84, 227–279.
- Fahle, S. R., & Thomason, J. C. (2008). Measurement of jaw viscoelasticity in newborn and adult lesser spotted dogfish *Scyliorhinus canicula* (L., 1758). *Journal of Fish Biology*, 72, 1553–1557.
- Francis, M. P., & Duffy, C. (2005). Length at maturity in three pelagic sharks (*Lamna nasus*, *Isurus oxyrinchus*, and *Prionace glauca*) from New Zealand. *Fishery Bulletin*, 103(3), 489–500.
- Frédérich, B., Adriaens, D., & Vandewalle, P. (2008). Ontogenetic shape changes in Pomacentridae (Teleostei, Perciformes) and their relationships with feeding strategies: a geometric morphometric approach. *Biological Journal of the Linnean Society*, 95, 92–105.
- Freitas, R., Zhang, G., & Cohn, M. J. (2007). Biphase Hoxd gene expression in shark paired fins reveals an ancient origin of the distal limb domain. *PLoS One*, 2, e754.
- Fu, A. L., Hammerschlag, N., Lauder, G. V., Wilga, C. D., Kuo, C. Y., & Irschick, D. J. (2016). Ontogeny of head and caudal fin shape of an apex marine predator: the tiger shark (*Galeocerdo cuvier*). *Journal of Morphology*, 277, 556–564.
- Garman, S. (1884). An extraordinary shark. *Bulletin of the Essex Institute*, 16, 47–55.
- Genbrugge, A., Heyde, A., Adriaens, D., Boone, M., Van Hoorebeke, L., Dirckx, J., ... Herrel, A. (2011). Ontogeny of the cranial skeleton in a Darwin's finch (*Geospiza fortis*). *Journal of Anatomy*, 219, 115–131.
- Gillis, J. A., Modrell, M. S., & Baker, C. V. (2012). A timeline of pharyngeal endoskeletal condensation and differentiation in the shark, *Scyliorhinus canicula*, and the paddlefish, *Polyodon spathula*. *Journal of Applied Ichthyology*, 28, 341–345.
- Gilmore, R. G., Dodrill, J. W., & Linley, P. A. (1983). Reproduction and embryonic development of the sand tiger shark, *Odontaspis taurus* (Rafinesque). *Fishery Bulletin*, 81, 201–225.
- Girard, M., & Du Buit, M. H. (1999). Reproductive biology of two deep-water sharks from the British Isles, *Centroscymnus coelolepis* and *Centrophorus squamosus* (Chondrichthyes: Squalidae). *Journal of the Marine Biological Association of the United Kingdom*, 79, 923–931.
- Goto, M. (1987). *Chlamydoselachus anguineus*—A living cladodont shark. *Report of Japanese Society for Elasmobranch Studies*, 23, 11–13.
- Goto, M. (1991). Evolutionary trends of the tooth structure in Chondrichthyes. In S. Suga & H. Nakahara (Eds.), *Mechanisms and phylogeny of mineralization in biological systems* (pp. 447–451). Tokyo: Springer.
- Goto, M., & Hashimoto, I. (1976). Studies on the teeth of *Chlamydoselachus anguineus*, a living archaic fish. I. On the morphology, structure and composition of the teeth. *Japanese Journal of Oral Biology*, 18(3), 362–377.
- Gudger, E. W. (1940). The breeding habits, reproductive organs, and external embryonic development of *Chlamydoselachus* based on notes and drawings left by Bashford Dean. In E. W. Gudger (Ed.), *The Bashford Dean memorial volume: Archaic fishes* (pp. 525–633). New York, NY: American Museum of Natural History.
- Gudger, E. W., & Smith, B. G. (1933). The natural history of the frilled shark, *Chlamydoselachus anguineus*. In E. W. Gudger (Ed.), *The Bashford Dean memorial volume: Archaic fishes* (pp. 243–330). New York, NY: American Museum of Natural History.
- Gunz, P., & Mitteroecker, P. (2013). Semilandmarks: a method for quantifying curves and surfaces. *Hystrix*, 24, 103–109.
- Hall, J., Jheon, A. H., Ealba, E. L., Eames, B. F., Butcher, K. D., Mak, S. S., ... Schneider, R. A. (2014). Evolution of a developmental mechanism: species-specific regulation of the cell cycle and the timing of events during craniofacial osteogenesis. *Developmental Biology*, 385, 380–395.
- Harrison, B. M. (1931). Developmental stages of the chondrocranium in some selachians. *Journal of Morphology*, 52, 565–592.
- Holmgren, N. (1940). Embryological, morphological, and phylogenetical researches. *Acta Zoologica*, 21, 51–266.
- Huber, D. R., Claes, J. M., Mallefet, J., & Herrel, A. (2008). Is extreme bite performance associated with extreme morphologies in sharks? *Physiological and Biochemical Zoology*, 82, 20–28.
- Jollie, M. (1971). Some developmental aspects of the head skeleton of the 35–37 mm *Squalus acanthias* foetus. *Journal of Morphology*, 133, 17–40.
- Joung, S. J., & Hsu, H. H. (2005). Reproduction and embryonic development of the shortfin mako, *Isurus paucus* Rafinesque, 1810, in the northwestern Pacific. *Zoological Studies*, 44, 487–496.
- Kirali, S. J., Moore, J. A., & Jasinski, P. H. (2000). Deepwater and other sharks of the U.S. Atlantic Ocean exclusive economic zone. *Marine Fisheries Review*, 65(4), 1–63.
- Kubota, T., Shiobara, Y., & Kubodera, T. (1991). Food habits of the frilled shark *Chlamydoselachus anguineus* collected from Suruga Bay, central Japan. *Nippon Suisan Gakkaishi*, 57, 15–20.
- Litherland, L., Collin, S. P., & Fritsches, K. A. (2009). Visual optics and ecomorphology of the growing shark eye: a comparison between deep and shallow water species. *Journal of Experimental Biology*, 212, 3583–3594.
- Lowry, D., & Motta, P. J. (2008). Relative importance of growth and behaviour to elasmobranch suction-feeding performance over early ontogeny. *Journal of the Royal Society Interface*, 5, 641–652.
- Loy, A., Mariani, L., Bertelletti, M., & Tunesi, L. (1998). Visualizing allometry: geometric morphometrics in the study of shape changes in the early stages of the two-banded sea bream, *Diplodus vulgaris* (Perciformes, Sparidae). *Journal of Morphology*, 237, 137–146.
- Mabee, P. M., Crotwell, P. L., Bird, N. C., & Burke, A. C. (2002). Evolution of median fin modules in the axial skeleton of fishes. *Journal of Experimental Zoology*, 294, 77–90.
- Maisey, J. G., & Wolfram, K. (1984). Notidanus. In N. Eldredge & S. M. Stanley (Eds.), *Living Fossils* (pp. 170–180). New York, NY: Springer.
- Malmgren, J. C., & Thollessen, M. (1999). Sexual size and shape dimorphism in two species of newts, *Triturus cristatus* and *T. vulgaris* (Caudata: Salamandridae). *Journal of Zoology*, 249, 127–136.
- Maxwell, E. E., Fröbisch, N. B., & Heppleston, A. C. (2008). Variability and conservation in late chondrichthyan development: ontogeny of the winter skate (*Leucoraja ocellata*). *The Anatomical Record*, 291, 1079–1087.
- McGowan, C. (1988). Differential development of the rostrum and mandible of the swordfish (*Xiphias gladius*) during ontogeny and its possible functional significance. *Canadian Journal of Zoology*, 66, 496–503.
- Mei, W., Yu, G., Lai, J., Rao, Q., & Umezawa, Y., (2018). basicTrendline: Add Trendline and Confidence Interval of Basic Regression Models to Plot. R package version 2.0.3.
- Meyer, A. (1990). Morphometrics and allometry in the trophically polymorphic cichlid fish, *Cichlasoma citrinellum*: Alternative adaptations and ontogenetic changes in shape. *Journal of Zoology*, 221, 237–260.
- Monnet, J. M., & Cherry, M. I. (2002). Sexual size dimorphism in anurans. *Proceedings of the Royal Society of London (B) Biological Sciences*, 269, 2301–2307.
- Onimaru, K., Motone, F., Kiyatake, I., Nishida, K., & Kuraku, S. (2018). A staging table for the embryonic development of the brownbanded bamboo shark (*Chiloscyllium punctatum*). *Developmental Dynamics*, 247, 712–723.
- Openshaw, G. H., & Keogh, J. S. (2014). Head shape evolution in monitor lizards (*Varanus*): interactions between extreme size disparity, phylogeny and ecology. *Journal of Evolutionary Biology*, 27, 363–373.
- O'Shaughnessy, K. L., Dahn, R. D., & Cohn, M. J. (2015). Molecular development of chondrichthyan claspers and the evolution of copulatory organs. *Nature Communications*, 6, 6698.
- R Core Team (2019). *R: A language and environment for statistical computing*. Vienna, Austria: R Foundation for Statistical Computing.
- Reiss, K. L., & Bonnan, M. F. (2010). Ontogenetic scaling of caudal fin shape in *Squalus acanthias* (Chondrichthyes, Elasmobranchii): A geometric morphometric analysis with implications for caudal fin functional morphology. *The Anatomical Record*, 293, 1184–1191.



- Rigby, C., & Simpfendorfer, C. A. (2013). Patterns in life history traits of deep-water chondrichthyans. *Deep-Sea Research II*, 115, 30–40.
- Rodda, K., & Seymour, R. (2007). Functional morphology of embryonic development in the Port Jackson shark *Heterodontus portusjacksoni* (Meyer). *Journal of Fish Biology*, 72, 961–984.
- Rogers, T. D., Cambiè, G., & Kaiser, M. J. (2017). Determination of size, sex and maturity stage of free swimming catsharks using laser photogrammetry. *Marine Biology*, 164, 213.
- Rohlf, F. J. (2002). *tpsDig, digitize landmarks and outlines, version 1.37*. Stony Brook, NY: Department of Ecology and Evolution, State University of New York.
- Rohlf, F. J., & Slice, D. (1990). Extensions of the procrustes method for the optimal superimposition of landmarks. *Systematic Biology*, 39(1), 40–59.
- Rollim, F. A., Caltabellotta, F. P., Rotundo, M. M., & Vaske-Júnior, T. (2015). Sexual dimorphism based on body proportions and ontogenetic changes in the Brazilian electric ray *Narcine brasiliensis* (von Olfers, 1831) (Chondrichthyes: Narcinidae). *African Journal of Marine Sciences*, 37(2), 167–176.
- Rose, C. (2009). Generating, growing and transforming skeletal shape: insights from amphibian pharyngeal arch cartilages. *BioEssays*, 31, 287–299.
- Rose, C. S., Murawinski, D., & Horne, V. (2015). Deconstructing cartilage shape and size into contributions from embryogenesis, metamorphosis, and tadpole and frog growth. *Journal of Anatomy*, 226, 575–595.
- Russo, T., Costa, C., & Cataudella, S. (2007). Correspondence between shape and feeding habit changes throughout ontogeny of gilthead sea bream *Sparus aurata* L., 1758. *Journal of Fish Biology*, 71, 629–656.
- Semba, Y., Aoki, I., & Yokawa, K. (2011). Size at maturity and reproductive traits of shortfin mako, *Isurus oxyrinchus*, in the western and central North Pacific. *Marine and Freshwater Research*, 62, 20–29.
- Shiobara, Y., Abe, H., & Hioki, K. (1987). Some biological information on the frill shark in Suruga Bay. *Report of the Japan Group for Elasmobranch Studies*, 23, 7–10.
- Shirai, S. (1992). Identity of extra branchial arches in Hexanchiformes (Pisces, Elasmobranchii). *Bulletin of the Faculty of Fisheries Hokkaido University*, 43, 24–32.
- Smith, B. G. (1937). The anatomy of the frilled shark *Chlamydoselachus anguineus* Garman. In E. W. Gudger (Ed.), *The Bashford Dean memorial volume: Archaic fishes* (pp. 331–520). New York, NY: American Museum of Natural History.
- Smith, J. L. B. (1967). The Lizard shark, *Chlamydoselachus anguineus* Garman, in South Africa. *Occasional Papers of the Department of Ichthyology, Rhodes University, South Africa*, 10, 105–115.
- Smith, M. M., Underwood, C., Clark, B., Kriwet, J., & Johanson, Z. (2018). Development and evolution of tooth renewal in neoselachian sharks as a model for transformation in chondrichthyan dentitions. *Journal of Anatomy*, 232, 891–907.
- Soares, M. C., & de Carvalho, M. R. (2013). Comparative myology of the mandibular and hyoid arches of sharks of the order hexanchiformes and their bearing on its monophyly and phylogenetic relationships (Chondrichthyes: Elasmobranchii). *Journal of Morphology*, 274(2), 203–214.
- Strauss, R. E., & Fuiman, L. A. (1985). Quantitative comparisons of body form and allometry in larval and adult Pacific sculpins (Teleostei: Cottidae). *Canadian Journal of Zoology*, 63(7), 1582–1589.
- Tanaka, K., Shiina, T., Tomita, T., Suzuki, S., Hosomichi, K., Sano, K., et al. (2013). Evolutionary relations of Hexanchiformes deep-sea sharks elucidated by whole mitochondrial genome sequences. *BioMed Research International*, 2013, 11.
- Tanaka, S., Shiobara, Y., Syozo, H., Abe, H., Nishi, G., Yano, K., & Suzuki, K. (1990). The reproductive biology of the frilled shark, *Chlamydoselachus anguineus*, from Suruga Bay, Japan. *Japanese Journal of Ichthyology*, 37, 273–291.
- Tomita, T., Toda, M., Miyamoto, K., Oka, S., Ueda, K., & Sato, K. (2018). Development of the lunate-shaped caudal fin in white shark embryos. *The Anatomical Record*, 301, 1068–1073.
- Wilga, C. A., Diniz, S. E., Steele, P. R., Sudario-Cook, J., Dumont, E. R., & Ferry, L. A. (2016). Ontogeny of feeding mechanics in smoothhound sharks: morphology and cartilage stiffness. *Integrative and Comparative Biology*, 56, 442–448.
- Witten, P. E., & Huyseune, A. (2007). Mechanisms of chondrogenesis and osteogenesis in fins. In B. K. Hall (Ed.), *Fins into limbs: Development, evolution and transformation* (pp. 79–92). Chicago, IL: Chicago University Press.
- Woolbright, L. L. (1983). Sexual selection and size dimorphism in anuran amphibia. *American Naturalist*, 121, 110–119.
- Zelditch, M. L., Sheets, H. D., & Fink, W. L. (2000). Spatiotemporal reorganization of growth rates in the evolution of ontogeny. *Evolution*, 54, 1363–1371.

## SUPPORTING INFORMATION

Additional supporting information may be found online in the Supporting Information section at the end of this article.

How to cite this article: López-Romero FA, Klimpfinger C, Tanaka S, Kriwet J. Growth trajectories of prenatal embryos of the deep-sea shark *Chlamydoselachus anguineus* (Chondrichthyes). *J Fish Biol.* 2020;97:212–224. <https://doi.org/10.1111/jfb.14352>



# **CHAPTER 3: COMPARATIVE MORPHOLOGY OF LABIAL CARTILAGES IN SHARKS (CHONDRICHTHYES, ELASMOBRANCHII)**

## **Author Information**

Klimpfinger C.<sup>1\*</sup> & Kriwet J.<sup>2</sup>

<sup>1</sup> Claudia Klimpfinger MSc.MEd., Department of Paleontology, University of Vienna, Vienna, Austria

\*Corresponding Author: Claudia Klimpfinger c.klimpfinger@gmx.at

<sup>2</sup> Prof. Dr. Jürgen Kriwet, Department of Paleontology, University of Vienna, Vienna, Austria

Own contributions: I developed this project together with my supervisor (J. K.). I downloaded published ct-scans of sharks from the platform figshare.com and used the Amira software package to crop the stacks, as well as reconstruct and mark the jaws and labial cartilages within all scans. Furthermore, I introduced the numeration system, used the freeware inkscape to produce sketches and established the morphogroups. Finally, I interpreted the results, wrote the whole manuscript and produced all included figures.

## **Bibliography**

Klimpfinger C. & Kriwet J., 2020, Comparative morphology of labial cartilages in sharks (Chondrichthyes, Elasmobranchii), European Zoological Journal, Volume 87, pp. 741-753, doi: 10.1080/24750263.2020.1844323

Processing status: Published







# Comparative morphology of labial cartilages in sharks (Chondrichthyes, Elasmobranchii)

C. KLIMPFINGER & J. KRIWET



Department of Palaeontology, University of Vienna, Vienna, Austria (Re-

ceived 24 June 2020; accepted 27 October 2020)

## Abstract

During the last years, feeding mechanisms of sharks have been documented mainly based on their stomach contents supplemented by video footages of feeding behaviours in some species. Rare kinematic analyses of shark jaws contributed additionally to our knowledge. However, not all structures important to prey capture in sharks have been investigated yet. Here, we summarize the current knowledge about labial cartilages in sharks and compare them on a morphological base. Labial cartilages are considered a plesiomorph character found in extinct and extant species and their number and size varies a lot between species. We identified labial cartilages in representatives of 27 from 36 shark families and detected different numbers, sizes and forms of labial cartilages, as well as differing positioning along the jaws. The morphology of labial cartilages can help to identify suction-feeding in sharks and to estimate the quality of the suction generated by a species. We were able to summon different shark taxa according to their morphology and positioning of labial cartilages into eight groups, which we consider morphological modules. To determine if these modules bear a phylogenetic signal further testing with rigorous methodologies and more shark species as well as batomorphs needs to be done. This study therefore only can represent a first starting point providing future research pathways.

**Keywords:** Jaws, function, morphogroup, suction, ram-feeding

## Introduction

Sharks form together with rays and skates a monophyletic clade (Neoselachii *sensu* Compagno 1977; Elasmobranchii *sensu* Maisey 2012), with a fossil record probably extending back into the Early Permian (295 mya; Ivanov 2005). This long period of evolution has shaped diverse sets of biological traits that allowed them to develop a wide range of lifestyles and feeding strategies (Compagno 1990; Wilga et al. 2007). The evolution of a large variety of different tooth morphologies (see for instance Cappetta 2012) is considered to be a key feature for their success and allowed modern sharks to explore different food niches from giant plankton feeders like the whale shark (*Rhincodon typus*) via large apex predators like the white shark (*Carcharodon carcharias*) and the tiger shark (*Galeocerdo cuvier*) down to small and highly adapted predators like the cookie-cutter shark (*Isistius brasiliensis*) representing ectoparasites. Most information about their diet is derived from stomach content

analyses (e.g., Strasburg 1963; Braccini 2008; Cabrera-Chávez-Costa et al. 2010; Wieczorek et al. 2018), whereas feeding strategies are known only in few species based on video captured behaviour of popular species or species that can be bred in captivity (e.g. Motta & Wilga 1999, 2001). To reconstruct the feeding strategy of sharks, intense investigations of the jaw and tooth morphologies are obligatory and those structures are studied worldwide in present, but also past species (e.g. Moss 1977; Huber et al. 2005; Compagnucci et al. 2013). However, skeletal features associated with the jaws, like the labial cartilages (LC), which vary in numbers and have different morphologies and sizes, are most often neglected. These LCs, nevertheless, are common features in cartilaginous fishes and were described for both, extant and extinct shark species in the past (e.g., Maisey 1986, 1987; Wu 1994; Veran 1995; Klug et al. 2009), as well as in batoids (e.g., Dean et al. 2006, 2007) and chimaeras (e.g., Dean 1906; Dean et al. 2012). LCs are paired generally elongated skeletal structures located labially to the jaws, spanning the mouth gape at different locations and

Correspondence: C. Klimpfinger, Department of Palaeontology, University of Vienna, Vienna 1090, Austria. Email: [c.klimpfinger@gmx.at](mailto:c.klimpfinger@gmx.at)

© 2020 The Author(s). Published by Informa UK Limited, trading as Taylor & Francis Group.  
This is an Open Access article distributed under the terms of the Creative Commons Attribution License (<http://creativecommons.org/licenses/by/4.0/>), which permits unrestricted use, distribution, and reproduction in any medium, provided the original work is properly cited.

therefore limiting or extending the mouth gape. Reviewing the sparse literature considering LCs suggests that their number and form have an important function in prey capture. At this point two kinds of suction have to be differentiated: on the one hand the inertial suction, which is used to suck in close prey, on the other hand the compensatory suction, which is used to – as the name suggests – compensate for the forward-movement of the actively hunting predator. Both forms of suction comprise a rapid depression of the lower jaw and a connected LC protrusion in species, which have LCs. Also, the size of the mouth gape, which is influenced by the LCs, generally has functional implications for the mode of prey capture, since it was shown that a small, roundish mouth opening combined with a large buccal volume is useful to create effective suction, while a large mouth gape can be connected to ram or biting feeding behaviours (Ferry et al. 2015). There is a wide range of different combinations of all kinds of feeding strategies (ram/biting/ suction) and the LCs play a more or less important role in these feeding behaviours. LCs are either connected to the jaws or freely embedded in the surrounding tissue and their number varies from none to five pairs in extant shark species. Despite the general knowledge about these structures in some selected taxa, it remains ambiguous whether these elements only have functional properties or also include phylogenetic signals. Such phylogenetic considerations, however, are beyond the scope of this paper, which presents a review of the morphology of the LCs in 72 different sharks and complements that with available descriptive information of another 14 species.

### Brief historical review

The origin and also function of LCs have been discussed for almost 150 years. Gegenbauer (1872) considered labial cartilages in chondrichthyan fishes as “vestiges of pre-mandibular visceral arches”, whereas Pollard (1895) assumed that they represent “remains of skeletal supports of a primitive set of oral cirrhi” and compared them to those found in *Amphioxus*. Swertsoff (1916) returned to Gegenbauer's assumption and described the LCs more precisely as “vestiges of 2 segments of visceral arches”. Goodrich (1930), on the other hand, rejected Swertsoff's interpretation of the visceral arch origin, but conversely proposed that the LCs are a secondary structure in gnathostomes and of no great morphological importance at all. Smith

(1937), conversely, hypothesized that the LCs strengthen and mobilize the mouth corners and suggested that they should be described as “extravisceral cartilages of the mandibular arch”. Nevertheless, the function of these skeletal structures continued to be controversial. Veran (1995), for example, considered them to be “without functional utility” and therefore being “in decline” in chondrichthyans, while Motta and Wilga (2001), using sophisticated analyses employing state-of-the-art procedures, were able to identify the role of the LCs in the feeding behaviour of some species and it turned out that they are obviously very important to generate significant suction forces for ingesting possible prey items.

Phylogenetic signals or evolutionary pathways for the origin and distribution of LCs among chondrichthyan fishes also have been suggested. For example chimeroids, representing the sister group to all shark-like chondrichthyans and hybodontiforms, which forms the extinct sister group of Elasmobranchii (extant sharks, rays, skates), have five pairs of LCs (Maisey 1983; Didier 1995) that could be considered as the plesiomorphic condition for chondrichthyans and Klug (2010) hypothesized that two dorsal and two ventral pairs of LCs represent the plesiomorphic condition for modern sharks, which would indicate that LCs were reduced during the evolution of sharks.

### Materials and methods

To identify the number, size and position of LC in sharks, we reviewed the available literature, used published X-ray computed tomography scans provided on figshare.com by Kamminga et al. (2017), and analysed one specimen of *Etmopterus lucifer* and one specimen of *Etmopterus baxteri* using CT-microtomography. The etmopterid CT scans were prepared at the Department of Palaeontology of the University of Vienna with a Bruker Skyscan 1173 Desktop-Micro-CT. This resulted in detailed information on LCs for 86 representatives of 27 shark families (Supplementary Table I). We downloaded CT stacks from figshare.com and used Amira software packages to reconstruct the scanned individuals and to mark the jaws and LCs if there were any detectable. We used the volume-rendering function for a first overview, marked jaws and LCs in the slices using the orthogonal view and the brush-tool and rechecked the tagged areas in the volume-rendering view. Then we employed the surface-rendering tool to search a second time for LCs we might have missed in the first trial. After that we examined similarities in the shape and size and

Table I. Types of labial cartilages (LC) according to their positions (compare Figure 1). The number following LC denotes the element counted from anterior to posterior and from dorsal to ventral. LC 2.1 and LC 3.1 are sub-forms of LC2 and LC3 (see Wu 1994). LC1 = blue, LC2 = green, LC2.1 = yellow, LC3.1 = orange, LC3 = red

<b>LC1:</b> located at the most anterior position along the upper jaw; sometimes connected to the jaw on the anterior end; mostly oriented along anterior-posterior-axis; variable shape
<b>LC2:</b> located between LC1 & LC3 or between LC1 & LC3.1; never connected to the jaw; oriented antero-posteriorly in differing angles to the dorso-ventral axis; shape elongated; forking on the anterior end in <i>Orectolobidae</i>
<b>LC2.1:</b> a segregated part of the forking of LC2; located dorsally of the LC1; never connected to the jaw; orientated antero-posteriorly; slender cartilage only present in <i>Orectolobidae</i>
<b>LC3.1:</b> a segregated part of the LC3; located in the more posterior position along the lower jaw between LC2 & LC3; oriented antero-posteriorly; mostly short and stout
<b>LC3:</b> located at the most anterior position along the lower jaw; often connected to the jaw on the anterior ventral end; oriented antero-posteriorly in differing angles to the dorso-ventral axis; variable shape

manually drew sketches of different types of jaws and their LCs. Next we used the free software inkscape to transform these sketches into a digital format and used the same colour for LCs that we assume to be homologous.

Subsequently, we identified LCs according to their position and introduced a numeration based

on the maximum number of LCs found in extant species and the derivation of sub-categories according to Wu (1994) (Table I; Figure 1). We assembled taxa, in which we identified LCs, in a next step into eight morphogroups based on the number, shape and arrangement of the LCs found (Figure 2(a-h)) and also included taxa with similar jaw-shapes, which are lacking LCs in these morphogroups. Variations of single LC shapes or positions between different species within one morphogroup are coloured with different shadings of the same colour (Figures 1, 2).

## Results

Examination of LCs in sharks in combination with Wu's (1994) description of the segregation of smaller parts from the most frequently detected number of three LCs allows us to introduce a generally usable numeration system for these skeletal elements in sharks. Consequently, it is possible to differentiate between LC1, LC2, LC2.1, LC3.1 and LC3 (Table I). In the following we refer to the Meckel's cartilage as lower jaw and to the palatoquadrate as upper jaw. The most obvious difference between the eight morphogroups relates to the number of LC pairs, which vary from zero to five (in the following, we refer only to LCs on the left side of the jaws as representatives for the paired structures). The eight morphogroups (A to H) combine taxa with similar morphological traits in jaw shape and labial cartilage number, position and

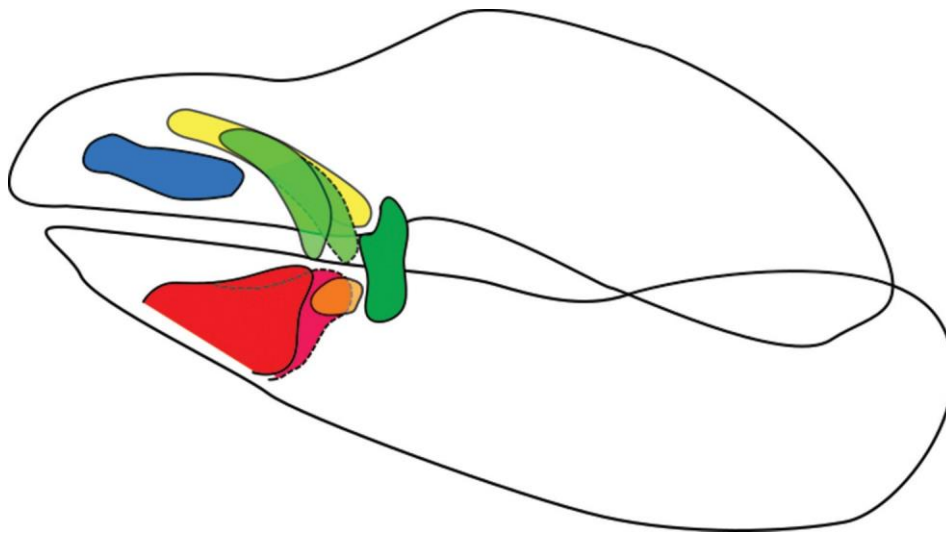


Figure 1. Generalized shark jaws including palatoquadrate and Meckel's cartilage and all possible five labial cartilages in their defined positions (see Table I), as well as their variations by change in number. Blue = LC1, green = LC2, yellow = LC2.1, orange = LC3.1, red = LC3.

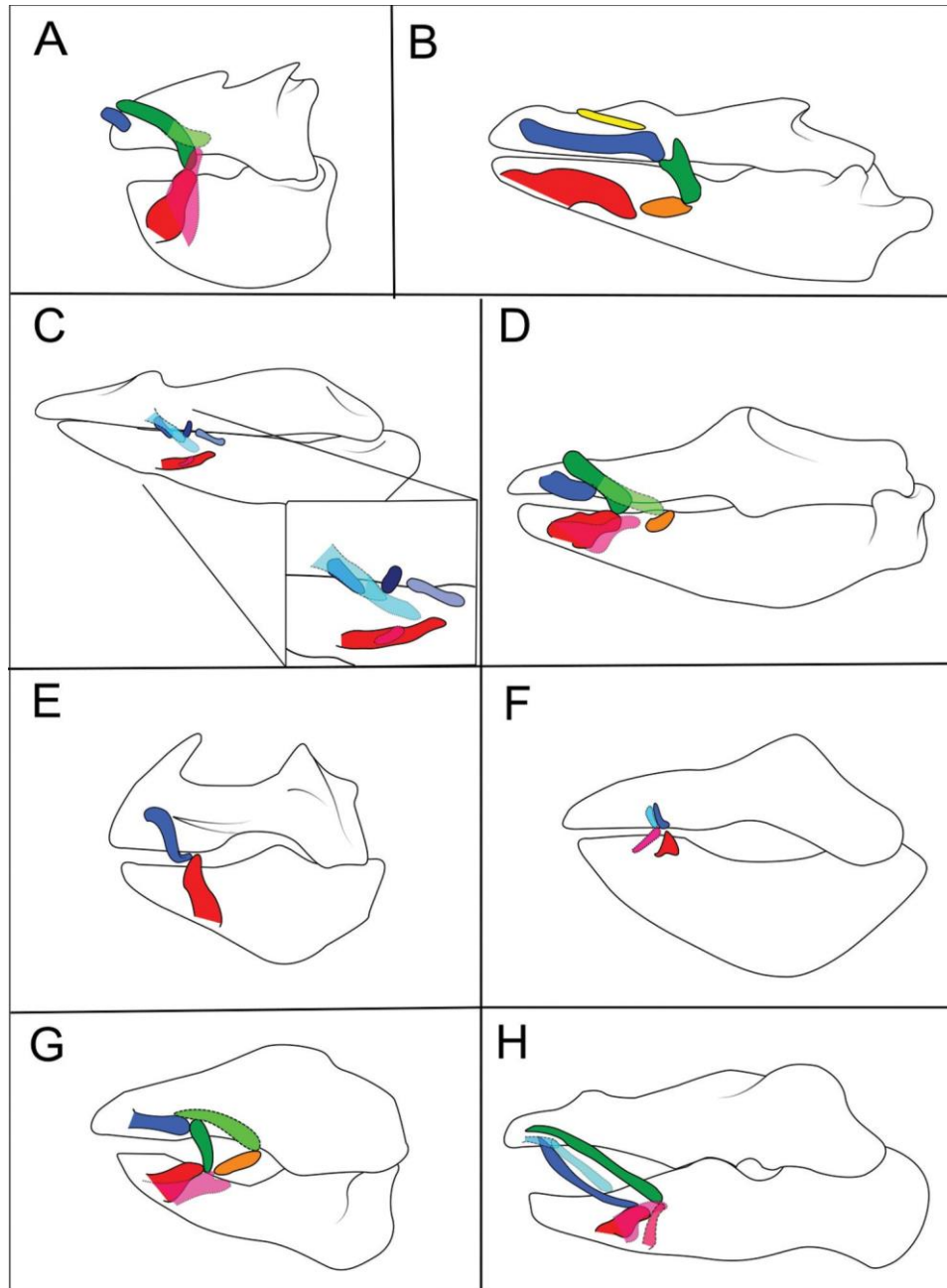


Figure 2. Morphogroups A to H according to the number and morphology of labial cartilages and the shape of the jaws. A = Dalatiidae; B = Orectolobidae; C = Alopiidae, Cetorhinidae, Lamnidae, Megachasmidae, Mitsukurinidae, Odontaspidae, Carcharhinidae, Hemigaleidae, Scyliorhinidae, Sphyrnidae, Triakidae; D = Squatinidae; E = Etmopteridae; F = Heterodontiformes; G = Brachaeluridae, Ginglymostomatidae, Hemiscylliidae, Stegostomatidae, Rhincodontidae, Pristiophoridae; H = Hexanchidae, Chlamydoselachidae, Centrophoridae, Oxinotidae, Somniosidae, Squalidae. Blue = LC1, green = LC2, yellow = LC2.1, orange = LC3.1, red = LC3.

arrangement (Figure 2) and are defined by the combination of jaw shape with the shape and arrangement of the LCs. We found that the highest numbers of LCs (5 or 4 pairs) are restricted to three families of orectolobiforms, namely the

Stegostomatidae with four LCs, the Hemiscylliidae with at least one species displaying also four LCs and the Orectolobidae with five LCs. Also, one species of the Squatinidae, the African angel shark (*Squatina africana*) presents four pairs of LCs.



Three pairs of LCs are the most frequent number of LCs we came across in this study, comprising 23 of the described species, followed by two LC pairs, comprising further 14 species.

Morphogroup A (Figures 2(a) and 3(a)) comprises only members of the squaliform family Dalatiidae, which have a very peculiarly shaped jaw that is antero-posteriorly shorter and dorso-ventrally

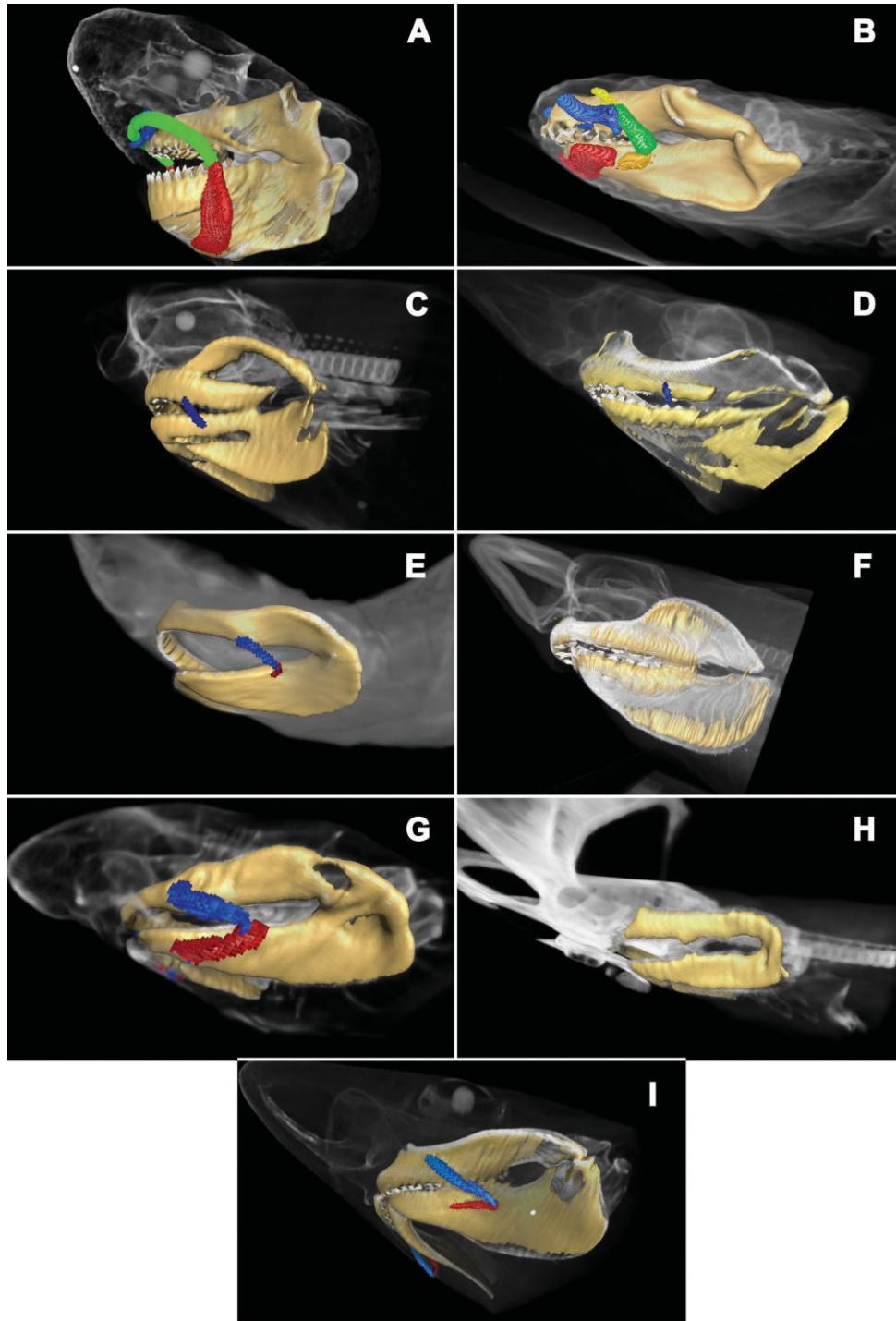


Figure 3. CT-scans of representatives of the morphogroups A to C. Morphogroup A: A = *Dalatias licha*; morphogroup B: B = *Orectolobus japonicus*; morphogroup C: C = *Alopias vulpinus*, D = *Prionace glauca*, E = *Chaenogaleus macrostoma*, F = *Lamna nasus*, G = *Atelomycterus marmoratus*, H = *Sphyrna corona*, I = *Galeorhinus galeus*. Blue = LC1, green = LC2, yellow = LC2.1, orange = LC3.1, red = LC3.

higher than in other taxa. Their LCs also are different from those of the other examined categories: all examined species have three pairs of LCs positioned in one of two possible ways. The “dalatiine” group (sensu Shirai 1992, 1996) displays a comparatively small LC1 that is positioned more anteriorly than in the other groups, almost at the symphysis. A rather long and thick LC2, which overlaps dorso-ventrally at its meeting point above the symphysis, is followed by a broad LC3 that is orientated almost upright dorso-ventrally and is attached to the lower jaw with its broad ventral base. This broad LC3 base narrows down to a tip that has about the same width as the LC2. According to Denton et al. (2018) the pocket shark, *Mollisquama parini*, an “euprotomicrinine” (sensu Shirai 1992, 1996) possesses a longer LC1 that starts dorsal of the symphysis and supports the LC2, which is rather thin, along its full length down to the LC3. The LC3 is of almost steady width along its whole length and is connected on its ventral end to the lower jaw.

Morphogroup B (Figures 2(b) and 3(b)) comprises only members of the family Orectolobidae, which are the only ones with five LCs. Their LC1 is one of the longest of all eight groups. It is broad, bends slightly dorsally on its anterior end and has a short extension pointing ventrally on its posterior end. It lines up with the upper jaw antero-posteriorly, contacts the LC2 on its posterior end but is not connected to the upper jaw at any point. The LC2.1, which only is present in this morphogroup, is a slender and antero-posteriorly elongated cartilage that is a presumably separated segment of LC2 (see Wu 1994). It is located dorsally of the LC1 and does not attach to the upper jaw. LC2 too is unusual in this group for it is oriented nearly vertically and has a furcation on its dorsal end that contacts with the LC1. The LC3.1 is located between LC2 and LC3, is oval shaped and lines up antero-posteriorly with the lower jaw. The LC3 is nearly as broad as the lower jaw’s anterior end and retains this width for almost its complete length. It is connected to the lower jaw by its anteriorly located end and describes a slight, ventrally directed curve up to its contact point with the LC3.1. Wu (1994) stated LCs in all Orectolobidae and described three to four LCs in the spotted wobbegong (*Orectolobus maculatus*).

The number of LCs in Morphogroup C (Figures 2(c), 3(c-i)) ranges from zero to two in carcharhiniform and, according to published information, also in lamniform sharks (Lavenberg & Seigel 1985; Shimada et al. 2009). Ten families are included in this morphogroup: Alopiidae, Cetorhinidae, Carcharhinidae,

Hemigaleidae, Scyliorhinidae, Sphyrnidae, Triakidae, Megachasmidae, Mitsukurinidae, Odontaspidae, Lamnidae, as well as the tiger shark, *Galeocerdo cuvier*. The LCs in those species of carcharhiniform and lamniform sharks possessing LCs generally are very small and are varying in their positioning along the jaws. Some of the most popular shark species are comprised in this group and do not possess any LCs, like the basking shark (*Cetorhinus maximus*) according to Compagno (1990) and Shimada et al. (2009), the megamouth shark (*Megachasma pelagios*) according to Lavenberg & Seigel (1985) and Shimada et al. (2009), the great white shark (*Carcharodon carcharias*) according to Shimada et al. (2009), the goblin shark (*Mitsukurina owstoni*) according to Shimada et al. (2009) or the tiger shark (*Galeocerdo cuvier*) according to personal observations of Simon de Marchi (Sydney, Australia) (pers. comm. 2020), but all their jaws resemble the group C morphotype. Shimada et al. (2009) provided additional descriptions of LCs for the shortfin mako (*Isurus oxyrinchus*), the longfin mako (*Isurus paucus*), the salmon shark (*Lamna ditropis*), and the smalltooth sandtiger shark (*Odontaspis ferox*). The species with one LC among this group are all belonging to carcharhiniforms and have the LC embedded in the connective tissue of the labial fold. Thus, the single LC is very small, not connected to the jaw at any point and its orientation varies between a slight and an almost vertical dorso-ventral tilt along the upper jaw.

None of the members of this morphogroup displays a LC2. The LC3, if there is one, is in contact with the LC1 and also contacts the lower jaw with its anterior end in some species. It is comparatively slender, orientated rather horizontally along the antero-posterior axis labially of the lower jaw and is also embedded in the labial fold tissue.

Morphogroup D (Figures 2(d) and 4(a)) includes all squatinid sharks investigated in this study. Squatinidae have labial cartilages very similar to those of the orectolobiforms (morphogroup B), even though both groups are phylogenetically not closely related. Nevertheless, differences between both groups are existing. All LCs in Squatinidae are located comparably further anteriorly with the LC1 being rather short and broad and connected to the upper jaw on its anterior end. It is oriented antero-posteriorly along the upper jaw in an almost horizontal position. The LC2 is partially located dorsally of the LC1 and is a rather massive structure orientated diagonally from the dorsal point of the upper jaw above the LC1 down to a more posterior position on the dorsal side of the lower jaw where it

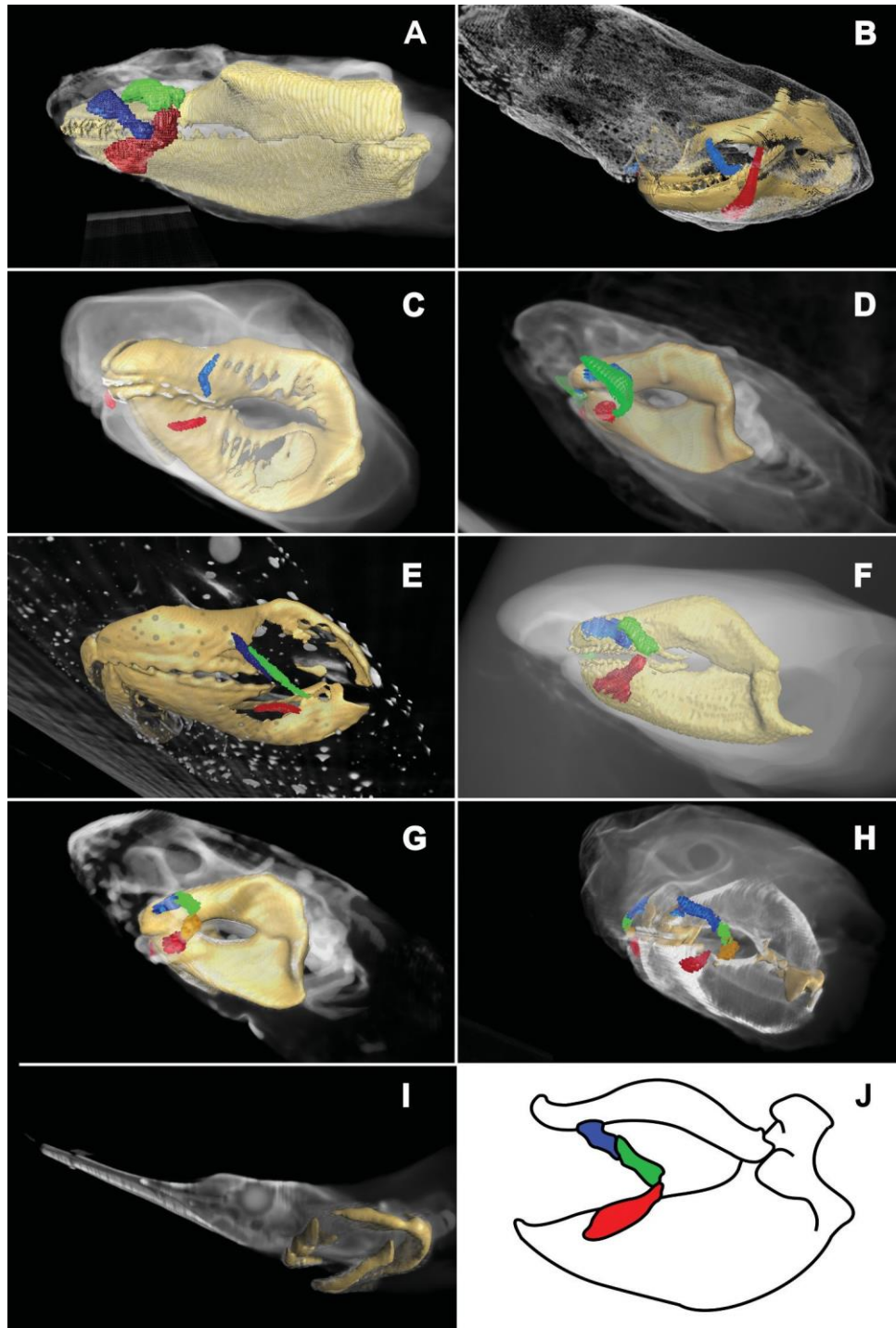


Figure 4. CT-scans of representatives of the morphogroups D to G. Morphogroup D: A = *Squatina squatina*; morphogroup E: B = *Etmopterus baxteri*; morphogroup F C = *Heterodontus francisci*; morphogroup G: D = *Brachaelurus waddi*, E = *Echinorhinus brucus*, F = *Ginglymostoma cirratum*, G = *Chiloscyllium punctatum*, H = *Stegostoma fasciatum*, I = *Pristiophorus japonicus*, J = *Rhincodon typus* sketch after Denison (1937). Blue = LC1, green = LC2, yellow = LC2.1, orange = LC3.1, red = LC3.

makes contact to the LC3.1 in the African angel shark (*Squatina Africana*) or to the LC3 in the other squatinid species, which possess only three LCs. The LC3.1 in the African angel shark is, like in orectolobiforms, a stout, kidney-shaped cartilage between LC2

and LC3, whereas the LC3 represents more a cone-shaped structure with a broad base that is connected to the lower jaw antero-ventrally and a thinner posterior ending that makes contact to the next LC in all investigated squatinid species.



Morphogroup E (Figures 2(e) and 4(b)) incorporates only deep-water sharks of the family Etmopteridae. They are characterized by a very special jaw-shape with large dorsally extending structures on the anterior jaw end and also a very special shaped LC1. This LC1 is not attached to the upper jaw but is orientated nearly vertical and is sticking out laterally away from the jaws in an inverse S-curved shape. The dorsal end of the LC1 is flattened parallel to the upper jaw, while the ventral end is more hook-shaped pointing towards the upper jaw's ventral side. There is no LC2 developed in this morphogroup. The LC3 follows the out-sticking tendency of the LC1 but not so intensely and dorsally makes contact to the base of the hook-shaped ventral ending of the LC1. The whole LC3 is orientated almost vertically with the ventral end being connected to the lower jaw.

Morphogroup F (Figures 2(f) and 4(c)) is characterized by heterodontiform sharks (comprising only the family Heterodontidae) having two pairs of LCs, which display two different kinds of orientation in diverse species. In general the LC1 is very small and rod-shaped and is always orientated practically vertical in all species. There exists no LC2 in members of this morphogroup. The LC3 is comparatively the smallest among all described morphogroups and is either rod-shaped and orientated antero-posteriorly inclining or isoscel triangular-shaped with the tip pointing dorsally. None of the LCs is connected to the jaws.

Morphogroup G (Figures 2(g) and 4(d-j)) merges all non-orectolobid orectolobiforms, the echinorhiniforms and the pristiophoriforms. The orectolobiforms of this group (members of the Stegostomatidae, Hemiscylliidae, Brachaeluridae, Ginglystomatidae, Rhincodontidae) all have either three or four pairs of LCs. *Echinorhinus* (the only member of the Echinorhinidae within echinorhiniformes) and the pristiophoriforms (only comprising one family Pristiophoridae) do not display any LCs but their general jaw shape matches that of the morphogroup G. The LC1 is of medium length compared to the other groups described, is orientated almost horizontally along the upper jaw and is connected to the upper jaw on its anterior end in all cases.

The LC2 is an elongated structure that is orientated either almost vertically in species with three LCs or antero-posteriorly declining, starting dorsally

of the posterior end of LC1 and ending in a more posterior ventral point of the upper jaw. In both scenarios the LC2 contacts either the LC3.1 in species with four LCs or the LC3 in species with 3 LCs. The LC3.1, which is present in Stegostomatidae and Hemiscylliidae, is more elongated than in other morphogroups possessing an LC3.1, and is oriented antero-posteriorly with inclination starting at the dorsal side of the lower jaw above the LC3 and contacting the LC2 with its posterior end. In any case, the LC3 is connected to the lower jaw on its broader anterior end. It then either narrows dorsally and contacts the LC2 or keeps its anterior width and ends posteriorly in an emargination making contact to the LC3.1. Additionally to our findings in the CT-scans, LCs have been described in the epaulette shark (*Hemiscyllium ocellatum*) by Wu (1994), and in the whale shark (*Rhincodon typus*) by Denison (1937).

Morphogroup H (Figures 2(h) and 5(a-f)) encompasses members of two hexanchiform families (Chlamydoselachidae and Hexanchidae) and members of four squaliform families (Centrophoridae, Somniosidae, Squalidae). All are possessing three LCs, except for the members of Hexanchidae who do not display any LCs. The LC1 varies between being and not being attached with its anterior end to the upper jaw. In cases where it is not attached it is remarkably slender and elongated and is orientated antero-posteriorly in a declining curve. In some Centrophoridae and Squalidae the LC1 even makes contact to the LC3 by its posterior end. In cases where the LC1 is attached to the upper jaw by its anterior end, it is short and rod-shaped and oriented antero-posteriorly parallel to the upper jaw. The LC2 is similarly positioned as in morphogroup D (Squatinae) being located dorsally of the LC1, not being connected to the upper or lower jaw at any point, but being of very long and slender shape. It is oriented antero-posteriorly declining starting anteriorly dorsal of the LC1 (labially to the upper jaw) and ending posteriorly dorsal of the LC3 (labially of the lower jaw). The LC3 is shaped in two ways: either broader and shaped like an antero-posteriorly stretched S-shape or narrow and rod-like and oriented almost vertically. In both cases the LC3 is connected ventrally to the lower jaw. Additionally to our findings in the CT-scans, LCs were described for some more species. The three LCs of the frilled shark (*Chlamydoselachus anguineus*) were first described by Smith (1937), while White (1895) stated that the Greenland shark (*Somniosus microcephalus*) does not possess any LCs.



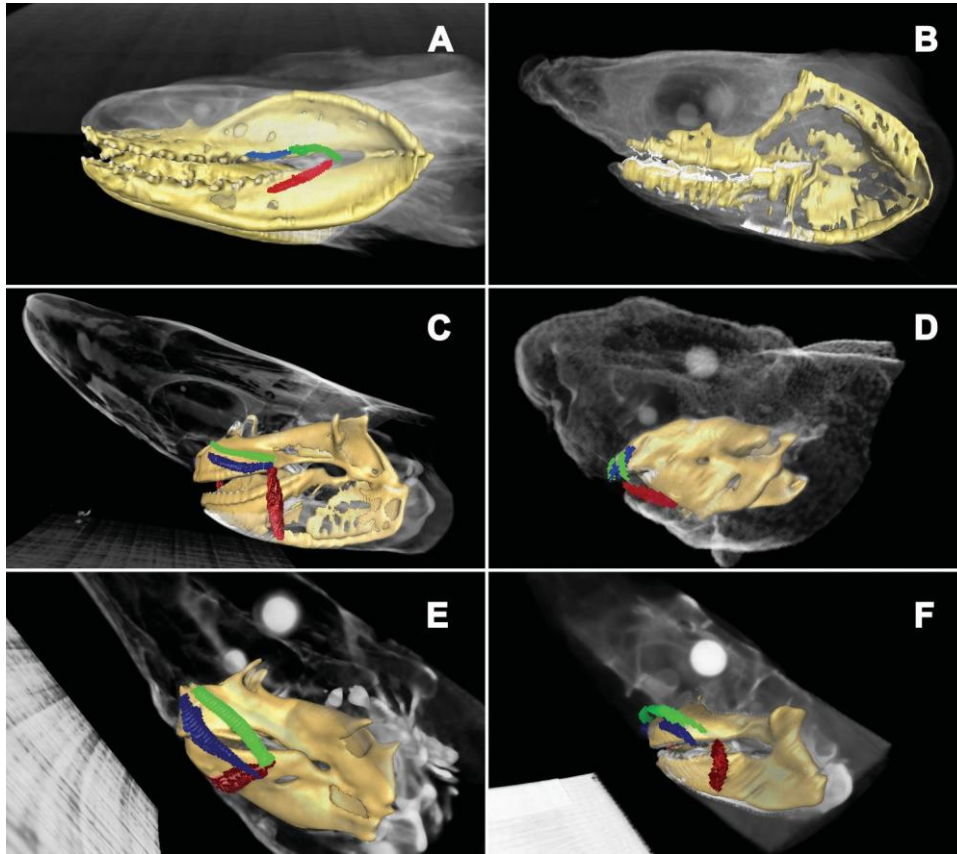


Figure 5. CT-scans of representatives of the morphogroup H: A = *Chlamydoselachus anguineus*, B = *Hexanchias perlo*, C = *Centrophorus uyato*, D = *Oxynotus centrina*, E = *Centroselachus crepidater*, F = *Squalus acanthias*. Blue = LC1, green = LC2, yellow = LC2.1, orange = LC3.1, red = LC3.

## Discussion

The large number of shark species with three LC pairs identified here indicates that three pairs of LC is the most common number among sharks and therefore could represent the plesiomorphic condition according to the in-group commonality assumption, which also would be in agreement with the hypothetical neoselachian (= elasmobranch *sensu* Maisey 2012) morphotype constructed by Compagno (1977) depicting three slender labial cartilages located in the assumed corner of the mouth but not attached to the jaws – a construction that is very similar to the LC-situation in the Chlamydoselachidae. This would also indicate a reduction from four labial cartilages (Klug 2010) in putative stem-elasmobranchs to three pairs in crown elasmobranchs. Consequently, one could hypothesize that further reduction of labial cartilage numbers within different selachimorph clades represents derived conditions. Such a scenario, however, needs to be tested employing rigorous cladistics principles, which is beyond the scope of this review.

Many carcharhiniform and most lamniform sharks do not have any LCs, which we consider a secondary reduction probably related with a shift in life styles accompanied with changes in feeding kinematics. We also consider the small LCs in carcharhiniform and lamniform sharks a vestigial structure, since those taxa are considered derived groups, which are known to use ram feeding techniques (like cranial elevation), at which LCs would be rather hindering than helping (see Ferry et al. 2015). Individuals possessing one labial cartilage barely can be expected to create inertial suction, because the one remaining labial cartilage in sharks generally is very small and can be considered to be a remnant of what once was a larger LC and now is without significant function. None or one pair of labial cartilages characterizes ram or biting feeding strategies such as in carcharhiniform and lamniform sharks that cannot create significant suction in feeding (Motta & Wilga 2001; Wilga et al. 2007).

Although lamniform sharks are only very imperfectly represented in our sample, we still agree with

Shimada et al. (2009) concerning the non-synapomorphic loss of labial cartilages in lamniform families. We even detected a small labial cartilage in a specimen of the common thresher shark, *Alopias vulpinus* (Figure 3(c)), though Shimada et al. (2009) stated that all members of Alopiidae are devoid of labial cartilages.

Aside from the lamniform and carcharhiniform sharks the inspected species of the Hexanchidae also lack LCs. As in most other sharks without LCs their absence can be considered a secondary reduction. The investigated sharpnose sevengill shark (*Heptranchias perlo*) is assumed to use an in modern sharks unusual way of feeding, as it is suspected to perform a backward ripping movement to break up larger prey items (Kryukova & Kuznetsov 2020). Additionally the increased number of gill slits is considered to reduce the water-wave in a ram-feeding attack (Kryukova 2017).

In those carcharhiniform sharks possessing two LC pairs, the LCs are embedded in the labial fold tissue and are too small to be used for generating a functional suction while feeding. Nevertheless, other groups possessing two pairs of LCs can be considered to be able to generate suction strong enough to be used during feeding. This applies for example to durophagous heterodontiform sharks (like *Heterodontus francisci*), which have either two or three LCs depending on the species (Edmonds et al. 2001). The LCs in heterodontiforms, independent of the number, are located close to the posterior corner of the mouth-opening, which is located rather far anteriorly. This position of the mouth-opening and LCs along the jaws might explain why heterodontiforms can produce inertial suction despite their small sized LCs. The LCs are often embedded in the labial fold tissue. Since also species without LCs possess labial folds their presence does not necessarily indicate the presence of LCs.

The group of shark species presenting three pairs of LCs is the largest in this study (19 species based on CT-scans, including literature data 23 species). All of the different forms of three LC pairs can be considered to be useful in creating a suction that can be advantageous during prey capture. The very special constellation seen in the Dalatiidae, with their LC2-pair overlapping anteriorly, leads us to the assumption that a special kind of suction can be generated here. The separation of dalatiid sharks into “euprotomicrinines” (*Euprotomicrus*, *Squaliolus*) and “dalatiines” (*Dalatis*, *Isistius*) sensu Shirai (1992, 1996) is supported by our study, since the LCs are arranged differently among the investigated species. The knowledge about the unique feeding strategy of the cookie-cutter shark, *Isistius brasiliensis*, which

sucks on to much larger prey and cuts out round pieces of flesh by rotating its body around its axis, makes us assume that also other representatives of this family – especially of the “dalatiine” group – might use a similar feeding strategy due to their morphologically similar LCs. Based on the very elongated LCs 1 and 2 located at the anterior half of the jaws in squaliforms we hypothesize that they are only able to create a suction of medium strength, since the thin cartilages cannot be assumed to be resilient to strong forces. We still suppose that the pocket shark (see Denton et al. 2018) might be capable of creating a slightly stronger suction than other squaliforms, since its LC2 is supported by the LC1 and, therefore, could bear stronger forces. If this pattern of LC2-supporting LC1 is found in other squaliforms a stronger suction could be assumed in these species, too.

The three LC pairs described in the whale shark, *Rhincodon typus*, by Denison (1937) are rather stout and imply that the whale shark is, controversially to the outdated assumption that they are pure ram-feeders, also using suction, which Motta et al. (2010) already described. Although it seems that the use of suction during the vertical feeding position (also called “bottling”) results in a very small amount of energy expended, still the ram-feeding technique is more popular in whale sharks around the globe, which is connected to the occurrence of prey items. In areas with lower prey density suction-feeding is more frequent, while in areas with denser prey population ram-feeding is more productive (Cade et al. 2020).

In squatiniforms, a group possessing three or four LCs (Morphogroup D), the generation of a strong suction can be expected since their LCs are located very far anterior, therefore, forming a small mouth gape and a large buccal volume with the LCs rotating labially when the mouth opens (see Ferry et al. 2015). This gives the angel sharks, i.e., an adaptive advantage as ambush predators, similar to the condition seen in members of Orectolobidae (which also have very similar dental morphologies) that, nevertheless, evolved independently. Four LCs were described for all members of the Heterodontidae by Compagno (1977), which we cannot confirm after reviewing all available evidence. The encompassing amount of four LCs was also contradicted before for the Port Jackson shark (*Heterodontus portusjacksoni*) by Dean (1895), a description that might not have been taken into account by Compagno (1977).

The small number of sharks possessing four or five pairs of LCs (Stegostomatidae, Orectolobidae and some members of the Hemiscylliidae and Squatinidae) would have retained the plesiomorphic condition for elasmobranchs, with four LCs in

Stegostomatidae, Hemiscylliidae and Squatinidae according to Klug (2010), or represents the plesiomorphic condition for all chondrichthyans, with five LCs in Orectolobidae according to Didier (1995) and Maisey (1985), respectively. However, the life styles and modes of feeding (ram-feeder, pure biting, suction feeding or different combinations of the mentioned) that correlate with a certain LC construction, suggest that LCs predominantly bear a functional rather than a phylogenetic signal.

Orectolobiform sharks with four to five LCs are generally assumed to be capable of creating a strong suction, which was already demonstrated for some species (e.g., Motta & Wilga 1999, 2001; Gardiner et al. 2017). The LC2.1, which is present in Orectolobidae only, in combination with the LC3.1 enables these sharks to generate a very strong and effective suction flow. The high number of LCs in orectolobiforms combined with the knowledge about their hunting tactics and feeding strategies indicate that these families may have been adapted perfectly to suction feeding, as have the squatiniforms, rather than representing a plesiomorphic condition.

Intriguingly, there seems a close correlation between LC position and jaw shape indicating that these two skeletal units are forming distinct morphological modules (= morphogroups here). This consequently suggests that the modules contain at least partly a phylogenetic signal. However, the possible correlation of the morphogroups and their phylogenetic relationships needs to be tested in the future employing robust analytical procedures (e.g., ancestral trait identification, trait analyses).

## Conclusions

This work represents a first step to a better understanding of the morphology, number and role of LCs in elasmobranch fishes, however, without employing sophisticated statistical procedures here. It is evident that position and dimension of LCs are connected to the shape of the jaws, forming distinct morphological modules. The number and shape of LCs vary even within families and seemingly are related to the feeding strategy supporting our interpretation that LCs bear a strong functional signal. It is possible to use the number, shape and position of LCs to identify the probability of sharks to create a functional useful suction in order to improve their chances of prey capture and to estimate the suction strength qualitatively.

## Acknowledgements

We thank M. Stagg1 (Vienna, Austria), who produced the micro-CT scans of the etmopterid species, and the help of S. de Marchi (Sydney, Australia), who provided information about the existence of LCs in the tiger shark. We want to thank the European Elasmobranch Association (EEA) for their financial support enabling this publication, with special thanks to E. Sperone (Calabria, Italy) for managing the submissions for this special issue of the European Zoology Journal. We acknowledge P. Kamminga and his team (Leiden, Netherlands) for their great open access work providing multiple CT-scans. Last but not least, we express our gratitude to three anonymous reviewers for their constructive feedbacks, which improved the manuscript significantly.

## Disclosure statement

No potential conflict of interest was reported by the authors.

## Supplementary material

Supplemental data for this article can be accessed [here](#).

## ORCID

J. Kriwet  <http://orcid.org/0000-0002-6439-8455>

## References

- Braccini JM. 2008. Feeding ecology of two high-order predators from south-eastern Australia: The coastal broadnose and the deepwater sharpnose sevengill sharks. *Marine Ecology Progress Series* 371:273–284. DOI: 10.3354/meps07684.
- Cabrera-Chávez-Costa AA, Galván-Magana F, Escobar-Sánchez O. 2010. Food habits of the silky shark *Carcharhinus falciformis* (Müller & Henle, 1839) off the western coast of Baja California Sur, Mexico. *Journal of Applied Ichthyology* 26:499–503. DOI: 10.1111/j.1439-0426.2010.01482.x.
- Cade DE, Levenson JJ, Cooper R, de la Parra R, Webb DH, Dove ADM. 2020. Whale sharks increase swimming effort while filter feeding, but appear to maintain foraging efficiencies. *Journal of Experimental Biology* 223:jeb224402. DOI: 10.1242/jeb.224402.
- Cappetta H. 2012. Mesozoic and cenozoic elasmobranchii: Theeth. München, Germany: Pfeil Verlag. ISBN: 9783899371482.
- Compagno LJV. 1977. Phylogenetic relationships of living sharks and rays. *American Zoology* 17:303–322. DOI: 10.1093/icb/17.2.303.
- Compagno LJV. 1990. Relationships of the megamouth shark, *Megachasma pelagios* (Lamniformes, Megachasmidae), with comments on its feeding habits, IN: Elasmobranchs as living resources: Advances in the biology, ecology, systematics and the status of the fisheries (Pratt H.L. Jr., Gruber S.H. & Tanuchi T.). NOAA Technical Report 90, pp.357–379.

- Compagnucci C, Debiais-Thibaud M, Coolen M, Fish J, Griffin JN, Bertocchini F, Minoux M, Rijli FM, Borday- Birraux V, Casane D, Mazan S, Depew MJ. 2013. Pattern and polarity in the development and evolution of the gnathostome jaw: Both conservation and heterotopy in the branchial arches of the shark, *Scyliorhinus canicula*. *Developmental Biology* 377:428–448. DOI: 10.1016/j.ydbio.2013.02.022.
- Dean B. 1895. Fish, living and fossil – An outline of their forms and probable relationships, Columbia university biological series III. New York: MacMillan & Co. pp. 75.
- Dean B. 1906. Chimaeroid fishes and their development. Carnegie Institution of Washington, Publication No. 32.
- Dean MN, Bizzarro JJ, Summers AP. 2007. The evolution of cranial design, diet and feeding mechanisms in batoid fishes. *Integrative and Comparative Biology* 47(1):7–81.
- Dean MN, Huber DR, Nance HA. 2006. Functional morphology of jaw trabeculation in the lesser electric Ray *Narcine brasiliensis*, with comments on the evolution of structural support in the batoida. *Journal of Morphology* 367:1137–1146. DOI: 10.1002/jmor.10302.
- Dean MN, Summers AP, Ferry LA. 2012. Very low pressure drive ventilatory flow in chimaeroid fishes. *Journal of Morphology* 273:461–479. DOI: 10.1002/jmor.11035.
- Denison RH. 1937. Anatomy of the head and pelvic fin of the Whale Shark, *Rhineodon*. *Bulletin of the American Museum of Natural History* 73, Article 5:477–515.
- Denton JSS, Maisey JG, Grace M, Pradel A, Doosey MH, Bart Jr. HL, Naylor GJP. 2018. Cranial orphology in *Mollisquamia* sp. (Squaliformes, Dalatiidae) and patterns of cranial evolution in dalatiid sharks. *Journal of Anatomy* 233:15–32. DOI: 10.1111/joa.12823.
- Didier AD. 1995. Phylogenetic systematics of extant chimaeroid fishes (Holocephali, Chimaeroidei). *American Museum Novitates*, Number 3119, pp. 1–86.
- Edmonds MA, Motta PJ, Hueter RE. 2001. Food capture kinematics on the suction feeding horn shark, *Heterodontus francisci*. *Environmental Biology of Fishes* 62:415–427. DOI: 10.1023/A:1012205518704.
- Ferry LA, Paig-Tran EM, Gibbs AC. 2015. Suction, ram, and biting: Deviations and limitations to the capture of aquatic prey. *Integrative and Comparative Biology* 55(1):97–109. DOI: 10.1093/icb/icc028.
- Figshare. <https://figshare.com/> Accessed Jun 2020 11.
- Gardiner JM, Atema J, Hueter RE, Motta PJ. 2017. Modulation of shark prey capture kinematics in response to sensory deprivation. *Elsevier Zoology* 120:42–52.
- Gegenbauer C. 1872. Untersuchungen zur vergleichenden Anatomie der Wirbeltiere – Heft 3: Das Kopfskelett der Sela- chier, Leipzig.
- p. 316 ff Goodrich E.S., 1930, studies on the structure and development of vertebrates. London: MacMillan & Co. pp. 837 & 754.
- Goodrich, ES. 1930. Studies on the structure & development of vertebrates. London: Macmillan & Company.
- Huber DR, Eason TG, Hueter RE, Motta PJ. 2005. Analysis of the bite force and mechanical design of the feeding mechanism of the durophagous horn shark *Heterodontus francisci*. *The Journal of Experimental Biology* 208:3553–3571. DOI: 10.1242/jeb.01816.
- Ivanov. 2005. Dentition of late Palaeozoic xenacanthoid shark *Bransonella*. *Journal of Vertebrate Palaeontology* 25(3):47A.
- Kamminga P, de Bruin PW, Geleijns J, Brazeau MD. 2017. Data descriptor: X-ray computed tomography library of shark anatomy and lower jaw surface models. *Nature Scientific Data* 4:170047. DOI: 10.1038/sdata.2017.47.
- Klug S. 2010. Monophyly, phylogeny and systematic position of the synchondontiformes (Chondrichthyes, Neoselachii). *Zoologica Scripta* 39:37–49.
- Klug S, Kriwet J, Böttcher R, Schweigert G, Dietl G. 2009. Skeletal anatomy of the extinct shark *Paraorthacodus jurensis* (Chondrichthyes; Palaeospinacidae), with comments on synchondontiform and palaeospinacid monophyly. *Zoological Journal of the Linnean Society* 157:107–134. DOI: 10.1111/j.1096-3642.2009.00534.x.
- Kryukova NV. 2017. Functional analysis of the musculo-skeletal system of the gill apparatus in *Heptranchias perlo* (Chondrichthyes: Hexanchidae). *Journal of Morphology* 278 (8):1075–1090. DOI: 10.1002/jmor.20695.
- Kryukova NV, Kuznetsov AN. 2020. Suboccipital muscle of sharpnose sevengill shark *Heptranchias perlo* and its possible role in prey dissection. *Journal of Morphology* 281:842–861. DOI: 10.1002/jmor.21142.
- Lavenberg RJ, Seigel JA. 1985. The Pacific's megamystery – Megamouth. *Terra* 23(4):29–31.
- Maisey JG. 1983. Cranial anatomy of *Hybodus basanus* Egerton from the lower cretaceous of England. *American Museum Novitates*, Number 2758:1–64.
- Maisey, JG. 1985. Cranial morphology of the fossil elasmobranch *Synechodus dubrisiensis*. *American Museum Novitates* 2804:1–28.
- Maisey JG. 1986. Anatomical revision of the Fossil Shark *Hybodus fraasi* (Chondrichthyes: Elasmobranchii). New York: American Museum of Natural History, Novitates No. 2857, pp. 1–16.
- Maisey JG. 1987. Cranial anatomy of the lower Jurassic shark *Hybodus reticulatus* (Chondrichthyes: Elasmobranchii), with comments on hybodontid systematics. New York: American Museum of Natural History, Novitates No. 2878, pp. 1–39.
- Maisey JG. 2012. What is an 'elasmobranch'? The impact of palaeontology in understanding elasmobranch phylogeny and evolution. *Journal of Fish Biology* 80(5):918–951. DOI: 10.1111/j.1095-8649.2012.03245.x.
- Moss SA. 1977. Feeding mechanisms in sharks. *American Zoologist* 17(2):355–364. DOI: 10.1093/icb/17.2.355.
- Motta PJ, Maslanka M, Hueter RE, Davis RL, de la Parra R, Mulvaney SL, Habegger ML, Strother JA, Mara KR, Gardiner JM, Tyminski JP, Zeigler LD. 2010. Feeding anatomy, filter-feeding rate, and diet of the whale sharks *Rhincodon typus* during surface ram filter feeding off the Yucatan Peninsula, Mexico. *Elsevier Zoology* 113:199–212.
- Motta PJ, Wilga CD. 1999. Anatomy of the feeding apparatus of the nurse shark, *Ginglymostoma cirratum*. *Journal of Morphology* 241:33–60. DOI: 10.1002/(SICI)1097-4687-(199907)241:1<33::AID-JMOR3>3.0.CO;2-1.

- Motta PJ, Wilga CD. 2001. Advances in the study of feeding behaviors, mechanisms, and mechanics of sharks. *Environmental Biology of Fishes* 60:131–156. DOI: 10.1023/A:1007649900712.
- Pollard HB. 1895. Oral cirrhi of siluroids and the origin of the head in vertebrates. *Zoologisches Jahrbuch (Abteilung Anatomie)* 8:379–424.
- Shimada K, Rigsby CK, Kim SH. 2009. Labial cartilages in the smalltooth Sandtiger shark, *Odontaspis ferox* (Lamniiformes: Odontaspidae) and their significance to the phylogeny of lamniform sharks. *The Anatomical Record* 292:813–817. DOI: 10.1002/ar.20903.
- Shirai S. 1992. Squalan phylogeny: A new framework of 'squaloid' sharks and related taxa. Sapporo: Hokkaido University Press.
- Shirai S. 1996. Phylogenetic interrelationships of neoselachians (Chondrichthyes: Euselachii). In: Stiassny MLJ, Parenti LR, Johnson GD, editors. *Interrelationships of Fishes*. New York: Academic Press. pp. 9–34.
- Smith BG. 1937. The bashford dean memorial volume of archaic fishes – Article VI: The anatomy of the frilled shark *Chlamydoselachus anuineus* Garman. New York: American Museum of Natural History. pp. 330–498.
- Strasburg DW. 1963. The diet and dentition of *Isistius brasiliensis*, with remarks on tooth replacement in other sharks. *Copeia* No. 1, pp. 33–40.
- Swertzoff AN. 1916. Etudes sur l'évolution des vertébrés inférieurs – 1. Morphologie du squaloïde et de la musculature de la tête des cyclostomes. *Archiv Russes Anatomical Histological, Embryological* 1:1–104.
- Veran M. 1995. Are the labial cartilages of Chondrichthyes homologous to the labial bone of the primitive fossil Actinopterygians? *Geobios*, M.S. No. 19, pp. 161–166.
- White PJ. 1895. The skull and visceral skeleton of the Greenland shark. London: Transactions of the Royal Society of Edinburgh. pp. 287–306.
- Wieczorek AM, Power AM, Browne P, Graham CT. 2018. Stable-isotope analysis reveals the importance of soft-bodied prey in the diet of the lesser spotted dogfish *Scyliorhinus canicula*. *Journal of Fish Biology* 93:685–693. DOI: 10.1111/jfb.13770.
- Wilga CD, Motta PJ, Sanford CP. 2007. Evolution and ecology of feeding in elasmobranchs. *Integrative and Comparative Biology* 47(1):55–69. DOI: 10.1093/icb/icm029.
- Wu EH. 1994. Kinematic analysis of jaw protrusion in oreotolbiform sharks: A new mechanism for jaw protrusion in elasmobranchs. *Journal of Morphology* 222(2):175–190. DOI: 10.1002/jmor.1052220205.



# **CHAPTER 4: MORPHOLOGICAL VARIABILITY AND FUNCTION OF LABIAL CARTILAGES IN SHARKS (CHONDRICHTHYES, ELASMOBRANCHII)**

## **Author Information**

Klimpfinger C.<sup>1\*</sup> & Kriwet J.<sup>2</sup>

<sup>1</sup> Claudia Klimpfinger MSc.MEd., Department of Paleontology, University of Vienna, Vienna, Austria

\*Corresponding Author: Claudia Klimpfinger c.klimpfinger@gmx.at

<sup>2</sup> Prof. Dr. Jürgen Kriwet, Department of Paleontology, University of Vienna, Vienna, Austria

Own contributions: I developed this project together with my supervisor (J. K.). I downloaded additional published ct-scans of sharks from the platform figshare.com and the chondrichthyan tree of life platform, used the Amira software package to crop the stacks, as well as reconstruct and mark the jaws and labial cartilages within all scans. Furthermore, I provided morphological descriptions and established morphotypes of labial cartilages. Finally, I interpreted and discussed the results, wrote the whole manuscript and produced all included figures.

## **Bibliography**

Klimpfinger C. & Kriwet J., 2023, Morphological Variability and Function of Labial Cartilages in Sharks (Chondrichthyes, Elasmobranchii), Biology, Volume 12, Article 1486, doi: 10.3390/biology12121486


Processing status: Published





Article

# Morphological Variability and Function of Labial Cartilages in Sharks (Chondrichthyes, Elasmobranchii)

Claudia Klimpfinger \* and Jürgen Kriwet 

Department of Paleontology, University of Vienna, 1090 Vienna, Austria; juergen.kriwet@univie.ac.at

\* Correspondence: c.klimpfinger@gmx.at

**Simple Summary:** Labial cartilages (LCs) are structures along the jaws of many sharks that are known, in some species, to enable or support suction, but there are many different shapes, numbers, and positions of LCs. This study is a morphological description of the large variety of LCs in sharks and an estimation of their suction potential according to the data of species known for their suction feeding. This additional information on their feeding strategies may help to accurately protect endangered shark species.

## Abstract:

(1) Background: Labial cartilages (LCs), as their name suggests, lie in the folds of the connective tissue, the lips, framing the gape of elasmobranch chondrichthyans. As such, these cartilages lie laterally to the jaws and marginal teeth. They are considered to influence the ability of creating suction during the feeding process. As past studies have shown, LCs in sharks are as diverse as their varied feeding techniques and differ between species in number, size, shape, and position. This allows establishing parameters for inferring the feeding and hunting behaviors in these ecologically important fishes. (2) Methods: We present a study of LCs based on the CT scans of more than 100 extant shark species and, therefore, represent at least one member of every living family within the Euselachii, excluding batoids. (3) Results: Accordingly, sharks without labial cartilages or that have only small remnants are ram feeders or use pure biting and mainly occupy higher trophic levels (tertiary and quaternary consumers), whereas suction-feeding sharks have higher numbers (up to five pairs) of well-developed LCs and occupy slightly lower trophic levels (mainly secondary consumers). Species with unique feeding strategies, like the cookie-cutter shark (*Isistius brasiliensis*, an ectoparasite), display distinct shapes of LCs, while generalist species, conversely, exhibit a simpler arrangement of LCs. (4) Conclusions: We propose a dichotomous identification key to classify single LCs into different morphotypes and propose combinations of morphotypes that result in suction feeding differing in strength and, therefore, different hunting and feeding strategies. The conclusions of this study allow to infer information about feeding strategies not only in extant less-known sharks but also extinct sharks.



**Citation:** Klimpfinger, C.; Kriwet, J. Morphological Variability and Function of Labial Cartilages in Sharks (Chondrichthyes, Elasmobranchii). *Biology* **2023**, *12*, 1486. <https://doi.org/10.3390/biology12121486>  
Academic Editor: Vincent L. Bels

Received: 25 October 2023  
Revised: 29 November 2023  
Accepted: 1 December 2023  
Published: 3 December 2023



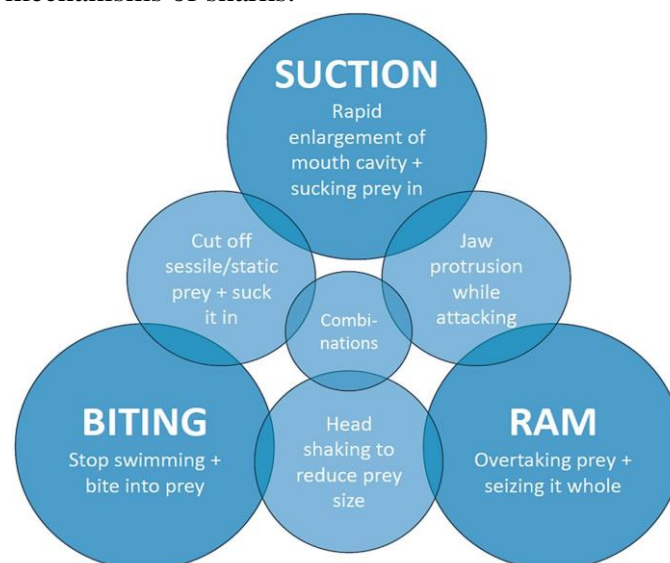
**Copyright:** © 2023 by the authors. Licensee MDPI, Basel, Switzerland. This article is an open access article distributed under the terms and conditions of the Creative Commons Attribution (CC BY) license (<https://creativecommons.org/licenses/by/4.0/>).

**Keywords:** feeding mechanisms; feeding strategies; jaw morphology; suction; ram feeding; feeding behavior

## 1. Introduction

The group Elasmobranchii (sensu [1]; Neoselachii sensu [2]) encompasses all modern sharks, rays, and skates in a monophyletic clade [1,2]. The fossil records of Elasmobranchii [1] extend back to the Early Permian period (ca. 295 mya) [3] and they adapted to a wide range of niches during their evolutionary history. This resulted in the development of various feeding mechanisms [4] (Scheme 1) as exemplified in apex predators, like the great white shark (*Carcharodon carcharias*) and the tiger shark (*Galeocerdo cuvier*); small, highly adapted species, like the cookie-cutter shark (*Isistius brasiliensis*) hunting in an ectoparasitic way; the Japanese wobbegong (*Orectolobus japonicus*) being a very sufficient benthic living suction feeder; or giant plankton feeders, like the whale shark (*Rhincodon typus*). These niche adaptations required different

developments in tooth and jaw structures to solve the requirements for prey capture. In this paper, we focus on the labial cartilages (LCs) of sharks. The LCs are paired structures located on both sides of the head, laterally to the jaws. Their position along the jaws varies and therefore constrains the mouth-gape to a higher or lesser extent. LCs are considered a shared derived character as they are present in extinct shark species [5–10] and their sister groups [11–14], supporting that these structures are symplesiomorphic for living sharks. They vary in number (0–5 pairs), size and orientation, and have been described previously in some species, e.g., [8,15–17], but only insufficiently or not at all in others, e.g., [18,19]. Their origin and function have been discussed for over 100 years (e.g., [20–25]), but since 2001, it is well established that LCs support suction during feeding in sharks [8]. Still, not all LCs enable suction [26], but a certain number and size is necessary to form an efficient tunnel for generating a suction flow. The objective of this work is to provide precise descriptions of the number, position, structure, and orientation of LCs in different shark species. Previously, Klimpfinger and Kriwet [26] introduced a general identification system for LCs in sharks and arranged extant shark families according to their jaw and LC structure into eight morphotypes (groups A to H). The present study represents an extension of this work providing novel information about the morphology and variability of LCs in sharks and installing a dichotomous identification key for different morphotypes of LCs. Secondly, we discuss the combinations of LC morphotypes that account for different suction performances, deduced from physiological and biomechanical studies, e.g., [8,16,27,28]. This provides an additional insight into the feeding mechanisms of sharks.



**Scheme 1.** Main feeding mechanisms of sharks, including common intermediate forms and possible combinations.

## 2. Materials and Methods

We used published CT and micro-CT scans as well as pictures from published studies resulting in a dataset of 120 shark species, for which information about the presence/absence and nature of labial cartilages could be retrieved. Thirty-four species of the dataset lack labial cartilages and subsequently were excluded from the study, resulting in 86 species (Supplementary Table S1). The main sources for the descriptions of LCs in the remaining 86 species were based on X-ray-computed scans provided in [www.figshare.com](http://www.figshare.com) (accessed on 24th

October 2023) [29] by Kamminga et al. [30] and the Chondrichthyan Tree of Life [31] by Corrigan, Naylor, Yang et al. [32]. Additionally, we retrieved information for the whale shark (*Rhincodon typus*) from Denison [15]; the Greenland shark (*Somniosus microcephalus*) from White [33]; the Port Jackson shark (*Heterodontus portusjacksoni*) from Summers [34]; the blackbelly lanternshark (*Etmopterus lucifer*) from Staggl [35]; for the white shark (*Carcharodon carcharias*), the shortfin mako (*Isurus oxyrinchus*), the longfin mako (*Isurus paucus*), the salmon shark (*Lamna ditropis*), and the smalltooth sand tigershark (*Odontaspis ferox*) from Shimada [19]; and the megamouth shark (*Megachasma pelagios*) from Seigel [36] and Shimada [19]. This resulted in the representation of at least one species of each of the currently known nine shark orders (Hexanchiformes, Squaliformes, Squatiniformes, Pristiophoriformes, Echinorhiniformes, Heterodontiformes, Orectolobiformes, Lamniformes, and Carcharhiniformes) and almost one species for each of the currently identified families.

### Morphological Descriptions

We downloaded 52 CT stacks from figshare.com and used the Amira software (<https://www.thermofisher.com/at/en/home/electron-microscopy/products/software-em-3d-vis/amira-software.html>, accessed on 24 October 2023) packages to reconstruct the scanned individuals and to mark the jaws and detectable LCs, which was also conducted for *Etmopterus lucifer*, of which a micro-CT scan was provided by Staggl [35]. We used the volume-rendering function for an initial overview; then, the jaws and LCs were marked using the orthogonal view and the brush tool, in order to visualize the structures. We rechecked the selected areas in the volume-rendering view and applied the surface-rendering tool to search for any LC we might have missed. We transferred the processed scans to the Autodesk program Sketchbook and used a stylus pen to highlight the LCs according to the assigned colors (see Table 1). The same was performed with the micro-CT-scan of *E. lucifer*. After reconstructing the jaws and LCs, we also compared our reconstructions to other reconstructions published in sharksrays.org to check for similarities and aberrations and added those species for which we did not have scans (29 species). For LC identifications, we employed the definitions of LCs of Klimpfinger and Kriwet [26], who numbered LCs as 1, 2, 2.1, 3, and 3.1 (Table 1; Figure 1). We also established a dichotomous identification key for the different morphotypes of LCs (Figures 2–5).

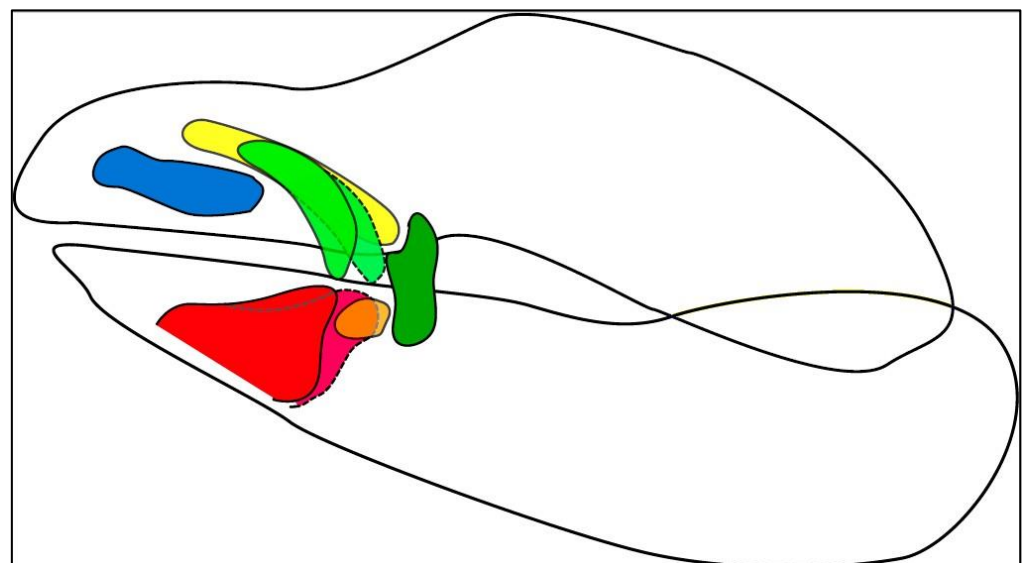


**Figure 1.** Hypothetical sketch of a shark jaw depicting all possible LCs in their resting positions. LC 1 = blue; LC 2 = green; LC 2.1 = yellow; LC 3.1 = orange; LC 3 = red.

**Table 1.** LC definitions and color-coding from Klimpfinger and Kriwet [26].

Color Code	LC No.	Description
Blue	LC1	Located/onset at the most anterior position along the upper jaw; sometimes connected to the jaw on the anterior end; mostly oriented along the anterior–posterior-axis; variable shapes
Green	LC2	Located between LC1 and LC3 or between LC1 and LC3.1; never connected to the jaw; oriented antero-posteriorly in differing angles to the dorso-ventral axis; shape is elongated; forking on the anterior end in Orectolobidae
Yellow	LC2.1	A segregated part of the forking of LC2 (see [27]); located dorsally to that of the LC1; never connected to the jaw; orientated antero-posteriorly; slender cartilage only present in Orectolobidae
Orange	LC3.1	A segregated part of the LC3 (see [27]); located in the more posterior position along the lower jaw between LC2 and LC3; oriented antero-posteriorly; mostly short and stout
Red	LC3	Located at the most anterior position along the lower jaw; often connected to the jaw on the anterior ventral end; oriented antero-posteriorly in differing angles to the dorso-ventral axis; variable shape

The following descriptions always refer to the LC in the corresponding sub-heading and the position always refers to the onset of the LC or its anterior end. The total number of LCs for each species was added in brackets next to the species name. Types comprise three or more species; Subtypes contain a maximum of two species, except for LCs 2.1 and 3.1. Since only few species possess those two, all groups were considered types, independent of the species number included. The orientation of the LCs was described with “posteriorly declining” if the anterior end was positioned more dorsally than the posterior end (for example, see Figure 1 for LC 2.1). If the anterior end was positioned more ventrally than the posterior end, the orientation was described as “posteriorly inclining” (for example, see Figure 1 for LC 3).

### 3. Results

#### 3.1. Morphological Descriptions

##### 3.1.1. LC1 (Figure 2)

**Type A:** The LCs1 of *Hexanchus nakamurai* (1), *Poroderma africanum* (1), *Alopias vulpinus* (1), *Scyliorhinus canicula* (1), *Scyliorhinus meadi* (1), *Scyliorhinus boa* (1), *Scyliorhinus stellaris* (1), *Mustelus higmani* (1), *Mustelus asterias* (2), *Atelomyxerus macleayi* (2), *Oxynotus centrina* (3), *Centrophorus seychellorum* (3), *Mollisquama parini* (3), *Isistius brasiliensis* (3), *Euprotomicrus bispinatus* (3), *Squalus acanthias* (3), and *Squatina nebulosa* (3) are small (< 1/3 length of the upper jaw), located in the anterior half of the upper jaw in a posteriorly declining or vertical position, and do not protrude from the jaws. In *A. macleayi* and *H. nakamurai*, they display a convex bend, while in *P. africanum*, *C. seychellorum*, *S. nebulosa*, *S. canicula*, and *S. meadi*, they display a concave bend. In all other group members, there is no detectable bend. A ligamentous connection to the upper jaw is possible but not necessarily present.

**Type B:** In *Schroederichthys chilensis* (2), *Brachaelurus waddi* (3), *Chiloscyllium arabicum* (3), *Rhincodon typus* (3), *Squalus brevirostris* (3), *Squalus megalops* (3), *Stegostoma fasciatum* (4), and *Parascyllium collare* (4), the LCs1 are small, positioned in the anterior half of the upper jaw in a posteriorly declining orientation, and protrudes labially. Except for *R. typus*, the LCs1 of all members are slender (< 1/2 length of the upper jaw) and they are tightly connected to the upper jaw in *B. waddi*, *S. megalops*, and *C. arabicum* by ligaments.

**Type C:** The hemiscyliid species *Chiloscyllium indicum* (3), *Chiloscyllium punctatum* (4), *Chiloscyllium griseum* (4), *Hemiscyllium ocellatum* (4), and *Hemiscyllium strahani* (4) possess small LCs1 that are located in the anterior half of the upper jaw, oriented horizontally, and protrude labially.

**Type D:** The LCs1 of *Scoliodon laticaudus* (1), *Sphyrna lewini* (1), *Sphyrna zygaena* (1), *Carcharhinus galapagensis* (2), and *Negaprion brevirostris* (2) are small and slender, located in the posterior half of the upper jaw in a vertical or posteriorly declining position, and do not protrude from the jaw.

**Type E:** In *Triakis semifasciata* (2), *Galeorhinus galeus* (2), *Atelomyxerus marmoratus* (2), *Mustelus manazo* (2) and *Mustelus mustelus* (2), *Centroscymnus crepidater* (3), *Centroscymnus owstonii* (3), *Scymnodon ringens* (3), *Centrophorus uyato* (3) and *Centrophorus tessellatus* (3), *Zameus squamulosus* (3), *Echinorhinus brucus* (3), *Squatina squatina* (3), and *Orectolobus japonicus* (5), the LCs1 are large ( $\geq 1/3$  length of the upper jaw), located in the anterior half of the upper jaw in a posteriorly declining or vertical position, and without any protrusion. Only *S. squatina* displays a notch at the posterior end and, except for *S. ringens* and *G. galeus*, none of the LCs1 are connected to the upper jaw. In *C. crepidater*, *C. uyato*, and *T. semifasciata*, a concave bend is detectable; in *O. japonicus*, multiple bends (S-shaped) are detectable; all other species of this type do not display any bends in their LCs1.

**Type F:** *Galeus melastomus* (2), *Galeus sauteri* (3), *Ginglymostoma cirratum* (3), *Squatina africana* (4), *Eucrossorhinus dasypogon* (5), and *Orectolobus maculatus* (5) possess large LCs1, located in the anterior half of the jaw in a horizontal position, without any labial or anterior protrusion. In *E. dasypogon*, *O. maculatus*, and *G. cirratum*, multiple bends are detectable.

**Type G:** In *Apristurus macrostomus* (2), *Apristurus laurussonii* (2), *Etmopterus lucifer* (2), *Etmopterus sheikoi* (2), and *Etmopterus splendidus* (2), *Squalus suckleyi* (3), *Squalus mitsukurii* (3), *Squalus cubensis* (3), *Chiloscyllium hasselti* (3), and *Deania calcea* (3), the LCs1 are large, located in the anterior half of the upper jaw in a vertical or posteriorly declining position, and protrude labially. They all are slender and, in *S. suckleyi*, *C. hasselti*, *A. macrostomus*, and *A. laurussonii*, they are tightly connected to the upper jaw by ligaments. A convex bend is detectable in the LCs1 of *S. suckleyi* and *E. lucifer*, while in those of *A. macrostomus*, *S. mitsukurii*, and *D. calcea*, a concave bend is detectable. The others display no bends.

**Type H:** The LCs1 of *Carcharhinus macroti* (1), *Hemigaleus microstoma* (1), *Bythaelurus canescens* (2), *Odontaspis ferox* (2), *Chaenogaleus macrostoma* (2), *Hemipristis elongata* (2), *Lepidion smithii* (3), and *Scymnodalatias albicauda* (4) are large, located at half-length of the upper jaw in a posteriorly declining position, and without any protrusion. In *L. smithii* and *C. macroti*, they display a slight concave bend and are connected tightly to the upper jaw by ligaments, as is also the case in *H. microstoma*.

**Subtype i:** In *Nebrius ferrugineus* (3) and *Squatina japonica* (3), the LCs1 are small, located in the anterior half of the upper jaw in a horizontal position without protrusion. They are broad ( $\geq 1/2$  length of the upper jaw) and display a concave bend.

**Subtype ii:** In *Dalatias licha* (3), the LCs1 are small, located in the anterior half in a posteriorly declining or vertical position, and protrude anteriorly.

**Subtype iii:** In *Prionace glauca* (1), *Pristiophorus nudipinnis* (1), and *Carcharhinus falciformis* (2), the LCs1 are small, slender ( $< 1/2$  length of the upper jaw), and without protrusion. In *P. glauca* and *C. falciformis*, they are oriented in a posteriorly declining position, while in *P. nudipinnis*, the LCs1 are oriented horizontally.

**Subtype iv:** The LCs1 of *Chlamydoselachus anguineus* (3) are small, slender, located in the posterior half of the lower jaw in a horizontal position, and display a concave bend.

**Subtype v:** *Mitsukurina owstoni* (2) has small, slender LCs1, located in the posterior half of the upper jaw in a vertical position and that protrude labially.

**Subtype vi:** In *Chiloscyllium plagiosum* (3) and *Hemiscyllium trispeculare* (4), the LCs1 are large ( $\geq 1/3$  length of the upper jaw) and broad, located in the anterior half of the upper jaw in a horizontal position and protrude labially. They are tightly connected to the upper jaw.

**Subtype vii:** In *Heterodontus francisci* (2) and *Heterodontus japonicus* (2), the LCs1 are large, slender, located at half-length of the upper jaw in an almost vertical position, and protrude labially.



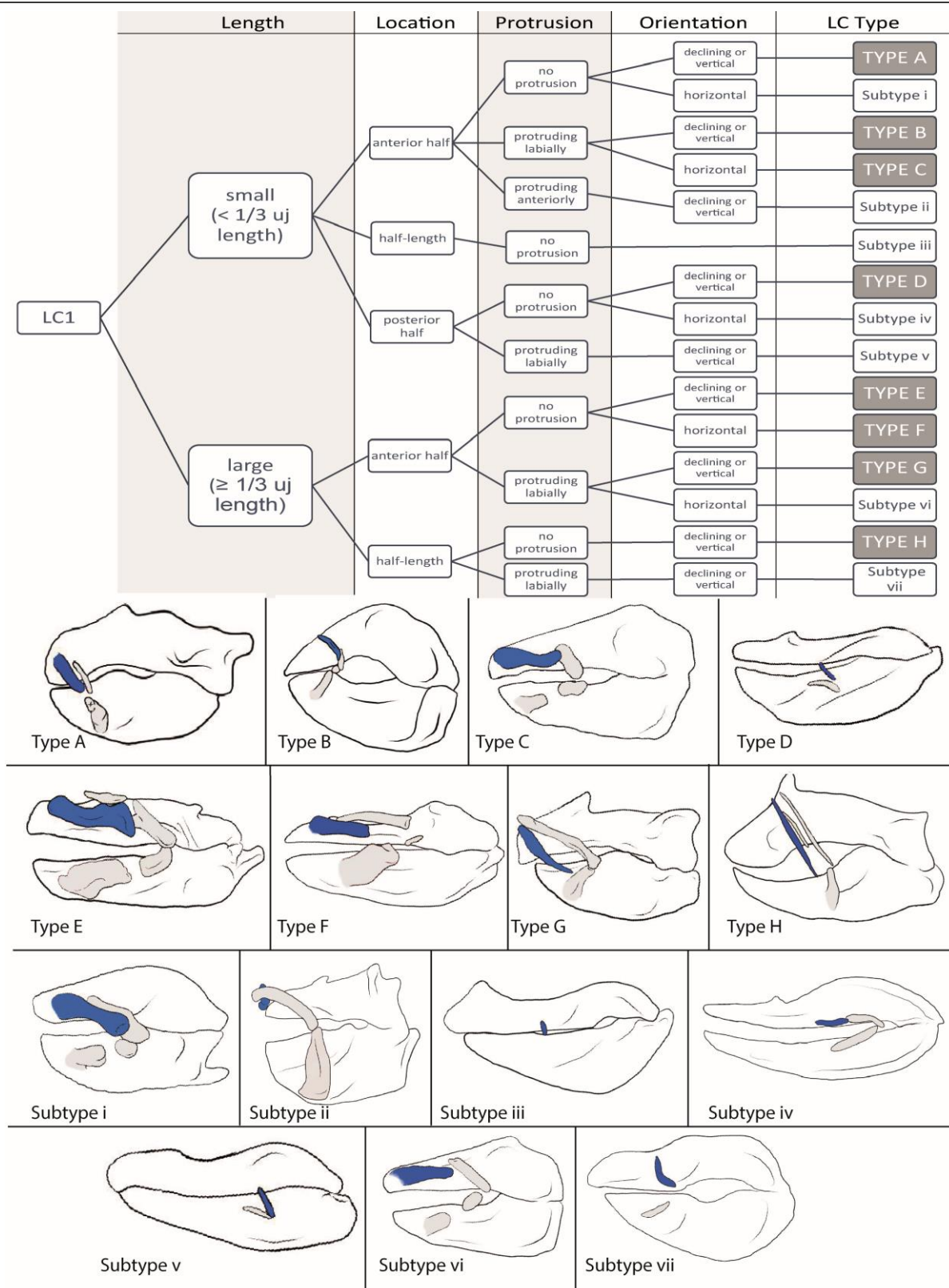


**Figure 2.** Dichotomous identification key for LC1 and sketches of example species of each LC type. Type A = *Oxynotus centrina*; Type B = *Stegostoma fasciatum*; Type C = *Hemiscyllium strahani*; Type D = *Negaprion brevirostris*; Type E = *Orectolobus japonicas*; Type F = *Squatina africana*; Type G = *Deania calcea*; Type H = *Scymnodalatias albicauda*; Subtype i = *Nebrius ferrugineus*; Subtype ii = *Dalatias licha*; Subtype iii = *Prionace glauca*; Subtype iv = *Chlamydoselachus anguineus*; Subtype v = *Mitsukurina owstoni*; Subtype vi = *Hemiscyllium trispeculare*; and Subtype vii = *Heterodontus francisci*.

### 3.1.2. LC2 (Figure 3)

**Type A:** In *Squalus cubensis* (3), *Squalus brevirostris* (3), *Squalus acanthias* (3), *Squalus megalops* (3), *Squalus suckleyi* (3), *Mollisquama parini* (3), *Leptocharias smithii* (3), the centrophorids *Centrophorus seychellorum* (3), *Centrophorus tessellatus* (3), *Centrophorus uyato* (3) and *Deania calcea* (3), the somniosids *Centroscymnus crepidater* (3), *Centroscymnus owstonii* (3), *Scymnodon ringens* (3), *Zameus squamulosum* (3), *Stegostoma fasciatum* (4), and *Scymnodalatias albicauda* (4) as well as in *Parascyllium collare* (4) and the ginglymostomatids *Ginglymostoma cirratum* (4), and *Nebrius ferrugineus* (4), the LCs2 are located in the anterior half of the upper jaw, dorsally to LC1, and in a vertical or posteriorly declining orientation. They are slender ( $< 1/2$  length of upper jaw), display a notch at the posterior end in the ginglymostomatids (*G. cirratum* and *N. ferrugineus*), *C. tessellatus*, and *S. brevirostris*, and is attached to the upper jaw in the somniosids *C. owstonii* and *C. crepidater* by ligaments.

**Type B:** The LCs2 in *Isistius brasiliensis* (3), *Dalatias licha* (3), and *Euprotomicrus bispinatus* (3) and the squatinids *Squatina nebulosa* (3), *Squatina squatina* (3), *Squatina japonica* (3), and *Squatina africana* (4) are located in the anterior tip of the upper jaw, with the onset dorsally to LC1 and extending posteriorly beyond the LC1. They are oriented horizontally, display no kinds of bends, and are, except for those of *S. nebulosa*, considered as broad ( $\geq 1/2$  length of the upper jaw).

**Type C:** In *Brachaelurus waddi* (3), *Rhincodon typus* (3), the hemiscylliids *Chiloscyllium hasselti* (3), *Chiloscyllium plagiosum* (3), *Chiloscyllium indicum* (3), *Chiloscyllium arabicum* (3), *Chiloscyllium griseum* (4), *Chiloscyllium punctatum* (4), *Hemiscyllium strahani* (4), *Hemiscyllium trispeculare* (4), and *Hemiscyllium ocellatum* (4) as well as in the orectolobid species *Eucrossorhinus dasypogon* (5), *Orectolobus japonicas* (5), and *Orectolobus maculatus* (5), the LCs2 are located in the anterior half of the upper jaw, posteriorly to LC1, and oriented vertically or in a posteriorly declining position. The LCs2 are slender ( $< 1/2$  length of upper jaw), except for the orectolobids, in which they are broad and display either no or a slight convex bend. *Rhincondon typus* displays a notch and the orectolobid species display a forking at the posterior end.

**Subtype i:** In *Galeus sauteri* (3) and *Chlamydoselachus anguineus* (3), the LCs2 are located in the posterior half of the upper jaw, posteriorly to LC1. They are slender and oriented obliquely.

**Subtype ii:** *Echinorhinus brucus* (3) and *Oxynotus centrina* (3) have their LCs2 located in the anterior half of the upper jaw, laterally to the LCs1, and in a posteriorly declining orientation. The LCs2 are slender and without bends or notches.

**Subtype iii:** *Squalus mitsukurii* (3) possesses slender LCs2, located in the anterior half of the jaw, ventrally to LC1, and in a posteriorly declining orientation

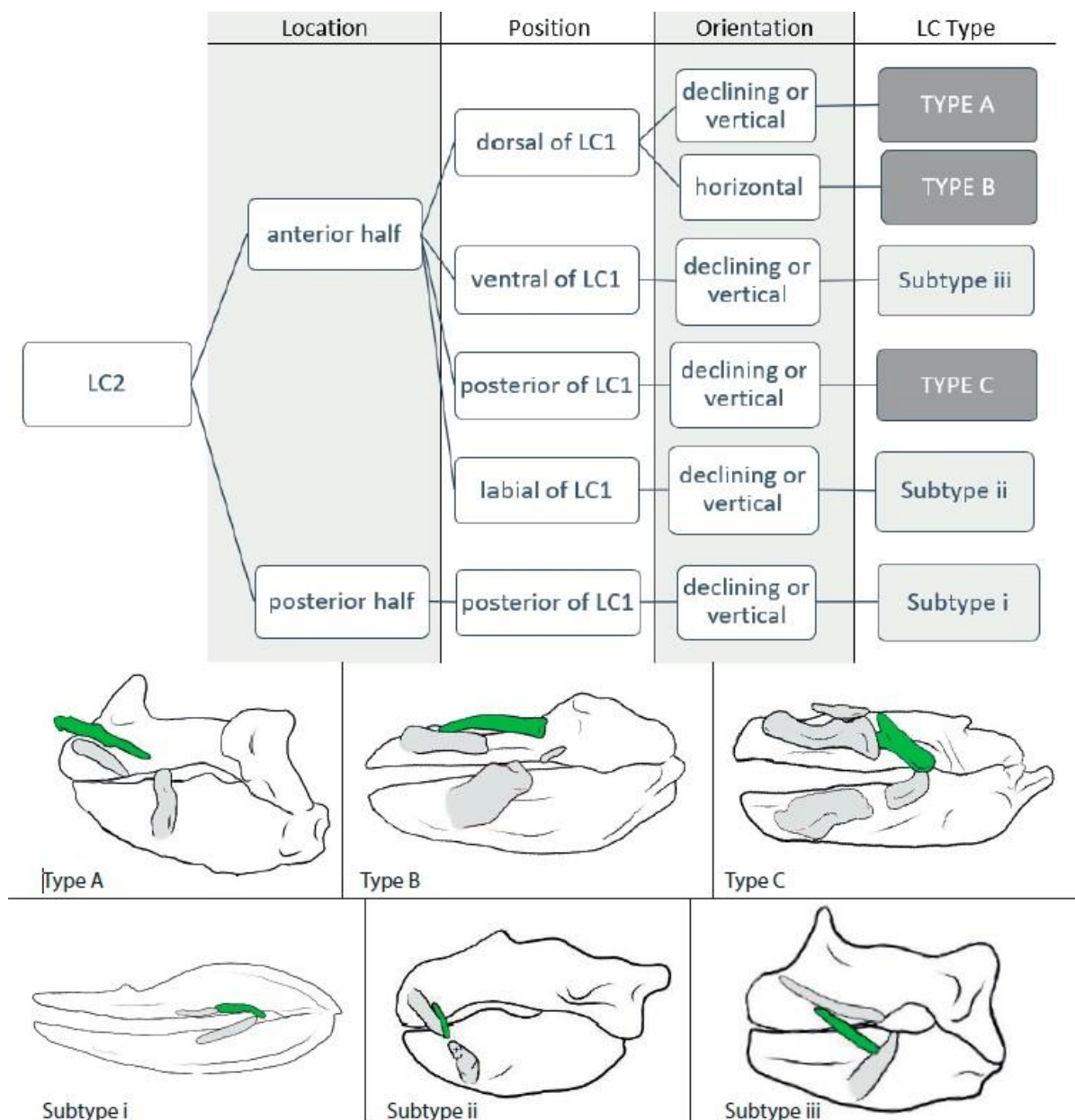


**Figure 3.** Dichotomous identification key for LC2 and sketches of example species of each LC type. Type A = *Squalus acanthias*; Type B = *Squatina africana*; Type C = *Orectolobus japonicus*; Subtype i = *Chlamydoselachus anguineus*; Subtype ii = *Oxynotus centrina*; and Subtype iii = *Squalus mitsukurii*.

### 3.1.3. LC2.1 (Figure 4)

**Type A:** In the orectolobid species *Eucrossorhinus dasypogon* (5), *Orectolobus japonicus* (5), and *Orectolobus maculatus* (5), the LC2.1 are located dorsally to LC1.

**Type B:** In *Scymnodalatias albicauda* (4), the LC2.1 are located between LC1 and LC2 and are oriented almost vertically, as are LC1 and LC2.

### 3.1.4. LC3.1 (Figure 4)

**Type A:** In *Chiloscyllium griseum* (4), *Chiloscyllium punctatum* (4), *Chiloscyllium plagiosum* (4), *Hemiscyllium ocellatum* (4), *Hemiscyllium strahani* (4), and *Hemiscyllium trispiculare* (4) as well as in the orectolobids *Eucrossorhinus dasypogon* (5), *Orectolobus japonicus* (5), and *Orectolobus maculatus* (5), the width of the LC3.1s is about the same as that of the LCs2 and,



therefore, considered as ‘stout’. They are elongated (length > width), oriented posteriorly inclining, and make contact with LC2.

**Type B:** Among *Stegostoma fasciatum* (4) and the members of the ginglymostomatids, *Ginglymostoma cirratum* (4) and *Nebrius ferrugineus* (4), the LC3.1s are also stout, but comparably spherical (length  $\approx$  width).

**Type C:** In *Squatina africana* (4), the LCs3.1 are slender (<  $\frac{1}{2}$  width of LC2) and elongated (length > width).

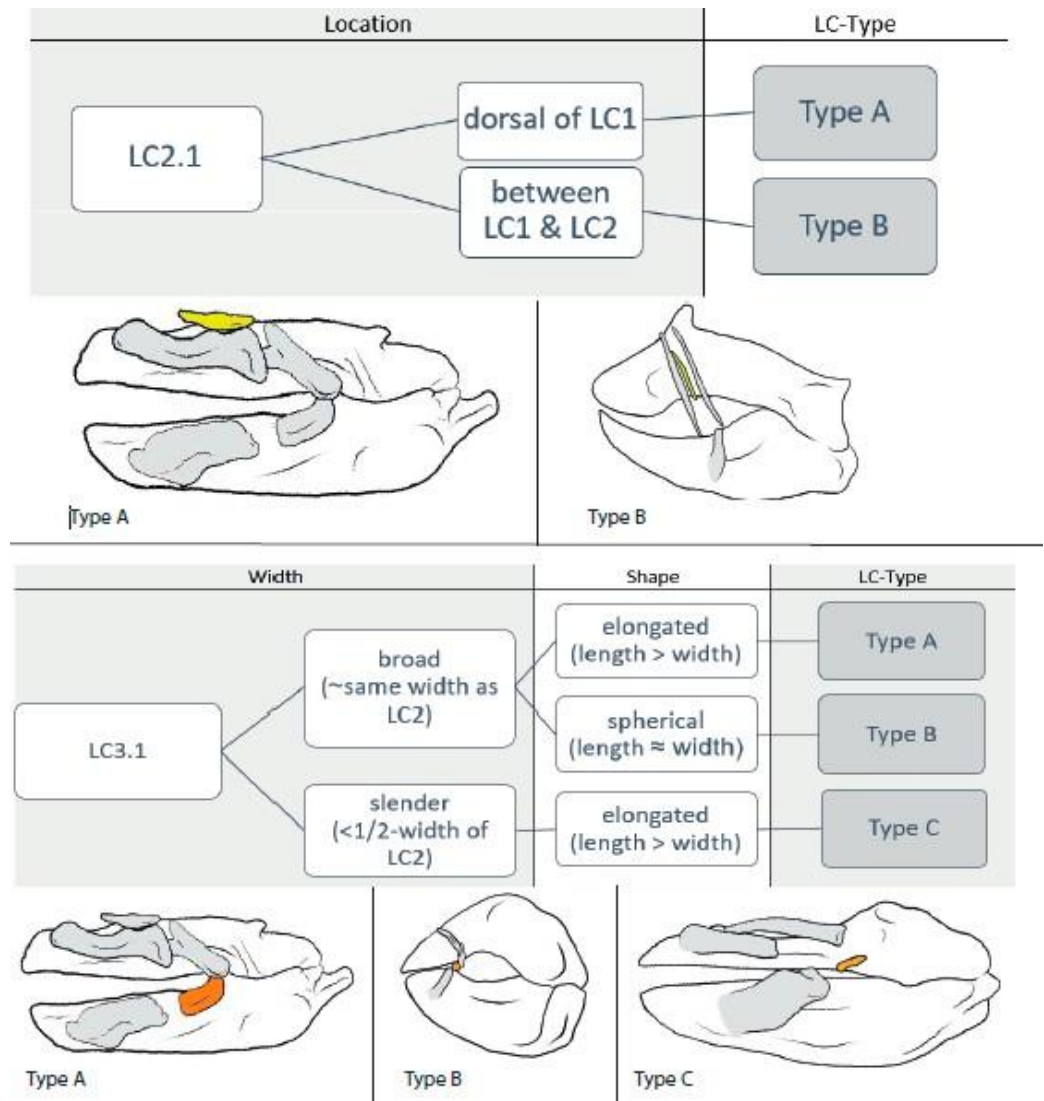


**Figure 4.** Dichotomous identification key for LC2.1 and LC3.1 and sketches of example species of each LC type. LC2.1: Type A = *Orectolobus japonicus*; and Type B = *Scymnodalatias albicauda*. LC3.1: Type A = *Orectolobus japonicus*; Type B = *Stegostoma fasciatum*; and Type C = *Squatina africana*.

### 3.1.5. LC3 (Figure 5)

**Type A:** The LCs3 in *Etmopterus splendidus* (2), *Zameus squamulosus* (3), *Mollisquama parini* (3), *Dalatias licha* (3), *Isistius brasiliensis* (3), *Euprotomicrus bispinatus* (3), *Centroscyrnus owstonii* (3), *Centroscyrnus crepidater* (3), and *Centrophorus tessellatus* (3) are long ( $\geq \frac{1}{3}$  of the lower jaw length) and located in the anterior half of the jaw. They do not protrude from the jaw and are oriented vertically or obliquely either being directed anteriorly or posteriorly. No notch can be detected, and they are always tightly connected to the lower jaw by ligaments.

**Type B:** In *Atelomycterus macleayi* (2), *Atelomycterus marmoratus* (2), *Galeus melastomus* (2), *Galeus sauteri* (2), and *Schroederichthys chilensis* (2), and the orectolobids *Eucrossorhinus dasypogon* (5), *Orectolobus japonicas* (5), and *Orectolobus maculatus* (5), the LCs3, again, are long and located in the anterior half of the jaw, but do protrude labially, are not connected to the lower jaw, and are oriented horizontally. Additionally, in orectolobid species, the LCs3 display a distinct notch or forking at their posterior end.

**Type C:** The LCs3 are long, located in the anterior half of the jaw, protrude labially, and are oriented vertically and obliquely either being directed anteriorly or posteriorly in *Etmopterus lucifer* (2), *Etmopterus sheikoi* (2), *Etmopterus splendidus* (2), *Oxynotus centrina* (3), *Squalus acanthias* (3), *Squalus megalops* (3), *Squalus brevirostris* (3), *Squalus cubensis* (3), *Squalus suckleyi* (3), *Squalus mitsukurii* (3), *Stegostoma fasciatum* (4), and *Parascyllium collare* (4).

**Type D:** Only in *Deania calcea* (3), *Centrophorus scychellorum* (3), and *Centrophorus uyato* (3) are the LCs3 are short ( $<1/3$  of the lower jaw length) and do not protrude from, but are tightly connected to, the lower jaw. They are located in the anterior half of the jaw and oriented posteriorly inclining.

**Type E:** The LCs3 in *Galeorhinus galeus* (2), *Mustelus asterias* (2), *Mustelus mustelus* (2), *Mustelus higmani* (2), *Mustelus manazo* (2), *Odontaspis ferox* (2), *Hemipristis elongata* (2), *Apristurus laurussonii* (2), *Bythaelurus canescens* (2), *Leptocharias smithii* (3), *Brachaelurus waddi* (3), *Rhincodon typus* (3), *Squatina nebulosa* (3), *Squatina squatina* (3), *Squatina japonica* (3), *Squatina africana* (4), *Chiloscyllium plagiosum* (3), *Chiloscyllium hasselti* (3), *Chiloscyllium griseum* (4), *Chiloscyllium punctatum* (4), *Hemiscyllium trispiculare* (4), *Hemiscyllium strahani* (4), and *Hemiscyllium ocellatum* (4) are short, located in the anterior half of the lower jaw, oriented horizontally, and protrude labially. They are roundish in cross-section, except for the LCs of the *Squatina* species, which are flat. Also, in all species of *Squatina*, *Chiloscyllium*, and *Hemiscyllium*, a notch at the posterior end is detectable.

**Type F:** In *Heterodontus francisci* (2), *Heterodontus japonicas* (2), *Apristurus macrostomus* (2), *Triakis semifasciata* (2), *Chiloscyllium indicum* (3), *Chiloscyllium arabicum* (3), *Ginglymostoma cirratum* (3), *Nebrius ferrugineus* (3), *Scymnodon ringens* (3), *Squatina japonica* (3), and *Echinorhinus brucus* (3), the LCs3 are short, located in the anterior half of the jaw, oriented vertically and obliquely either being directed anteriorly or posteriorly, and protrude labially from the jaw.

**Type G:** The carcharhinids *Carcharhinus falciformis* (2), *Carcharhinus galapagensis* (2), and *Negaprion brevirostris* (2) as well as the hemigaleid *Chaenogaleus macrosoma* (2) possess short LCs3 that are located in the posterior half of the jaw, do not protrude, and are oriented horizontally. They are not connected to the lower jaw, are flat, and do not display a notch at either end.

**Subtype i:** *Chlamydoselachus anguineus* (3) possesses a long ( $\geq 1/3$  of lower jaw length) LCs3, which are located in the posterior half of the jaw, oriented horizontally, and are not connected to and do not protrude from the lower jaw.

**Subtype ii:** *Mitsukurina owstonii* (2) has short ( $<1/3$  of the lower jaw length) LCs3, located in the posterior half, protrude labially, and are oriented horizontally, without any connection to the jaw or detectable notch.

**Subtype iii:** *Scymnodalatias albicauda* (4) has short LCs3 that are located in the posterior half of the jaw, protrude labially, are oriented posteriorly inclining, and are tightly connected to the lower jaw.

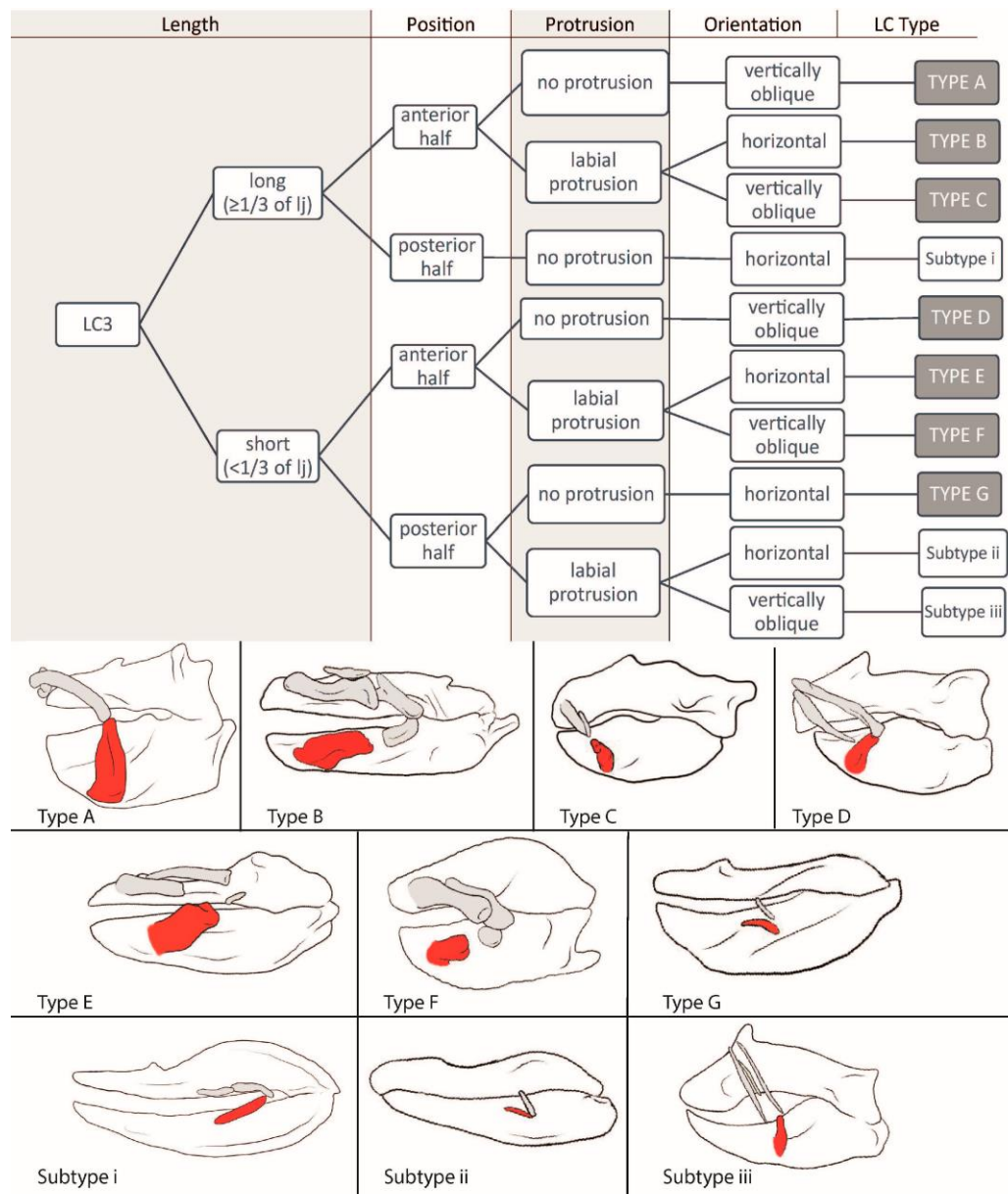


**Figure 5.** Dichotomous identification key for LC3 and sketches of example species of each LC type. Type A = *Dalatias licha*; Type B = *Orectolobus japonicus*; Type C = *Oxynotus centrina*; Type D = *Deania calcea*; Type E = *Squatina africana*; Type F = *Nebrius ferrugineus*; Type G = *Negaprion brevirostris*; Subtype i = *Chlamydoselachus anguineus*; Subtype ii = *Mitsukurina owstoni*; and Subtype iii = *Scymnodalatias albicauda*.

### 3.2. Interpretations

#### 3.2.1. LC1

LC Types D and H as well as Subtypes iii and iv are considered LC1 remnants and are not capable of supporting any kind of suction.

Type A and Subtype i correlate with a biting feeding behavior typical of scavengers or species feeding on immobile prey (as seen in *Oxynotus centrina* in [37]) if a maximum of two LCs is present; in cases with three LCs, a combination of biting and suction is suggested (as seen in *Scyliorhinus canicula* in [38]).

**Types B, C, E, F, and G** as well as **Subtypes ii and vi** are correlated with suction feeding of different strengths, and often occur in combination with another feeding technique (biting or ram) (as seen in *Etmopterus lucifer* in [35]). In Type F and Subtype vi, the suction is considered to be quite strong (as seen in *Chiloscyllium plagiosum* in [39]).

**Subtype v** only occurs in the goblin shark (*Mitsukurina owstoni*), which uses an extraordinary strong jaw protrusion for hunting, and Subtype vii only occurs in horn sharks (Heterodontidae) with their extraordinary massive labial tissues.

### 3.2.2. LC2

**Types A and B** are considered to reinforce LC1 (Type B more and Type A less) or serve as a pivoting point and, therefore, suggest a distinct usage in suction feeding (as seen in *Squatina californica* in [40] and in *Isistius plutodus* in [41]).

**Type C** is aligned with LC1 and, therefore, is considered to enlarge the mouth cavity, which suggests a certain amount of suction (as seen in *Rhincodon typus* in [42]).

**Subtype i** is considered to be a remnant of a formerly mouth-corner-enforcing LC2 (as seen in *Chlamydoselachus anguineus* in [43]), and Subtypes ii and iii suggest for minor suction (as seen in *Oxynotus centrina* in [37]).

### 3.2.3. LC2.1

**Type A** is found in species that create strong suction forces and probably reinforces LC1 so that it can endure higher pressures (as seen in *Orectolobus ornatus* in [44]).

**Type B** is only found in the whitetail dogfish (*Scymnodalatias albicauda*) and, since this is to date the only species with this kind of arrangement, we are not sure whether it is used for creating suction.

### 3.2.4. LC3.1

**Types A and B** are stout and more or less roundish in cross-section, both serving as additional elongations of LCs3 and as extra hinges for a more roundish mouth opening when extended (as seen in *Orectolobus maculatus* in [27]).

**Type C** is found only in one species of squatinids (*Squatina africana*), and we consider it to be the first hint of the development of an additional LC.

### 3.2.5. LC3

**Type A** is considered an anchor point and, therefore, is correlated with the possibility of establishing a longer lasting suction in combination with a biting movement (as seen in *Dalatias licha* in [45]).

**Type B** suggests for a strong suction; since it is oriented horizontally, it is quite moveable and long and sometimes provides a notch for a better joint function (as seen in *Orectolobus maculatus* in [27]).

**Types C, D, and F** are correlated with creating a medium suction force used in combination with other feeding techniques (as seen in *Squalus acanthias* in [44]). It also might correlate with an elongated duration of suction if the LC is directed anteriorly (as seen in *Etmopterus lucifer* in [35]).

**Type E** indicates a medium suction force if three or more LCs are expressed (as seen in *Chiloscyllium plagiosum* in [46]), but only minor suction if a maximum of two LCs is present (as seen in *Odontaspis ferox* in [19]).

**Type G** and Subtypes i, ii, and iii do not support suction behavior and are considered remnants of LCs3 that rather serve as a reinforcement of the mouth corners (as seen in *Chlamydoselachus anguineus* in [43]).

#### 4. Discussion

Feeding strategies in aquatic vertebrates are quite varied [4,47] (Scheme 1), with many groups using suction-feeding strategies for prey capture, since water is a denser medium than air [48]. Our results show that, in sharks, the number and size of LCs and LC combinations are very diverse and reflect the corresponding feeding strategies, ranging from pure ram feeding to all sorts of combinations and pure suction. They display a functional signal that correlates with their ecological niche and should not solely be used for phylogenetic classification [49].

There are several postulations concerning the feeding process that can be derived from the number, position, orientation, and size of the LCs in relation to feeding strategies in sharks. Species without LCs or with only one small LC1 in a position along the posterior half of the jaws (LC1 Types D and H and Subtypes iii and iv) use pure ram feeding or simple biting as the main feeding strategies (compare with [50–52]), whereas the opposite assembly of LCs (high number, strong shape, and anterior position) is related to the use of pure suction (compare with [8,16,28]).

To predict the effectiveness of suction performance during prey capture, we propose employing the following aspects in the following order:

- (1) **Number of LC pairs:** 0–1 = no suction; 2–3 = suction of different intensity used in combination with ram or biting behavior; and 4–5 = strong suction resulting in suction as the predominant or even exclusive feeding mechanism.
- (2) **Position of the LCs:** The further anterior the LCs 1 and 3 are located, the larger the volume of the mouth cavity. The strongest suction is developed when the LCs are in their extended position and the mouth opening is at its peak [8,53]. LCs 2, 2.1, and 3.1 can be aligned with LCs 1 or 3, or parallel to them, which again influences the mouth volume when the mouth is opened. Aligned LCs provide a volume enhancement, while parallel LCs reinforce the existing LCs and thus strengthen the lateral mouth gape walls, enabling them to bear a stronger suction and possibly can somewhat move along the other LCs.
- (3) **Orientation of the LCs:** The more horizontal the LCs are oriented in their resting position, e.g., when the mouth is closed, the larger their movement when the mouth is opened, since they then move antero-labially [28]. This results in a greater enlargement of the mouth cavity and therefore the volume, increasing the suction force. An LC that protrudes labially provides additional support for a larger mouth volume and therefore a stronger suction.
- (4) **Size of the LCs:** The larger a LC is, the more force it can endure, which influences the possible suction strength.

##### 4.1. Number of Labial Cartilages

Small numbers (1–2 pairs) or a complete lack of LCs as well as amplifications to four or five pairs can be considered divergences from the mean number of three pairs occurring in most species that possess LCs. Zero to one LCs are found in some of the most prominent ram-feeding apex predators. In the great white shark (*Carcharodon carcharias*) or the tiger shark (*Galeocerdo cuvier*), no LCs are developed at all. Other known ram-feeding species, such as the blue shark (*Prionace glauca*) or the bonnethead shark (*Sphyrna tiburo*), possess only one pair of very small LCs, which we consider to represent very reduced remnants having no function for creating suction. This led us to the conclusion that 0–1 LC pairs are a good predictor of pure ram feeding or biting behavior.



Two to three LCs are found in species that use a combination of suction and biting and/or ram feeding. Some of these sharks are generalists (e.g., *Chiloscyllium plagiosum* in [39] and *Galeus melastomus* in [54]), while others display a very distinct hunting behavior (e.g., *Heterodontus francisci* in [18], *Rhincodon typus* in [55], and *Isistius brasiliensis* in [56]).

Four to five LCs are found typically in ambush predators, such as the Japanese wobbegong shark (*Orectolobus japonicas*) or the nurse shark (*Ginglymostoma cirratum*), which predominantly employ effective suction to capture prey [16,28]. This led us to the conclusion that a high number of LCs reliably indicates a suction feeding behavior with a strong suction performance.

#### 4.2. Shapes of Labial Cartilages

The general shape of single LCs provides an insight into the movement capabilities of the whole LC apparatus. Small, roundish LCs are likely to serve as a kind of pivoting point, allowing a stronger rotation of the LC apparatus, while broad, elongated LCs add to the enlargement of the mouth cavity volume and LCs with a forking in their posterior end are assumed to provide a stronger connection to the next aligned LC, forming a joint with higher stability and therefore capable of enduring a stronger suction. The longer the LC, the more it adds to the total length of the complete LC arch and, therefore, allows for a larger mouth volume extension when the mouth is opened, which induces suction. Short, thin LCs are often located midway along the jaws or along the posterior half; we assume that they strengthen the mouth corners to prevent the prey from escaping [24], rather than being capable of creating a significant suction.

#### 4.3. Labial Cartilage Mobility and Adaptations for Special Feeding Strategies

The range of mobility seemingly increases if three or more LCs are developed. This relates to the fact that at least one of those LCs is not connected tightly to the jaw by ligaments and, therefore, allows a greater moveability. We postulate that the more freely moveable the LCs are, the greater is their influence on the feeding strategy (additionally to the above-stated number, position, orientation, and size). We assume that either the LC2 can partially slide over LC1 and therefore can extend the LC arch, similar to the movement actions of the premaxilla and maxilla in suction-feeding teleosts [57], or the LC2 reinforces the LC1, making this arrangement more robust and capable of enduring higher pressures in species in which the LC2 is located dorsally to LC1.

In the cookie-cutter shark (*Isistius brasiliensis*), the small LC1 can be considered to work as a rotation point, which extends the anatomically possible movement of LC2 labially, forming an entirely ovoid mouth opening that attaches perfectly to a smooth surface leaving no gaps. Also, Jones [58] described its basihyoid cartilage to be able to change its position so that it completely separates the mouth cavity from the pharynx. These modifications allow the cookie-cutter shark to generate a longer-lasting suction, comparable to that of a suction cup. This matches the current state of knowledge about the feeding strategy of the cookie-cutter shark, as it sucks onto larger prey animals, burying its teeth into the flesh and cutting out pieces of flesh by rotating around its own body axis, therefore combining suction and biting in its hunting strategy [56,58–60].

According to the LC arrangement, the kitefin shark (*Dalatias licha*) and probably also the pygmy shark (*Euprotomicrus bispinatus*), of which we cannot be sure due to the bad quality of the scan, might use a similar feeding strategy to that of the cookie-cutter shark or at least are capable of producing a suction of similar strength to that of the cookie-cutter shark.

Members of the Heterodontidae have developed another hunting strategy that is also reflected in their LC arrangement. Horn sharks mainly feed on benthic, sessile, or slow-moving prey. Usually, they make contact with the prey item with their snout first and then initialize a short suction strike, whose strength is comparable to the suction used by nurse sharks [4,16,18,47,53]. Their LCs differ from those of all other sharks since they are oriented in a unique way: from a lateral perspective, they resemble an arrow with the tip pointing slightly anteriorly (whereas in all other sharks it is pointing posteriorly); and from a frontal perspective, it can be seen that the LCs stick out labially, even during the resting position (mouth closed). The surrounding labial tissue is comparatively massive in horn sharks and allows a very rapid anterior movement of the LCs, which results in the observed short, but strong suction burst, enabling a precise hunting strike on a short distance. Also, the mouth opening is very small, which additionally intensifies the suction effect. The LCs move anteriorly when the jaw extension reaches its maximum [18], providing contact with the surface or the prey and therefore also preventing the prey from escaping, as was previously suggested by Huber et al. [61].

Many benthic living shark species, like angel sharks (Squatiniiformes) or some members of the carpet sharks (Orectolobiformes), specialize in ambush predation. They stay motionless on the ground until a potential prey comes within a certain range of their mouth and then rapidly expand their mouth cavity to create a strong suction that pulls the prey deep into the enlarged mouth cavity [27,40,44,62]. This hunting behavior is reflected in their LC apparatus too: All ambush predators possess at least three, sometimes even four or five pairs of LCs, which are located at the anterior end of the jaws. There are three possibilities in LC arrangement: (1) three pairs of massive LCs (e.g., *Squatina africana*), (2) four pairs of medium-sized LCs with an onset at the anterior tip of the jaws (e.g., *Chiloscyllium punctatum*), and (3) five pairs of massive LCs, with LC2.1 reinforcing LC1 and LC2 displaying a distinct posterior forking (e.g., *Orectolobus japonicas*). In the case of arrangements (2) and (3), the middle joint is formed by LC2 and the smaller, roundish LC3.1.

The whitetail dogfish (*Scymnodalatias albicauda*) is one of the least known species. It also displays a unique set of LCs that does not match any other combination, which makes suggesting a feeding strategy hard, but according to the scarce knowledge of its behavior and its overall body shape, we suggest that it is only capable of producing a minor suction force or no suction at all.

#### 4.4. Labial Cartilage Combinations

The possible LC combinations and their relation to the suction capability of the corresponding shark species are depicted in Table 2 (For a list of all the feeding mechanisms of the discussed species, see Supplementary Table S2).

**Table 2.** Combinations of LCs, the corresponding suction capabilities, and the suspected feeding strategy it leads to (marked by an arrow).

LC1	LC2	LC2.1	LC3.1	LC3	Suction capabilities	Example species from Dataset
ILC only (no matter which)						
D/H/iii	-	-	-	G	no suction → biting or ram	Blue shark ( <i>Prionace glauca</i> ) Lemon shark ( <i>Negaprion brevirostris</i> )
V	-	-	-	ii	no suction → extreme jaw protrusion	Goblin shark ( <i>Mitsukurina owstonii</i> )
H	-	-	-	E	minor to no suction → biting	Smalltooth sand tiger ( <i>Odontaspis ferox</i> )
H	A	-	B	iii	Minor to no suction (uncertain)	Whitetail dogfish ( <i>Scymnodalatias albicauda</i> )
A/E/F	(i)	-	-	B		Blacktip sawtail catshark ( <i>Galeus sauteri</i> )
A/E/G	-	-	-	E/F		Smooth-hound ( <i>Mustelus mustelus</i> )
G	-	-	-	C	minor suction → generalist, mainly biting	Blackbelly lanternshark ( <i>Etmopterus lucifer</i> )
iv	i	-	-	i		Frisled shark ( <i>Chlamydoselachus anguineus</i> )
H	A	-	-	E		Barbeled houndshark ( <i>Leptocharias smithii</i> )
E	ii	-	-	F	medium to minor suction	Bramble shark ( <i>Echinorhinus brucus</i> )
E	A	-	-	A	→ probably scavenger	Mosaic gulper shark ( <i>Centrophorus tessellatus</i> )
B/C/G/vi	C	-	(A)	E/F	medium suction + biting or ram → more effective when close to the ground or the surface	Whale shark ( <i>Rhincodon typus</i> )
A/E/G	A	-	-	A/D/F	medium suction →	Knifetooth dogfish ( <i>Scymnodon ringens</i> )
A/B/G	A/ii/iii	-	-	C	generalist, mainly benthic prey	Angular roughshark ( <i>Oxynotus centrina</i> )
B	-	-	-	B		Redspotted catshark ( <i>Schroederichthys chilensis</i> )
A/ii	A/B	-	-	A	strong to medium suction → capable of longer lasting (comparable to suction cup), used for ectoparasitism	Cookie-cutter shark ( <i>Isistius brasiliensis</i> )
vii	-	-	-	F	strong, short suction → mainly sessile prey	Horn shark ( <i>Heterodontus francisci</i> )
E/F	C	A	A	B	strong suction → benthic ambush predator	Japanese wobbegong ( <i>Orectolobus japonicus</i> )
A/E/F/i	B	-	(C)	E	strong suction → benthic ambush predator leaping from the bottom for strikes	Angelshark ( <i>Squatina squatina</i> )
B/F/i	A	-	B	C/F	strong suction → benthic generalist	Nurse shark ( <i>Ginglymostoma cirratum</i> )



## 5. Conclusions

Based on the knowledge of the feeding strategies in some species and the collected data on labial cartilages (LCs) of over 100 shark species, we were able to relate specific LC apparatus constellations to certain feeding strategies and consequently also to their probable hunting behaviors. The detailed account of the skeletal structures provided in this study allows some general and specific conclusions: (1) Sharks practicing ram feeding either lack LCs completely or only possess remnants of LCs, either of only LC1 or of LC1 and LC3, which then are generally located in the middle or in the posterior half of the jaws. Those sharks mainly occupy higher trophic levels, including apex predators representing tertiary and quaternary consumers, and the majority lives in pelagic waters, hunting actively. (2) Sharks using suction feeding, conversely, possess higher numbers (up to five pairs) of well-developed LCs that are located in the anterior half of the jaws. Such sharks occupy slightly lower trophic levels, representing mainly secondary consumers (e.g., Orectolobiforms and Heterodontiforms) and are, at least partially, benthic. (3) The whole LC apparatus is necessary to predict suction capabilities and therefore a feeding technique, since not only the number, but also the position, orientation, moveability, and combination of LCs are important contributors. This information and the conclusions derived from our study consequently allow to predict feeding and hunting strategies in rare extant sharks, for which behavioral observations are lacking, or even extinct sharks, for which corresponding behavioral observations are impossible. Such a study was beyond the scope of the present paper, but will be conducted in the near future by the authors. In extant shark species, it might even provide information that is helpful for defining conservation measures to protect sharks and their surrounding ecosystems along with them.

**Supplementary Materials:** The following supporting information can be downloaded at: <https://www.mdpi.com/article/10.3390/biology12121486/s1>, Table S1: species overview; Table S2: feeding mechanisms. References [17,18,27,28,37,39,41–46,50,55,56,58,59,61–67] are cited in the supplementary materials.

**Author Contributions:** Conceptualization, C.K. and J.K.; methodology, C.K.; data curation, C.K.; writing—original draft preparation, C.K.; writing—review and editing, J.K.; visualization, C.K.; supervision, J.K. All authors have read and agreed to the published version of the manuscript.

**Funding:** This research was funded in whole by the Austrian Science Fund (FWF) (P 33820). For the purpose of open access, the authors have applied a CC BY public copyright license to any Author Accepted Manuscript version arising from this submission. Open Access Funding by the Austrian Science Fund (FWF).

**Institutional Review Board Statement:** Not applicable.

**Informed Consent Statement:** Not applicable.

**Data Availability Statement:** The data presented in this study are openly available in <https://sharkrays.org/>; <https://figshare.com/>.

**Conflicts of Interest:** The authors declare no conflict of interest.

## References

1. Maisey, J.G. What is an ‘elasmobranch’? The impact of palaeontology in understanding elasmobranch phylogeny and evolution. *J. Fish Biol.* 2012, 80, 918–951. [[CrossRef](#)] [[PubMed](#)]
2. Cappetta, H. *Handbook of Paleoichthyology. Volume 3B. Chondrichthyes II. Mesozoic and Cenozoic Elasmobranchii*; Fischer Verlag: Stuttgart, Germany, 1987.
3. Klug, S. Monophyly, phylogeny and systematic position of the †Synchodontiformes (Chondrichthyes, Neoselachii). *Zool. Scr.* 2010, 39, 37–49. [[CrossRef](#)]
4. Huber, D.; Wilga, C.D.; Dean, M.; Ferry, L.; Gardiner, J.; Habegger, L.; Papastamatiou, Y.; Ramsay, J.; Whitenack, L. Feeding in Cartilaginous Fishes: An Interdisciplinary Synthesis. In *Feeding in Vertebrates: Evolution, Morphology, Behavior, Biomechanics*; Bels, V., Whishaw, I.Q., Eds.; Springer: Cham, Switzerland, 2019.
5. Dick, J.R.F. On the Carboniferous shark *Tristychius arcuatus* Agassiz from Scotland. *Earth Environ. Sci. Trans. R. Soc. Edinb.* 1978, 70, 63–109. [[CrossRef](#)]
6. Maisey, J.G. The Anatomy and Interrelationships of Mesozoic Hybodont Sharks. *Am. Mus. Novit.* 1982, 2724, 1–48.
7. Maisey, J.G. Cranial anatomy of *Hybodus basanus* Egerton from the Lower Cretaceous of England. *Am. Mus. Novit.* 1983, 2758, 59–64.
8. Motta, P.J.; Wilga, C.D. Advances in the study of feeding behaviors, mechanisms, and mechanics of sharks. *Environ. Biol. Fishes* 2001, 60, 131–156. [[CrossRef](#)]
9. Klug, S.; Kriwet, J.; Böttcher, R.; Schweitert, G.; Dietl, G. Skeletal anatomy of the extinct shark *Paraorthacodus jurensis* (Chondrichthyes; Palaeospinacidae), with comments on synchodontiform and palaeospinacid monophyly. *Zool. J. Linn. Soc.* 2009, 157, 107–134. [[CrossRef](#)]
10. Coates, M.I.; Tietjen, K.; Olsen, A.M.; Finarelli, J.A. High-performance suction feeding in an early elasmobranch. *Sci. Adv.* 2019, 5, eaax2742. [[CrossRef](#)]
11. Dean, M.N.; Huber, D.R.; Nanace, H.A. Functional Morphology of Jaw Trabeculation in the Lesser Electric Ray *Narcine brasiliensis*, With comments on the Evolution of Structural Support in the Batoidea. *J. Morphol.* 2006, 267, 1137–1146. [[CrossRef](#)] [[PubMed](#)]
12. Dean, M.N.; Azizi, E.; Summers, A.P. Uniform strain in broad muscles: Active and passive effects of the twisted tendon of the spotted ratfish *Hydrolagus collieli*. *J. Exp. Biol.* 2007, 210, 3395–3406. [[CrossRef](#)]
13. Dean, M.N.; Summers, A.P.; Ferry, L.A. Very Low Pressures Drive Ventilatory Flow in Chimaeroid Fishes. *J. Morphol.* 2012, 273, 461–479. [[CrossRef](#)]
14. Dearden, R.P.; Mansuit, R.; Cuckovic, A.; Herrel, A.; Didier, D.; Tafforeau, P.; Pradel, A. The morphology and evolution of chondrichthyan cranial muscles: A digital dissection of the elephantfish *Callorhynchus milii* and the catshark *Scyliorhinus canicular*. *J. Anat.* 2021, 238, 1081–1105. [[CrossRef](#)]
15. Denison, R.H. Anatomy of the head and pelvic fin of the Whale Shark, *Rhineodon*. *Bull. Am. Mus. Nat. Hist.* 1937, 73, 477–515.
16. Motta, P.J.; Wilga, C.D. Anatomy of the feeding apparatus of the nurse shark, *Ginglymostoma cirratum*. *J. Morphol.* 1999, 241, 33–60. [[CrossRef](#)]
17. Gardiner, J.M.; Atema, J.; Hueter, R.E.; Motta, P.J. Modulation of shark prey capture kinematics in response to sensory deprivation. *Zoology* 2017, 120, 42–52. [[CrossRef](#)] [[PubMed](#)]
18. Edmonds, M.A.; Motta, P.J.; Hueter, R.E. Food capture kinematics on the suction feeding horn shark, *Heterodontus francisci*. *Environ. Biol. Fishes* 2001, 62, 415–427. [[CrossRef](#)]
19. Shimada, K.; Rigsby, C.K.; Kim, S.H. Labial cartilages in the smalltooth Sandtiger shark, *Odontaspis ferox* (Lamniformes: Odontaspidae) and their significance to the phylogeny of lamniform sharks. *Anat. Rec.* 2009, 292, 813–817. [[CrossRef](#)]
20. Gegenbauer, C. *Untersuchungen zur vergleichenden Anatomie der Wirbeltiere—Heft 3: Das Kopfskelett der Selachier, als Grundlage zur Beurtheilung der Genese des Kopfskeletes der*

- Wirbelthiere*; W. Engelmann Verlag: Leipzig, Germany, 1872; p. 316 ff. [CrossRef]
21. Pollard, H.B. Oral cirrhi of siluroids and the origin of the head in vertebrates. *Zool. Jahrb. (Abt. Anat.)* 1895, 8, 379–424.
  22. Swertsoff, A.N. Etudes sur l'évolution des vertèbres inférieurs—1. Morphologie du squelette et de la musculature de la tête des cyclostomes. *Arch. Russes Anat. Histol. Embryol.* 1916, 1, 1–104.
  23. Goodrich, E.S. *Studies on the Structure & Development of Vertebrates*; Macmillan & Company: London, UK, 1930.
  24. Smith, B.G. *The Bashford Dean Memorial Volume of Archaic Fishes—Article VI: The Anatomy of the Frilled Shark *Chlamydoselachus anguineus* Garman*; American Museum of Natural History: New York, NY, USA, 1937; pp. 330–498.
  25. Veran, M. Are the labial cartilages of Chondrichthyans homologous to the labial bone of the primitive fossil actinopterygians? *Geobios* 1995, 19, 161–166. [CrossRef]
  26. Klimpfner, C.; Kriwet, J. Comparative morphology of labial cartilages in sharks (Chondrichthyes, Elasmobranchii). *Eur. Zool. J.* 2020, 87, 741–753. [CrossRef]
  27. Wu, E.H. Kinematic Analysis of Jaw Protrusion in Orectolobiform Sharks: A New Mechanism for Jaw Protrusion in Elasmobranchs. *J. Morphol.* 1994, 222, 175–190. [CrossRef]
  28. Motta, P.J.; Hueter, R.E.; Tricas, T.C.; Summers, A.P.; Huber, D.R.; Lowry, D.; Mara, K.R.; Matott, M.P.; Whitenack, L.B.; Wintzer, A.P. Functional Morphology of the Feeding Apparatus, Feeding Constraints, and Suction Performance in the Nurse Shark *Ginglymostoma cirratum*. *J. Morphol.* 2008, 269, 1041–1055. [CrossRef]
  29. Brazeau, M.; Kamminga, P.; De Bruin, P.W.; Geleijns, J. X-ray Computed Tomography Library of Shark Anatomy and Lower Jaw Models. On: Figshare. Collection. Available online: <https://doi.org/10.6084/m9.figshare.c.3662366.v1> (accessed on 15 November 2023).
  30. Kamminga, P.; de Bruin, P.W.; Geleijns, J.; Brazeau, M.D. X-ray computed tomography library of shark anatomy and lower jaw surface models. *Sci. Data* 2017, 4, 170047. [CrossRef] [PubMed]
  31. Chondrichthyan Tree of Life. Available online: <https://sharkrays.org/> (accessed on 25 October 2023).
  32. Corrigan, S.; Naylor, G.; Yang, L. The Chondrichthyan Tree of Life Project: Taking Stock of the World's Sharks and Rays, Copyright Experiment 2023. Available online: <https://experiment.com/projects/the-chondrichthyan-tree-of-life-project-taking-stock-of-the-world-s-sharks-and-rays> (accessed on 24 October 2023).
  33. White, P.J. XV.—The skull and visceral skeleton of the Greenland shark, *Læmargus microcephalus*. *Earth Environ. Sci. Trans. R. Soc. Edinb.* 1895, 37, 287–306. [CrossRef]
  34. Summers, A.P.; Ketcham, R.A.; Rowe, T. Structure and Function of the Horn Shark (*Heterodontus francisci*) Cranium Through Ontogeny: Development of a Hard Prey Specialist. *J. Morphol.* 2004, 260, 1–12. [CrossRef] [PubMed]
  35. Staggli, M.A.; Ruthensteiner, B.; Straube, N. Head anatomy of a lantern shark wet-collection specimen (Chondrichthyes: Etmopteridae). *J. Anat.* 2023, 242, 872–890. [CrossRef]
  36. Lavenberg, R.J.; Seigel, J.A. The Pacific's megamystery-Megamouth. *Terra* 1985, 23, 29–31.
  37. Capapé, C. Diet of the Angular rough shark *Oxynotus centrina* (Chondrichthyes: Oxynotidae) off the Languedocian coast (Southern France, North-Western Mediterranean). *Vie Milieu—Life Environ.* 2008, 58, 57–61.
  38. Wicczorek, A.M.; Power, A.M.; Browne, P.; Graham, C.T. Stable-isotope analysis reveals the importance of soft-bodied prey in the diet of lesser spotted dogfish *Scyliorhinus canicula*. *J. Fish Biol.* 2018, 93, 685–693. [CrossRef]
  39. Scott, B.; Wilga, C.A.D.; Brainerd, E.L. Skeletal kinematics of the hyoid arch in the suction-feeding shark *Chiloscyllium plagiosum*. *J. Exp. Biol.* 2019, 222, jeb193573. [CrossRef]
  40. Fouts, W.R.; Nelson, D.R. Prey Capture by the Pacific Angel Shark, *Squatina californica*: Visually Mediated Strikes an Ambush-Site Characteristics. *Copeia* 1999, 2, 304–312. [CrossRef]

41. De Figueiredo Petean, F.; de Carvalho, M.R. Comparative morphology and systematics of the cookiecutter sharks, genus *Isistius* Gill (1864) (Chondrichthyes: Squaliformes: Dalatiidae). *PLoS ONE* 2018, *13*, e0201913. [CrossRef] [PubMed]
42. Cade, D.E.; Levenson, J.J.; Cooper, R.; de la Parra, R.; Webb, D.H.; Dove, A.D.M. Whale sharks increase swimming effort while filter feeding, but appear to maintain high foraging efficiencies. *J. Exp. Biol.* 2020, *223*, jeb224402. [CrossRef]
43. Wilga, C.D. A functional analysis of jaw suspension in elasmobranchs. *Biol. J. Linn. Soc.* 2002, *75*, 483–502. [CrossRef]
44. Ramsay, J.B. A Comparative Investigation of Cranial Morphology, Mechanics, and Muscle Function in Suction and Bite Feeding Sharks. Ph.D. Thesis., University of Rhode Island, Kingston, RI, USA, 2012.
45. Denton, J.S.S.; Maisey, J.G.; Grace, M.; Pradel, A.; Doozey, M.H.; Bart, H.L., Jr.; Naylor, G.J.P. Cranial morphology in *Mollisquama* sp. (Squaliformes; Dalatiidae) and patterns of cranial evolution in dalatiid sharks. *J. Anat.* 2018, *233*, 15–32. [CrossRef]
46. Nauwelaerts, S.; Wilga, C.; Sanford, C.; Lauder, G. Hydrodynamics of prey capture in sharks: Effects of substrate. *J. R. Soc. Interface* 2007, *4*, 341–345. [CrossRef] [PubMed]
47. Bels, V.; Whishaw, I.Q. *Feeding in Vertebrates: Evolution, Morphology, Behavior, Biomechanics*; Springer: Cham, Switzerland, 2019. [CrossRef]
48. Cortés, E.; Papastamatiou, Y.P.; Carlson, J.K.; Ferry-Graham, L.; Wetherbee, B.M. An Overview of the Feeding Ecology and Physiology of Elasmobranch Fishes. In *Feeding and Digestive Functions of Fishes*; Cyrino, J.E.P., Bureau, D.P., Kapoor, B.G., Eds.; Science Publishers: Enfield, NH, USA, 2008; pp. 393–443. ISBN 9781578083756.
49. Klimpfinger, C. Variability of Labial Cartilages in Sharks—Functional or Phylogenetic Signal? Morphological Descriptions and Phylogenetic Analysis. Master Thesis, University of Vienna, Vienna, Austria, 2022. Available online: <https://ubdata.univie.ac.at/AC16587802> (accessed on 24 October 2023).
50. Tricas, T.C. Feeding Ethology of the White Shark, *Carcharodon carcharias*. *Memoirs* 1985, *9*, 81–91.
51. Ebert, D.A. Observations on the predatory behaviour of the sevengill shark *Notorynchus cepedianus*. *S. Afr. J. Mar. Sci.* 1991, *11*, 455–465. [CrossRef]
52. Moyer, J.K.; Shannon, S.F.; Irschick, D.J. Bite performance and feeding behaviour of the sand tiger shark *Carcharias taurus*. *J. Fish Biol.* 2019, *95*, 881–892. [CrossRef]
53. Ferry, L.A.; Paig-Tran, E.M.; Gibbs, A.C. Suction, ram, and biting: Deviations and limitations to the capture of aquatic prey. *Integr. Comp. Biol.* 2015, *55*, 97–109. [CrossRef]
54. D'Iglio, C.; Savoca, S.; Rinelli, P.; Spanò, N.; Capillo, G. Diet of the Deep-Sea Shark *Galeus melastomus* Rafinesque 1810, in the Mediterranean Sea: What We Know and What We Should Know. *Sustainability* 2021, *13*, 3962. [CrossRef]
55. Motta, P.J.; Maslanka, M.; Hueter, R.E.; Davis, R.L.; de la Parra, R.; Mulvany, S.L.; Habegger, M.L.; Strother, J.A.; Mara, K.R.; Gardiner, J.M.; et al. Feeding anatomy, filter-feeding rate, and diet of whale sharks *Rhincodon typus* during surface ram filter feeding off the Yucatan Peninsula, Mexico. *Zoology* 2010, *113*, 199–212. [CrossRef] [PubMed]
56. Papastamatiou, Y.P.; Wetherbee, B.M.; O'Sullivan, J.; Goodmanlowe, G.D.; Lowe, C.G. Foraging ecology of cookiecutter sharks (*Isistius brasiliensis*) on pelagic fishes in Hawaii, inferred from prey bite wounds. *Environ. Biol. Fishes* 2010, *88*, 361–368. [CrossRef]
57. Day, S.W.; Higham, T.E.; Holzmah, R.; van Wassenberg, S. Morphology, Kinematics, and Dynamics: The Mechanics of Suction Feeding in Fishes. *Soc. Integr. Comp. Morphol.* 2015, *55*, 21–35. [CrossRef] [PubMed]
58. Jones, E.C. *Isistius brasiliensis*, a Squaloid Shark, the Probable Cause of Crater Wounds on Fishes and Cetaceans. *Fish. Bull.* 1971, *69*, 791–798.
59. Shirai, S.; Nakaya, K. Functional morphology of feeding apparatus of the cookie-cutter shark,



- Isistius brasiliensis* (Elasmobranchii, Dalatiinae). *Zool. Sci.* 1992, 9, 811–821.
60. Hoyos-Padilla, M.; Papastamatiou, Y.P.; O’Sullivan, J.; Lowe, C.G. Observation of an attack by a cookiecutter shark (*Isistius brasiliensis*) on a White Shark (*Carcharodon carcharias*). *Pac. Sci.* 2013, 67, 129–134. [[CrossRef](#)]
  61. Huber, D.R.; Eason, T.G.; Hueter, R.E.; Motta, P.J. Analysis of the bite force and mechanical design of the feeding mechanism of the durophagous horn shark *Heterodontus fancisci*. *J. Exp. Biol.* 2005, 208, 3553–3571. [[CrossRef](#)]
  62. Motta, P.J.; Hueter, R.E.; Tricas, T.C.; Summers, A.P. Kinematic Analysis of Suction Feeding in the Nurse Shark, *Ginglymostoma cirratum* (Orectolobiformes, Ginglymostomatidae). *Copeia* 2002, 1, 24–38. [[CrossRef](#)]
  63. Kryukova, N.V.; Kuznetsov, A.N. Suboccipital muscle of sharpnose sevengill shark *Heptranchias perlo* and its possible role in prey dissection. *Journal of Morphology* 2020, 281, 842–861. [[CrossRef](#)] [[PubMed](#)]
  64. Grant, S.M.; Sullivan, R.; Hedges, K.J. Greenland shark (*Somniosus microcephalus*) feeding behavior on static fishing gear, effect of SMART (Selective Magnetic and Repellent-Treated) hook deterrent technology, and factors influencing entanglement in bottom longlines. *PeerJ* 2018, 6. [[CrossRef](#)]
  65. Wilga, C.D.; Motta, P.J.; Sanford, C.P. Evolution and ecology of feeding in elasmobranchs. *Integr. Comp. Biol.* 2007, 47, 55–69. [[CrossRef](#)]
  66. Tomita, T.; Sato, K.; Suda, K.; Kawauchi, J.; Nakaya, K. Feeding of the Megamouth Shark (Pisces: Lamniformes: Megachasmidae) Predicted by Its Hyoid Arch: A Biomechanical Approach. *J. Morphol.* 2011, 272, 513–524. [[CrossRef](#)] [[PubMed](#)]
  67. Motta, P.J.; Wilga, C.A.D. Anatomy of the Feeding Apparatus of the Lemon Shark, *Negaprion brevirostris*. *J. Morphol.* 1995, 226, 309–329. [[CrossRef](#)]

**Disclaimer/Publisher’s Note:** The statements, opinions and data contained in all publications are solely those of the individual author(s) and contributor(s) and not of MDPI and/or the editor(s). MDPI and/or the editor(s) disclaim responsibility for any injury to people or property resulting from any ideas, methods, instructions or products referred to in the content.



## **CHAPTER 5: CONCLUDING REMARKS AND FUTURE PERSPECTIVES**

Throughout my PhD studies the objective changed from deep-sea sharks only, to labial cartilages and feeding mechanisms of sharks in general. The early onset of labial cartilages (LCs) in the seemingly primordial frilled shark (*Chlamydoselachus anguineus*) as well as the description of LCs in fossil findings and the wide distribution among chondrichthyan fishes leads to the assumption that LCs are a plesiomorphic character.

A phylogenetic analysis of LCs showed a certain aggregation of species with similar lifestyle which happen to be related in single cases but a useful impact on or support of the phylogeny of sharks could not be provided by characters from LCs (Klimpfinger 2023) [Supplementary Material 1 & 2]. The analysis, however, fortifies my presumption that LCs are a useful tool to determine the feeding strategy of a species. The high differentiation between LCs emphasizes their usefulness concerning the designation of feeding and hunting mechanism and, likewise, their lifestyle and role in an ecosystem. This is especially advantageous for species which are not too popular or obtainable for research, such as deep-sea, endangered or extinct shark species.

As an application example on how information on LCs can enlarge or change the knowledge on the lifestyle of a shark species I want to adduce some examples among the deep-sea sharks. Deep-sea sharks, specified by the definition of Kyne and Simpfendorfer (2007), are species that predominantly or exclusively spend their lives at depths below 200m. Of the described 215 shark species mentioned by Kyne and Simpfendorfer (2007) I had 35 in my descriptions of LCs, many of which only sparse information on their lifestyle or feeding behavior is present. Due to my knowledge on the LCs, I can state now, that deep-sea species majorly are opportunistic feeders, using only minor suction and rely mainly on biting [Supplementary Table 1]. On the basis of my data only three deep-sea species can be assumed to use medium or strong suction, those are two members of the kitefin sharks (Dalatiidae), namely the kitefin shark (*Dalatias licha*) and the cookiecutter shark (*Isistius brasiliensis*), and the only member of the angelsharks (Squatinaidae) that spends its life in the required depths to count as deep-sea species, the African angelshark (*Squatina africana*). The members of the kitefin-shark family probably use their suction to suck onto larger prey or carcasses, hence biting out pieces of tissue (as it is known from *I. brasiliensis*) while the African angelshark is a benthic ambush predator like its relatives

and is capable of producing a strong suction flow that can be even more powerful when used close to solid underground.

Another example of how important more detailed information on LCs are, is the case of the Greenland shark (*Somniosus microcephalus*), who was already described with three pairs of LCs in 1895 (White 1895), but the sketch attached to the description depicts the LCs in a wrong location. The placement in the original sketch would lead to the assumption that those LCs only enforce the mouth corners. At the same time the described LCs are far too massive for enforcement only and, therefore, after gathering some photographs of living or at least whole specimen, I repositioned the LCs [Figure 8]. The new, further anterior position resembles the photographs much more and according to my studies, it would allow the Greenland shark to produce suction of some magnitude. During a subsequent literature research, it turned out that actually suction was documented in the only existing video of a Greenland shark feeding on stationary bait (Grant et al. 2018). This proves again that elaborate information on LCs provide valuable insights on hunting and feeding behavior and it also stresses the fact that older sketches and descriptions need to be updated. As my studies show, CT-scans are a viable method of achieving new information on the structure and position of LCs.

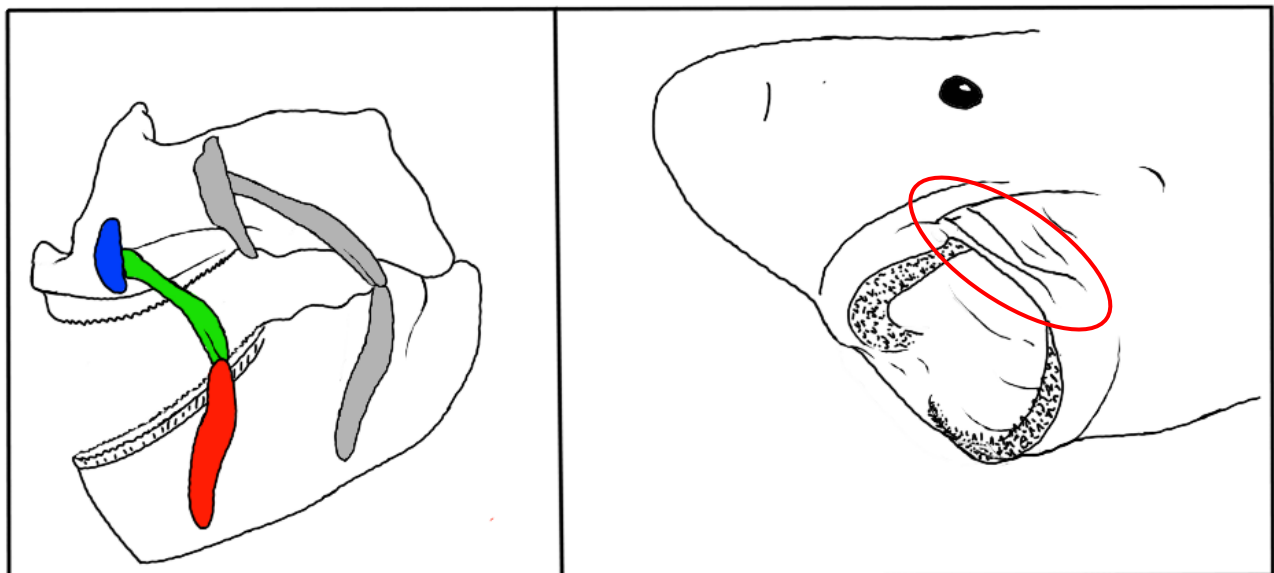


**Figure 8** Sketch of Greenland shark (*Somniosus microcephalus*). Left: sketch after White (1895) with the original placement of the LCs in grey and the updated placement using the color code of Klimpfinger & Kriwet (2020) – blue = LC 1, green = LC 2, red = LC 3. Right: sketch of a Greenland shark after capture with its mouth wide open and the detectable LCs encircled in red.

Generally, the extension of knowledge on extinct and extant organisms is a fundamental motivation in natural sciences. Therefore, also the gaining of new and additional information on the skeletal structures of sharks is an important contribution to our



understanding of those fascinating predators. The additional knowledge provided by the analysis of LCs can be crucial not only to expand our understanding of hunting and feeding behavior, but also to get a better idea on ecological roles and might even lead to useful conservation strategies, such as regulations for the use of certain baits or fishing methods.

Future research should encompass the expansion of scan data on sharks as well as the application of our findings to extinct sharks and species whose LCs have not been described so far. This additional information can possibly clarify existing questions concerning the lifestyle and feeding strategies of rare or extinct species and, therefore, alter their position in the current or paleontological ecosystem. Furthermore, the usage of suction is, according to our data, more common in sharks than often assumed and even specializations, like the one seen in the cookie-cutter shark *Isistius brasiliensis*, might be more prevalent than expected. The different kinds of suction utilized among species of different ecological niches may also lead to a redistribution of species within the currently defined ecotypes or might even open up new ecotypes. Another future branch of research is the extension of LC-research to other chondrichthyans, such as skates and rays, as well as the application of our results to those future findings to broaden the knowledge on their feeding strategies too. In a further step current data on bait and fishing methods can be collected and then compared to the knowledge on feeding strategies of cartilaginous fishes, so custom-tailored regulations for the conservation of certain shark and ray species can be established.

In conclusion, the newly gained information from this dissertation allows further insights on the lifestyle, as well as the hunting and feeding behavior of extant sharks. In addition, the information is applicable to extinct shark species as well as to relatives within the chondrichthyan fishes and offers new insights on their position within their respective ecosystems.

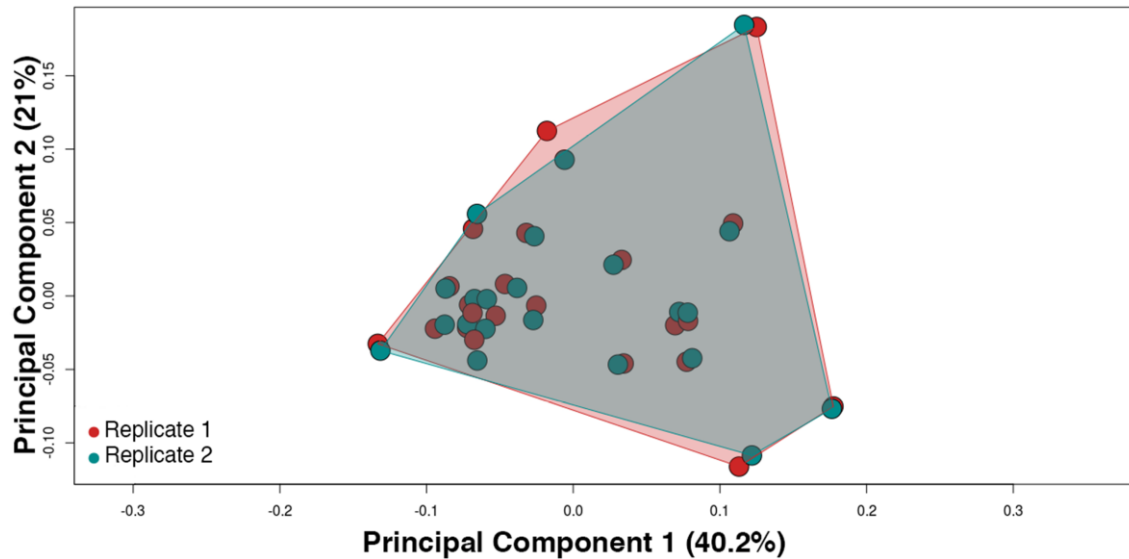
## References

- Klimpfinger, C. & Kriwet, J., 2020, *Comparative morphology of labial cartilages in sharks (Chondrichthyes, Elasmobranchii)*, European Zoological Journal, Volume 87, pp. 741–753
- Klimpfinger C., 2023, *Variability of Labial Cartilages in Sharks—Functional or Phylogenetic Signal? Morphological Descriptions and Phylogenetic Analysis*, Master Thesis, University of Vienna, Vienna, Austria, Available online: <https://ubdata.univie.ac.at/AC16587802> (accessed on 06 November 2024)
- Kyne P. M. & Simpfendorfer C. A., 2007, *A Collation and Summarization of Available Data on Deepwater Chondrichthyans: Biodiversity, Life History and Fisheries*, Report by IUCN SSC Shark Specialist Group for the Marine Conservation Biology Institute, Australia, pp. 1-137
- White P. J., 1895, *The Skull and Visceral Skeleton of the Greenland Shark*, Transactions of the Royal Society of Edinburgh, Volume 37, Part 2, pp. 287-306

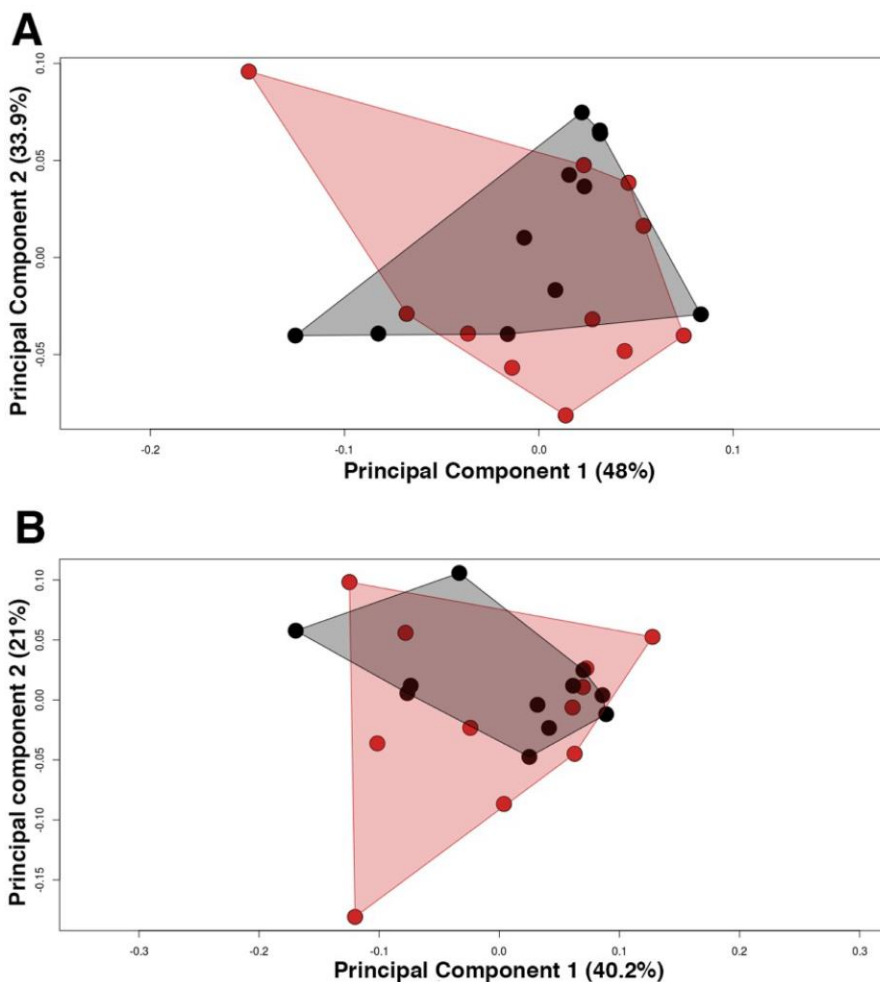
# SUPPLEMENTARY MATERIALS

## Manuscript 1

Supporting information figure S1: Morphospace of the landmarks replicates to test the repeatability of the coordinates capture



Supporting information figure S2: Morphospace of the shape variation between sexes (female = red; male = black). (a) Body shape and (b) head shape



## Manuscript 2

Supplementary Table: Sharkspecies (scientific and common name) and the number of labial cartilages detectable

species name	common name	Total Number of LC detected
<i>Alopias vulpinus</i>	common thresher shark	1
<i>Apristurus laurussonii</i>	Iceland catshark	2
<i>Atelomycterus macleayi</i>	Australian marbled atshark	2
<i>Atelomycterus marmoratus</i>	coral catshark	2
<i>Brachaelurus waddi</i>	blind shark	3
<i>Carcharhinus amboinensis</i>	pigeye shark	0
<i>Carcharhinus falciformis</i>	silky shark	2
<i>Carcharhinus hemiodon</i>	pondicherry shark	0
<i>Carcharhinus leucas</i>	bull shark	0
<i>Carcharhinus macroti</i>	hardnose shark	1
<i>Carcharhinus melanopterus</i>	blacktip reef shark	0
<i>Carcharodon carcharias</i> [Shimada 2009]	great white shark	0
<i>Centrophorus seychellorum</i>	Seychelles gulper shark	3
<i>Centrophorus uyato</i>	little gulper shark	3
<i>Centroselachus crepidater</i>	longnose velvet dogfish	3
<i>Cetorhinus maximus</i>	basking shark	0
<i>Chaenogaleus macrostoma</i>	hooktooth shark	2
<i>Chiloscyllium arabicum</i>	Arabian carpetshark	3
<i>Chiloscyllium griseum</i>	grey bamboo shark	4
<i>Chiloscyllium hasselti</i>	Hasselt's bamboo shark	3
<i>Chiloscyllium indicum</i>	slender bamboo shark	3
<i>Chiloscyllium punctatum</i>	brownbanded bamboo shark	4
<i>Chlamydoselachus anguineus</i> [Smith 1937]	frilled shark	3
<i>Dalatias licha</i>	kitefin shark	3
<i>Deania calcea</i>	birdbeak dogfish	3
<i>Echinorhinus brucus</i> alias <i>E. spinosus</i>	bramble shark	3
<i>Etmopterus baxteri</i>	New Zealand lanternshark	2

<i>Etmopterus lucifer</i>	black-belly lanternshark	2
<i>Etmopterus spinax</i>	velvet-belly lanternshark	0
<i>Eucrossorhinus dasypogon</i>	tasselled wobbegong	5
<i>Euprotomicrus bispinatus</i>	pygmy shark	1
<i>Eusphyra blochii</i>	winghead shark	0
<i>Galeorhinus galeus</i>	school shark	2
<i>Galeus melastomus</i>	blackmouth catshark	2
<i>Ginglymostoma cirratum</i>	nurse shark	3
<i>Halaelurus boesemani</i>	speckled catshark	0
<i>Halaelurus buergeri</i>	blackspotted catshark	0
<i>Hemigaleus microstoma</i>	sicklefin weasel shark	1
<i>Hemiscyllium ocellatum</i> [Wu 1994]	epaulette shark	4
<i>Hemiscyllium strahani</i>	hooded carpetshark	4
<i>Hemiscyllium trispeculare</i>	speckled carpetshark	4
<i>Heptranchias perlo</i>	sharpnose sevengill shark	0
<i>Heterodontus francisci</i>	horn shark	2
<i>Heterodontus japonicas</i>	japanese bullhead shark	2
<i>Heterodontus portusjacksoni</i> [Dean 1895]	Port Jackson shark	3
<i>Isistius brasiliensis</i>	cookiecutter shark	3
<i>Isogomphodon oxyrinchus</i>	daggernose shark	0
<i>Isurus oxyrinchus</i> [Shimada 2009]	shortfin mako	0
<i>Isurus paucus</i> [Shimada 2009]	longfin mako	0
<i>Lamna ditropis</i> [Shimada 2009]	salmon shark	0
<i>Lamna nasus</i>	porbeagle	0
<i>Megachasma pelagios</i> [Seigel 1985 / Shimada 2009]	megamouth shark	0
<i>Mitsukurina owstoni</i> [Shimada 2009]	goblin shark	0
<i>Mollisquama parini</i> [Denton et al. 2018]	pocket shark	3
<i>Mustelus asterias</i>	starry smooth-hound	2
<i>Mustelus higmani</i>	smalleye smooth-hound	1
<i>Mustelus mustelus</i>	common smooth-hound	1
<i>Nebrius ferrugineus</i>	tawny nurse shark	3
<i>Odontaspis ferox</i> [Shimada 2009]	smalltooth sand tiger shark	2
<i>Orectolobus japonicas</i>	Japanese Wobbegong	5
<i>Orectolobus maculatus</i> [Wu 1994]	spotted Wobbegong	4

<i>Oxynotus centrina</i>	angular roughshark	0
<i>Prionace glauca</i>	blue shark	1
<i>Pristiophorus japonicus</i>	Japanese sawshark	0
<i>Rhincodon typus</i> [Denison 1937]	whale shark	3
<i>Rhizoprionodon terraenovae</i>	Atlantic sharpnose shark	0
<i>Scoliodon laticaudus</i>	spadenose shark	1
<i>Scyliorhinus boa</i>	boa catshark	1
<i>Scyliorhinus canicula</i>	small-spotted catshark	1
<i>Scyliorhinus stellaris</i>	nursehound	1
<i>Scymnodalatias albicauda</i>	whitetail dogfish	4
<i>Somniosus microcephalus</i> [White 1895]	Greenland shark	3
<i>Sphyrna corona</i>	scalloped bonnethead	0
<i>Sphyrna lewini</i>	scalloped hammerhead	1
<i>Sphyrna tiburo</i>	bonnethead	0
<i>Sphyrna tudes</i>	smalleye hammerhead	0
<i>Sphyrna zygaena</i>	smooth hammerhead	1
<i>Squalus acanthias</i>	spiny dogfish	3
<i>Squalus cubensis</i>	Cuban dogfish	3
<i>Squalus megalops</i>	shortnose spurdog	3
<i>Squalus suckleyi</i>	Pacific spiny dogfish	3
<i>Squatina africana</i>	African angelshark	4
<i>Squatina japonica</i>	Japanese angelshark	3
<i>Squatina squatina</i>	angelshark	3
<i>Stegostoma fasciatum</i>	zebra shark	4
<i>Triaenodon obesus</i>	whitetip reef shark	0
<i>Triakis semifasciata</i>	leopard shark	2

## Manuscript 3

Supplementary Table 1: total number of labial cartilages in shark species and presence (1)/ absence (0) of single labial cartilages; color-coding only refers to the total number of LC-pairs present.

Family	Gattung	Art	Total Number of LC-Pairs	LC1	LC2	LC2.1	LC3.1	LC3
Chlamydoselachidae	Chlamydoselachus	C. anguineus	3	1	1	0	0	1
Hexanchidae	Heptranchias	H. perlo	0	0	0	0	0	0
	Hexanchus	H. nakamurai	1	1	0	0	0	0
Centrophoridae	Centrophorus	C. seychellorum	3	1	1	0	0	1
		C. uyato	3	1	1	0	0	1
		C. tessellatus	3	1	1	0	0	1
	Deania	D. calcea	3	1	1	0	0	1
Dalatiidae	Mollisquama	M. parini	3	1	1	0	0	1
	Dalatias	D. licha	3	1	1	0	0	1
	Isistius	I. brasiliensis	3	1	1	0	0	1
	Euprotomicrus	E. bispinatus	1	1	0	0	0	0
Etmopteridae	Etmopterus	E. lucifer	2	1	0	0	0	1
		E. sheikoi	2	1	0	0	0	1
		E. splendendus	2	1	0	0	0	1
		E. spinax	0	0	0	0	0	0
	Trigonognathus	T. kabeyai	0	0	0	0	0	0
Oxynotidae	Oxynotus	O. centrina	3	1	1	0	0	1
Somniosidae	Centroscymnus	C. crepidater	3	1	1	0	0	1
		C. owstonii	3	1	1	0	0	1
	Scymnodalatias	S. albicauda	4	1	1	1	0	1
	Scymnodon	S. ringens	3	1	1	0	0	1
	Somniosus	S. microcephalus [White 1895]	3	1	1	0	0	1
	Zameus	Z. squamosum	3	1	1	0	0	1
Squalidae	Squalus	S. acanthias	3	1	1	0	0	1
		S. suckleyi	3	1	1	0	0	1
		S. cubensis	3	1	1	0	0	1
		S. megalops	3	1	1	0	0	1
		S. mitsukurii	3	1	?	0	0	1
		S. brevirostris	3	1	1	0	0	1
Echinorhinidae	Echinorhinus	E. brucus = E. spinosus	3	1	1	0	0	1
Squatinidae	Squatina	S. squatina	3	1	1	0	0	1
		S. africana	4	1	1	0	1	1
		S. japonica	3	1	1	0	0	1
		S. nebulosa	3	1	1	0	0	1
Pristiophoridae	Pristiophorus	P. japonicus	0	0	0	0	0	0
		P. nudipinnis	1	1	0	0	0	0
Heterodontidae	Heterodontus	H. japonicas	2	1	0	0	0	1
		H. francisci	2	1	0	0	0	1
		H. portusjacksoni [Summers 2004]	2	1	0	0	0	1



Brachaeluridae	Brachaelurus	B. waddi	3	1	1	0	0	1
Ginglymostomatidae	Ginglymostoma	G. cirratum	3	1	1	0	0	1
	Nebrius	N. ferrugineus	3	1	1	0	0	1
Hemisylliidae	Chiloscyllium	C. hasselti	3	1	1	0	0	1
		C. arabicum	3	1	1	0	0	1
		C. indicum	3	1	1	0	0	1
		C. punctatum	4	1	1	0	1	1
		C. griseum	4	1	1	0	1	1
		C. plagiosum	3	1	1	0	0	1
	Hemisycyllium	H. trispeculare	4	1	1	0	1	1
		H. strahani	4	1	1	0	1	1
		H. ocellatum	4	1	1	1	0	1
Orectolobidae	Eucrossorhinus	E. dasyopogon	5	1	1	1	1	1
	Orectolobus	O. japonicus	5	1	1	1	1	1
		O. maculatus	5	1	1	1	1	1
Parascylliidae	Parascyllium	P. collare	4	1	1	1	0	1
Rhincodontidae	Rhincodon	R. typus [Denison 1937]	3	1	1	0	0	1
Stegostomatidae	Stegostoma	S. fasciatum	4	1	1	0	1	1
Alopiidae	Alopias	A. vulpinus	1	1	0	0	0	0
		A. superciliosus	0	0	0	0	0	0
Cetorhinidae	Cetorhinus	C. maximus	0	0	0	0	0	0
Lamnidae	Carcharodon	C. carcharias [Shimada 2009]	0	0	0	0	0	0
	Isurus	I. oxyrinchus [Shimada 2009]	0	0	0	0	0	0
		I. paucus [Shimada 2009]	0	0	0	0	0	0
	Lamna	L. ditropis [Shimada 2009]	0	0	0	0	0	0
		L. nasus	0	0	0	0	0	0
Megachasmidae	Megachasma	M. pelagios [Seigel 1985 / Shimada 2009]	0	0	0	0	0	0
Mitsukurinidae	Mitsukurina	M. owstoni	2	1	0	0	0	1
Odontaspidae	Carcharias	C. taurus	0	0	0	0	0	0
	Odontaspis	O. ferox [Shimada 2009]	2	1	0	0	0	1
Pseudocarchariidae	Pseudocarcharias	P. kamoharai	0	0	0	0	0	0
?	Galeocerdo	G. cuvier [pers. obs. Simon de Marchi]	0	0	0	0	0	0
Carcharhinidae	Scoliodon	S. laticaudus	1	1	0	0	0	0
		S. macrorhynchos	0	0	0	0	0	0
	Carcharhinus	C. falciformis	2	1	0	0	0	1
		C. macroti	1	1	0	0	0	0
		C. amboinensis	0	0	0	0	0	0
		C. hemiodon	0	0	0	0	0	0
		C. leucas	0	0	0	0	0	0
		C. melanopterus	0	0	0	0	0	0
		C. galapagensis	2	?	0	0	0	?
		C. plumbeus	0	0	0	0	0	0
	Prionace	P. glauca	1	1	0	0	0	0
	Negaprion	N. brevirostris	2	1	0	0	0	1
	Rhizoprionodon	R. terraenovae	0	0	0	0	0	0
	Isogomphodon	I. oxyrinchus	0	0	0	0	0	0
	Trienodon	T. obesus	0	0	0	0	0	0
Hemigaleidae	Chaenogaleus	C. macrostoma	2	1	0	0	0	1

	Hemigaleus	H. microstoma	1	1	0	0	0	0
	Hemipristis	H. elongatus	2	1	0	0	0	1
Leptochariidae	Leptocharias	L. smithii	2	1	0	0	0	1
Proscylliidae	Eridacnis	E. radcliffei	0-1	1	0	0	0	0
Scyliorhinidae	Apristurus	A. laurussonii	2	1	0	0	0	1
		A. macrostomus	2	1	0	0	0	1
	Atelomycterus	A. marmoratus	2	1	0	0	0	1
		A. macleayi	2	1	0	0	0	1
	Bythaelurus	B. canescens	2	1	0	0	0	1
	Cephaloscyllium	C. ventriosum	0	0	0	0	0	0
	Galeus	G. melastomus	2	1	0	0	0	1
		G. sauteri	3	1	?	0	0	1
	Halaaelurus	H. boesemani	0	0	0	0	0	0
		H. buergeri	0	0	0	0	0	0
	Poroderma	P. africanum	1	1	0	0	0	0
	Schroederichthys	S. chilensis	2	1	?	0	0	1
	Scyliorhinus	S. boa	1	1	0	0	0	0
		S. canicula	1	1	0	0	0	0
		S. stellaris	1	1	0	0	0	0
		S. meadi	1	1	0	0	0	0
Sphyrnidae	Eusphyras	E. blochii	0	0	0	0	0	0
	Sphyrna	S. zygaena	0	0	0	0	0	0
		S. lewini	1	1	0	0	0	0
		S. corona	0	0	0	0	0	0
		S. tiburo	0	0	0	0	0	0
		S. tudes	0	0	0	0	0	0
		S. media	0	0	0	0	0	0
Triakidae	Galeorhinus	G. galeus	2	1	0	0	0	1
	Mustelus	M. mustelus	2	1	0	0	0	1
		M. higmani	1	1	0	0	0	0
		M. asterias	2	1	0	0	0	1
		M. manazo	2	1	?	0	0	1
	Triakis	T. semifasciata	2	1	0	0	0	1

Supplementary Table 2: Shark species and their feeding behavior according to literature; color-coding only displays the total number of LC-pairs in a species. The stated feeding methods are either deduced from the collected Data (D) or described by a Reference (R)

Family	Gattung	Art	Total Number of LC-Pairs	Feeding Method	Reference (R) or Deduced from Data (D)
Chlamydoselachidae	Chlamydoselachus	C. anguineus	3	ram + biting	R: Wilga 2002
Hexanchidae	Heptranchias	H. perlo	0	Biting	R: Kryukova & Kuznetsov 2020
	Hexanchus	H. nakamurai	1	biting + suction	D
Centrophoridae	Centrophorus	C. seychellorum	3	biting + suction	D
		C. uyato	3	biting + suction	D
		C. tessellatus	3	biting + suction	D
	Deania	D. calcea	3	biting + suction	D
Dalatiidae	Mollisquama	M. parini	3	biting + suction	R: Denton et al. 2018
	Dalatias	D. licha	3	biting + suction	D
	Isistius	I. brasiliensis	3	biting + suction	R: Jones 1971; Shirai 1992; Figueiredo & Carvahlo 2018; Papastamatiou et al. 2010
	Euprotomicrus	E. bispinatus	1	biting	D
Etmopteridae	Etmopterus	E. lucifer	2	biting	D
		E. sheikoi	2	biting	D
		E. splenndidus	2	biting	D
		E. spinax	0	ram or biting	D
	Trigonognathus	T. kabeyai	0	ram or biting	D
Oxynotidae	Oxynotus	O. centrina	3	biting + suction	R: Capape 2008
Somniosidae	Centroscymnus	C. crepidater	3	biting + suction	D
		C. owstonii	3	biting + suction	D
	Scymnodalatias	S. albicauda	4	?	
	Scymnodon	S. ringens	3	biting + suction	D
	Somniosus	S. microcephalus [White 1895]	3	suction + biting	R: Grant et al. 2018
	Zameus	Z. squamosum	3	biting + suction	D
Squalidae	Squalus	S. acanthias	3	suction + biting (+ram)	R: Wilga 2001 & 2007
		S. suckleyi	3	biting + suction	D
		S. cubensis	3	biting + suction	D
		S. megalops	3	biting + suction	D
		S. mitsukurii	3	biting + suction	D
		S. brevirostris	3	biting + suction	D
Echinorhinidae	Echinorhinus	E. brucus = E. spinosus	3	ram + suction	D
Squatinaidae	Squatina	S. squatina	3	suction	D
		S. africana	4	suction	D
		S. japonica	3	suction	D
		S. nebulosa	3	suction	D
Pristiophoridae	Pristiophorus	P. japonicus	0	ram or biting	D
		P. nudipinnis	1	ram or biting	D
Heterodontidae	Heterodontus	H. japonicas	2	suction + biting	D
		H. francisci	2	suction + biting	R: Edmonds et al. 2001; Huber et al. 2005
		H. portusjacksoni [Summers 2004]	2	suction + biting	D

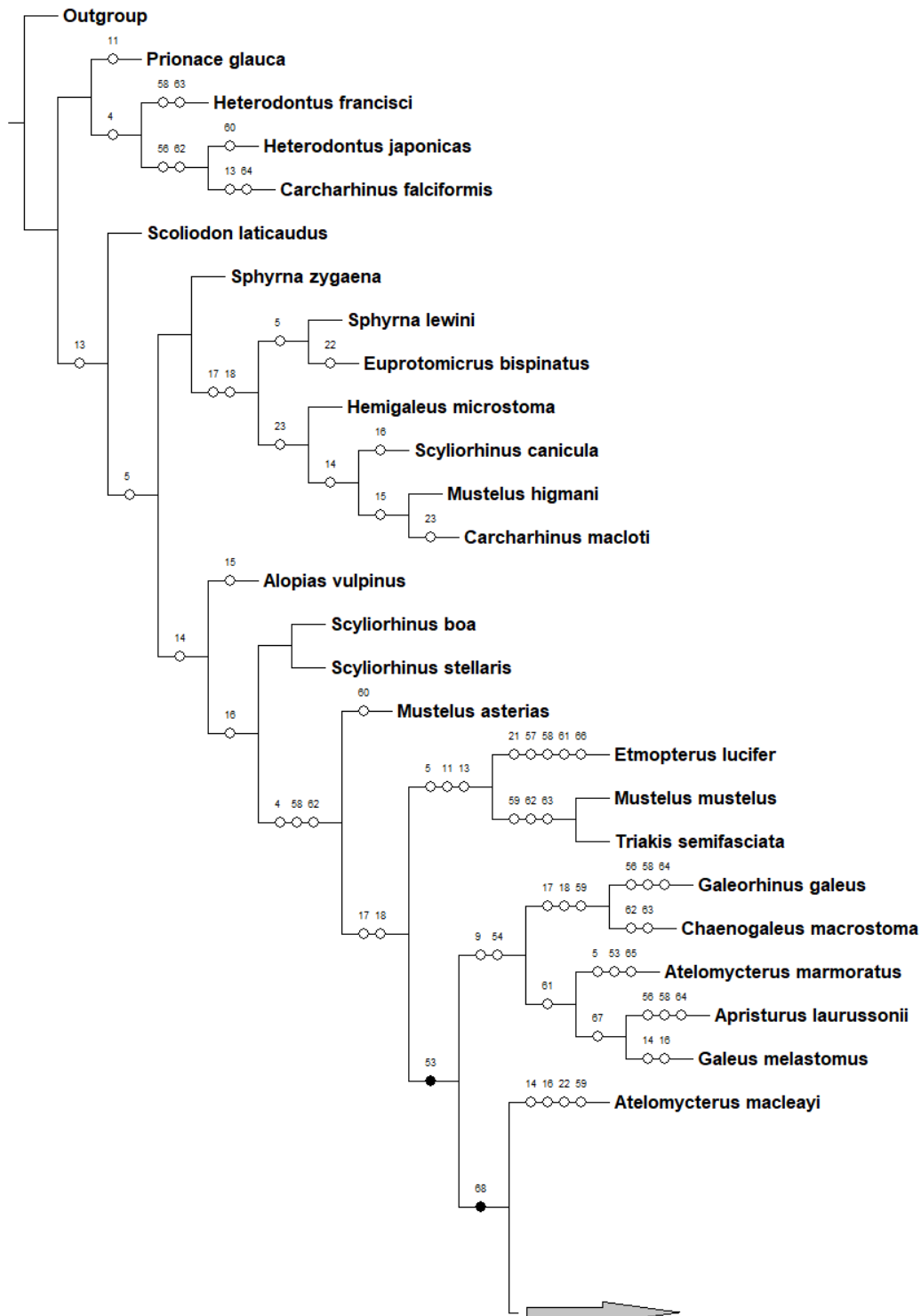
Brachaeluridae	Brachaelurus	B. waddi	3	biting + suction	D
Ginglymostomatidae	Ginglymostoma	G. cirratum	3	suction	R: Motta & Wilga 1999; Motta et al. 2002 & 2008; Wilga 2007; Gardiner et al. 2017
	Nebrius	N. ferrugineus	3	suction	D
Hemiscylliidae	Chiloscyllium	C. hasselti	3	biting + suction	D
		C. arabicum	3	biting + suction	D
		C. indicum	3	biting + suction	D
		C. punctatum	4	suction	D
		C. griseum	4	suction	D
		C. plagiosum	3	suction	R: Nauwelaerts 2007; Wilga 2007; Scott et al. 2019
	Hemiscyllium	H. trispeculare	4	suction	D
		H. strahani	4	suction	D
		H. ocellatum	4	suction + biting	R: Wu 1994
Orectolobidae	Eucrossorhinus	E. dasypogon	5	suction	D
	Orectolobus	O. japonicus	5	suction	D
		O. maculatus	5	suction	R: Wu 1994
Parascylliidae	Parascyllium	P. collare	4	biting + suction	D
Rhincodontidae	Rhincodon	R. typus [Denison 1937]	3	ram-filterfeeding or suction	R: Cade et al. 2020; Motta et al. 2010
Stegostomatidae	Stegostoma	S. fasciatum	4	suction + biting	D
Alopiidae	Alopias	A. vulpinus	1	ram + biting	D
		A. superciliosus	0	ram + biting	D
Cetorhinidae	Cetorhinus	C. maximus	0	ram	D
Lamnidae	Carcharodon	C. carcharias [Shimada 2009]	0	ram + biting	R: Tricas 1985
	Isurus	I. oxyrinchus [Shimada 2009]	0	ram (biting)	D
		I. paucus [Shimada 2009]	0	ram	D
	Lamna	L. ditropis [Shimada 2009]	0	ram (biting)	D
		L. nasus	0	ram	D
Megachasmidae	Megachasma	M. pelagios [Shimada 2009]	0	ram-filterfeeding	R: Tomita et al. 2011
Mitsukurinidae	Mitsukurina	M. owstoni	2	ram + biting	D
Odontaspidae	Carcharias	C. taurus	0	biting	D
	Odontaspis	O. ferox [Shimada 2009]	2	biting	R: Wilga 2007
Pseudocarchariidae	Pseudocarcharias	P. kamoharai	0	ram	D
?	Galeocerdo	G. cuvier [pers. obs. de Marchi]	0	ram + biting	D
Carcharhinidae	Scoliodon	S. laticaudus	1	ram or biting	D
		S. macrorhynchus	0	ram	D
	Carcharhinus	C. falciformis	2	ram (biting)	D
		C. macroti	1	biting	D
		C. amboinensis	0	ram	D
		C. hemiodon	0	ram	D
		C. leucas	0	ram	D
		C. melanopterus	0	ram	R: Gardiner et al 2017
		C. galapagensis	2	ram + suction	D
		C. plumbeus	0	biting	R: Ramsay 2012
	Prionace	P. glauca	1	ram (biting)	D
	Negaprion	N. brevirostris	2	ram	R: Motta et al. 1995
	Rhizoprionodon	R. terraenovae	0	ram	D
	Isogomphodon	I. oxyrhynchus	0	ram	D
	Trienodon	T. obesus	0	ram (biting)	D

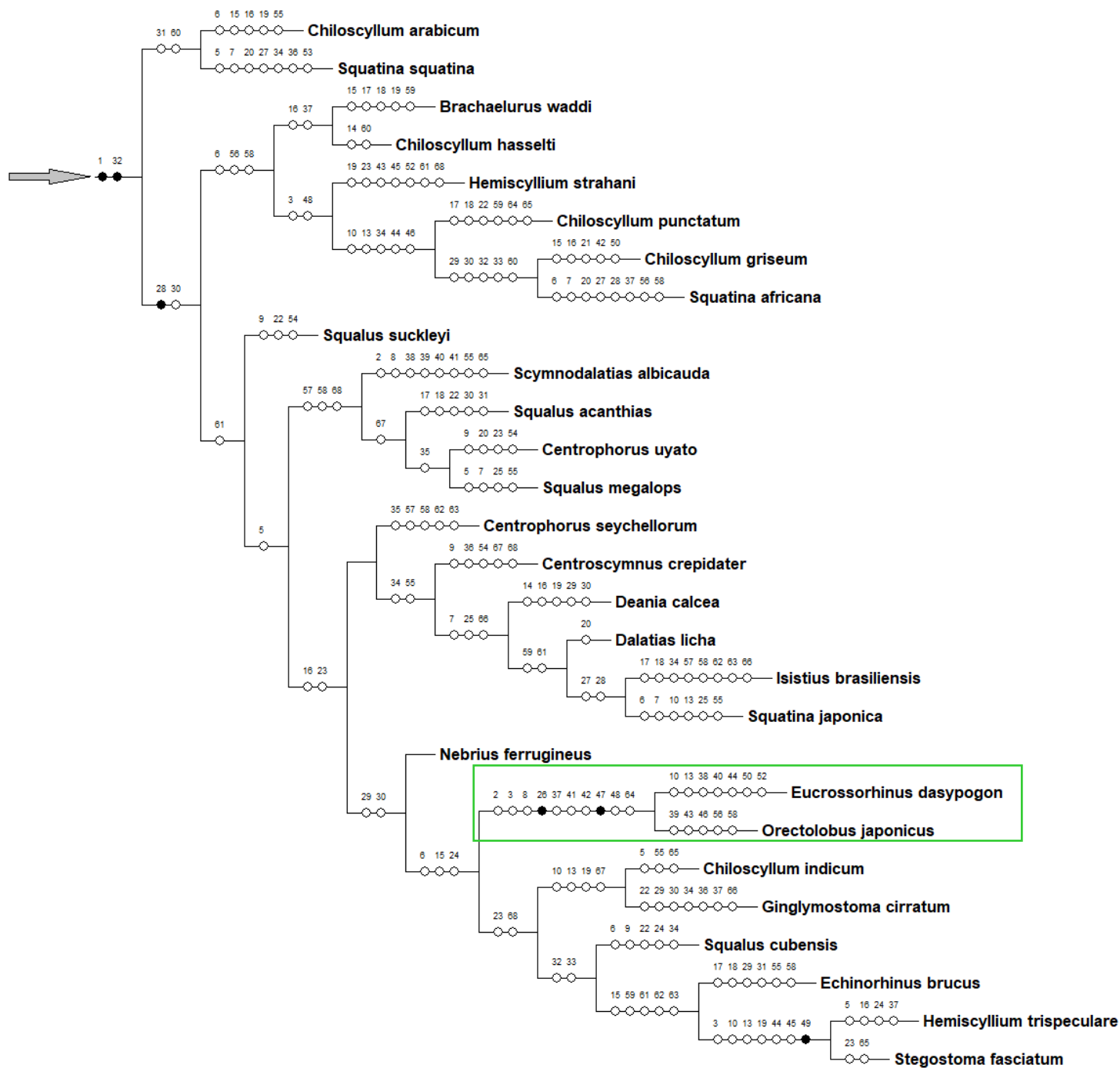
Hemigaleidae	Chaenogaleus	C. macrostoma	2	ram + biting	D
	Hemigaleus	H. microstoma	1	biting	D
	Hemipristis	H. elongatus	2	biting	D
Leptochariidae	Leptocharias	L. smithii	2	biting (suction)	D
Proscylliidae	Eridacnis	E. radcliffei	0-1	biting	D
Scyliorhinidae	Apristurus	A. laurussonii	2	biting (suction)	D
		A. macrostomus	2	biting (suction)	D
	Atelomycterus	A. marmoratus	2	biting (suction)	D
		A. macleayi	2	biting (suction)	D
	Bythaelurus	B. canescens	2	biting	D
	Cephaloscyllium	C. ventriosum	0	ram	D
	Galeus	G. melastomus	2	biting (suction)	D
		G. sauteri	3	biting (suction)	D
	Halaelurus	H. boesemani	0	biting or ram	D
		H. buergeri	0	biting or ram	D
	Poroderma	P. africanum	1	biting	D
	Schroederichthys	S. chilensis	2	suction + biting	D
	Scyliorhinus	S. boa	1	biting	D
		S. canicula	1	biting	D
		S. stellaris	1	biting	D
		S. meadi	1	biting	D
Sphyrnidae	Eusphyra	E. blochii	0	ram	D
	Sphyrna	S. zygaena	0	ram (biting)	D
		S. lewini	1	ram (biting)	D
		S. corona	0	ram	D
		S. tiburo	0	ram (biting)	R: Gardiner et al. 2017; Wilga 2001
		S. tudes	0	ram	D
		S. media	0	ram	D
Triakidae	Galeorhinus	G. galeus	2	biting (suction)	D
	Mustelus	M. mustelus	2	biting (suction)	D
		M. higmani	1	biting (ram)	D
		M. asterias	2	biting (suction)	D
		M. manazo	2	biting (suction)	D
	Triakis	T. semifasciata	2	suction + biting	D

## Conclusions

Supplementary Material 1: Phylogenetic analysis including only taxa possessing labial cartilages (LC) (54 taxa including a hypothetical outgroup) and based only on characters connected to the LCs (68 character) from Klimpfner (2022). Ci = 22

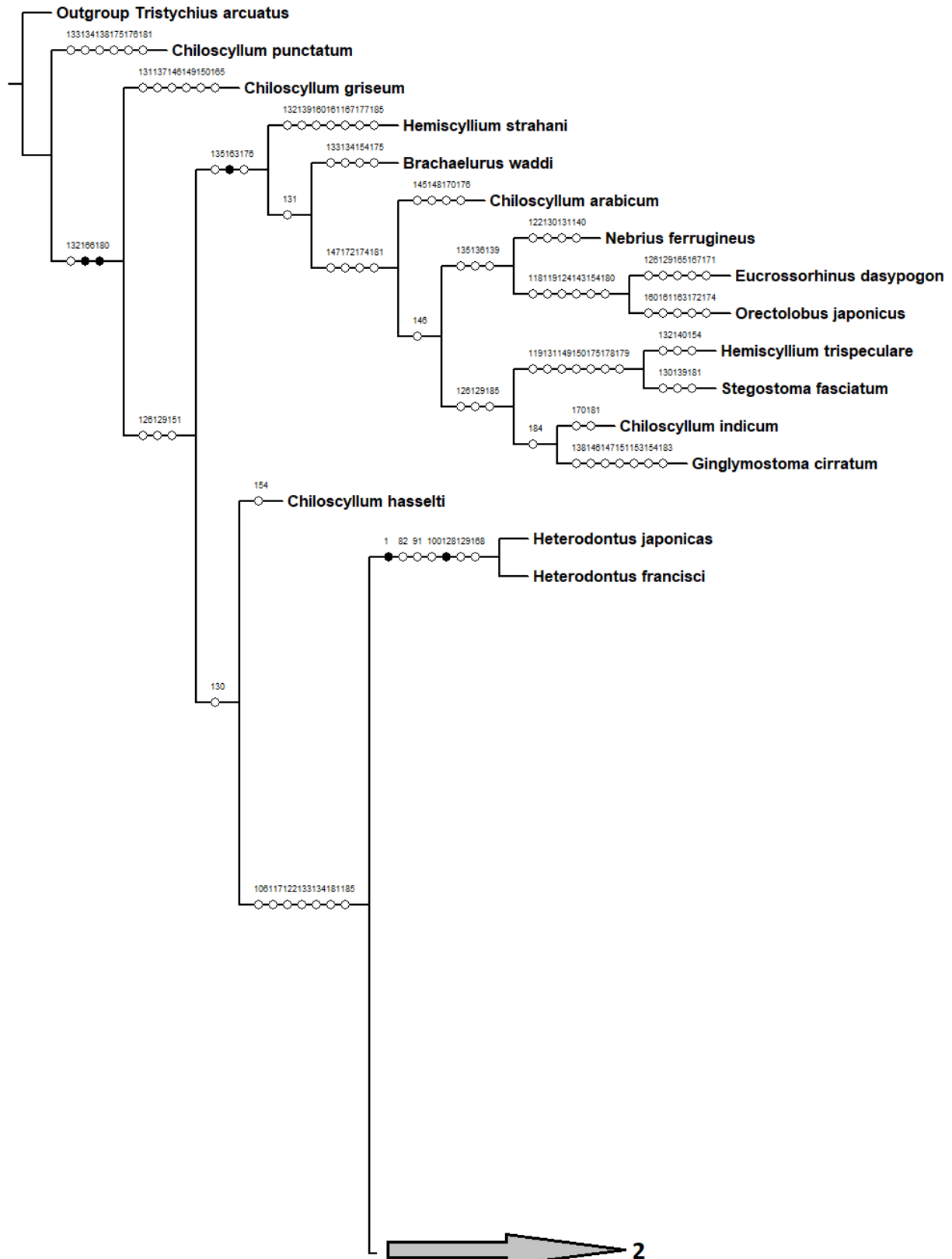
Only the members of the Orectolobidae family group together (boxed), else no genetically related taxa group together, which shows that the LCs do not provide good characters to determine the relationships between species.

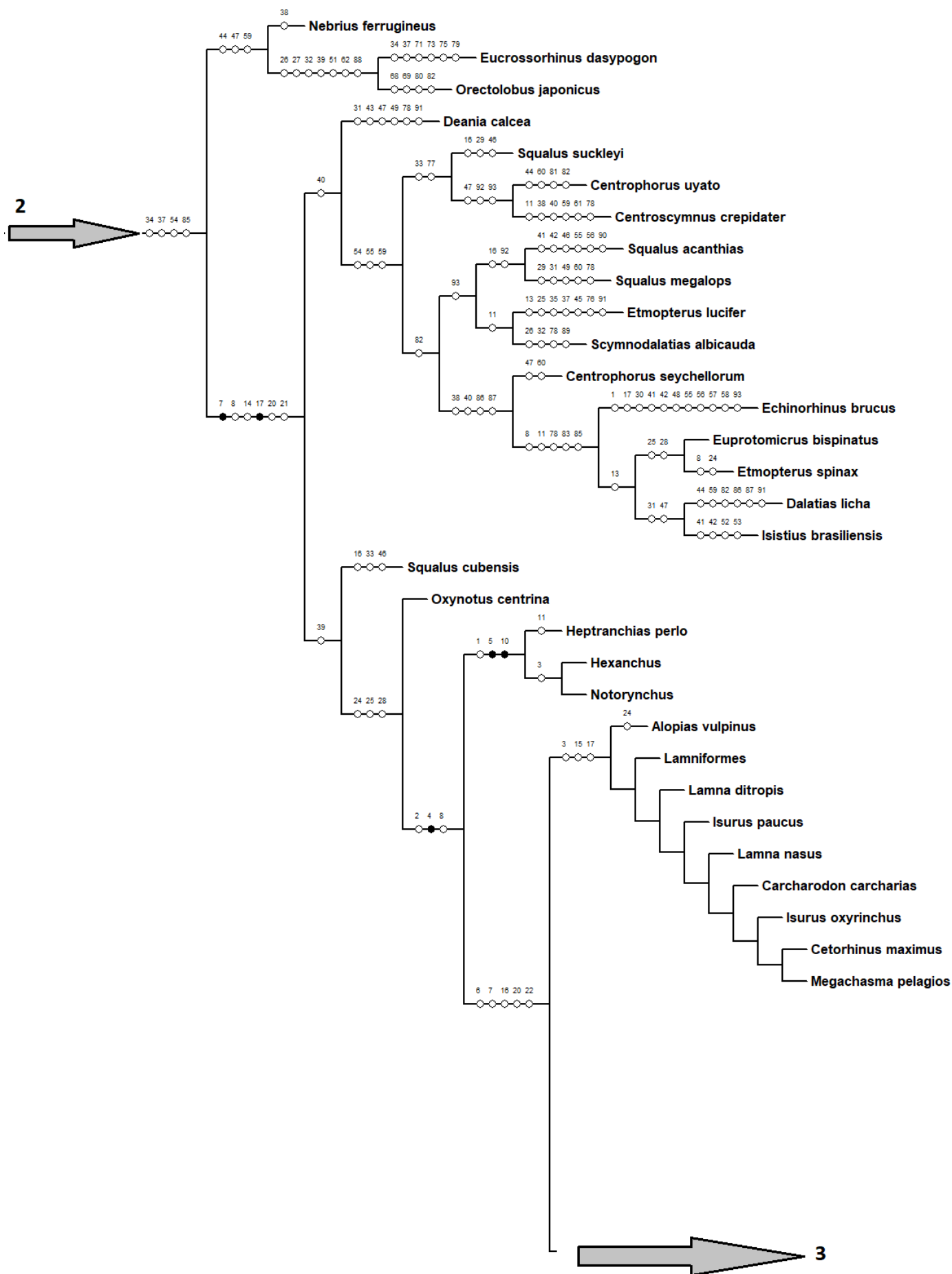






Supplementary Material 2: Phylogenetic analysis of 83 taxa of sharks, including species with and without labial cartilages (LC), based on general characters and characters connected to LCs (185 characters in total) including unknown character states from Klimpfinger (2022). Ci = 37







Supplementary Table 1: deep-sea shark species according to the definition by Kyne & Simpfendorfer (2007) that were represented in the study of Klimpfinger & Kriwet (2023) and their number and types of labial cartilages (LCs), coding for the amount of suction used while foraging. Color-code: red = no suction; orange = no to minor suction; yellow = minor suction (generalists using mainly biting); light green = medium suction; dark green = strong suction (benthic ambush predator).

Order	Species	Depth [m]	LC	LC-Type		
				LC1	LC2	LC3
Hexanchiformes	<i>Chlamydoselachus anguineus</i>	50-1500	3 LCs	iv	i	i
	<i>Heptranchias perlo</i>	27-1000	No LCs			
	<i>Hexanchus nakamurai</i>	90-621	1 LC	A		
Squaliformes	<i>Echinorhinus brucus</i>	18-900	3 LCs	E	ii	F
	<i>Squalus brevirostris</i>	0-730	3 LCs	B	A	C
	<i>Squalus cubensis</i>	60-380	3 LCs	G	A	C
	<i>Squalus megalops</i>	0-732	3 LCs	B	A	C
	<i>Squalus mitsukurii</i>	100-500	3 LCs	G	iii	C
	<i>Centrophorus seychellorum</i>	1000	3 LCs	A	A	D
	<i>Centrophorus tessellatus</i>	260-730	3 LCs	E	A	A
	<i>Centrophorus uyato</i>	50-1000	3 LCs	E	A	D
	<i>Deania Calcea</i>	70-1470	3 LCs	G	A	D
	<i>Etmopterus luzifer</i>	158-1357	2 LCs	G		C
	<i>Etmopterus splendidus</i>	210	2 LCs	G		C
	<i>Trigonognathus kabeyai</i>	270-360	No LCs			
	<i>Centroscymnus owstoni</i>	426-1459	3 LCs	E	A	A
	<i>Centroscymnus crepidater</i>	270-2080	3 LCs	E	A	A
	<i>Scymnodalatias albicauda</i>	150-500	4 LCs	H	A	iii
	<i>Scymnodon ringens</i>	200-1600	3 LCs	E	A	F
	<i>Zameus squamulosus</i>	0-6000	3 LCs	E	A	A
	<i>Oxynotus centrina</i>	50-660	3 LCs	A	ii	C
	<i>Dalatias licha</i>	37-1800	3 LCs	ii	B	A
	<i>Isistius brasiliensis</i>	0-3500	3 LCs	A	B	A
Squatiniformes	<i>Squatina africana</i>	60-494	4 LCs	F	B	E
Lamniformes	<i>Odontaspis ferox</i>	13-850	2 LCs	H		E
	<i>Pseudocarcharias kamoharai</i>	0-590	No LCs			
	<i>Mitsukurina owstoni</i>	270-1300	2 LCs	v		ii
	<i>Alopias superciliosus</i>	0-732	No LCs			
	<i>Cetorhinus maximus</i>	0-904	No LCs			
Carcharhiniformes	<i>Apristurus laurussoni</i>	560-2060	2 LCs	G		E
	<i>Apristurus macrostomus</i>	913	2 LCs	G		F
	<i>Bythaelurus canescens</i>	250-700	2 LCs	H		E
	<i>Galeus melastomus</i>	56-1440	2 LCs	F		B
	<i>Scyliorhinus boa</i>	229-676	1 LC	A		
	<i>Scyliorhinus meadi</i>	329-548	1 LC	A		